DESIGN AND ANALYSIS OF PROBE-FED CYLINDRICAL DIELECTRIC RESONATOR ANTENNA

A THESIS SUBMITTED IN PARTIAL FULFILMENT OF THE REQUIREMENTS FOR THE AWARD OF THE DEGREE

OF

MASTER OF ENGINEERING
IN
ELECTRONICS & TELE-COMMUNICATION ENGINEERING
IN SPECIALIZATION OF MICROWAVE ENGINEERING 2017-19

By:

ANUSRI PATRA

ROLL NO.: 001710702023

UNIVERSITY REGISTRATION NO.: 140706 OF 2017-18

EXAMINATION ROLL NO.: M4ETC19003

Under the supervision of

DR. MANOTOSH BISWAS

Professor

DEPARTMENT OF ELECTRONICS & TELE-COMMUNICATION ENGINEERING

JADAVPUR UNIVERSITY

KOLKATA-700032

MAY 2019

FACULTY OF ENGINEERING AND TECHNOLOGY

DEPARTMENT OF ELECTRONICS AND TELECOMMUNICATION ENGINEERING

JADAVPUR UNIVERSITY

CERTIFICATE OF RECOMMENDATION

This is to certify that the dissertation entitled **"DESIGN AND ANALYSIS OF PROBE-FED CYLINDRICAL DIELECTRIC RESONANTOR ANTENA"** submitted by **ANUSRI PATRA (Examination Roll No.: M4ETC19003, University Registration No.: 140706 of 2017-18)** to Jadavpur University, Kolkata, is a record of bonafide research work under my supervision and be accepted in partial fulfilment of the requirement for the degree of **Master of Engineering in Electronics and Telecommunication Engineering** of the institute. The research results presented in this thesis are not included in any other paper submitted for the award of any Degree or Diploma to any other University or Institute. The project in my opinion, is worthy for its acceptance.

_____

DR. MANOTOSH BISWAS

Thesis supervisor
(Professor)
Department of Electronics and Telecommunication Engineering
Jadavpur University
Kolkata 700032

_____

Prof. Sheli Sinha Chaudhuri
Head of the Department
Department of Electronics &
Telecommunication Engineering
Jadavpur University
Kolkata – 700 032

_____

Prof. Dr. Chiranjib Bhattacharjee
Dean
Faculty of Engineering & Technology
Jadavpur University
Kolkata – 700 032

FACULTY OF ENGINEERING AND TECHNOLOGY

DEPARTMENT OF ELECTRONICS AND TELECOMMUNICATION ENGINEERING

JADAVPUR UNIVERSITY

CERTIFICATE OF APPROVAL*

The foregoing THESIS is hereby approved as a creditable study of an Engineering Subject carried out and presented in a manner of satisfactory to warrant its acceptance as a pre-requisite to the degree for which it has been submitted. It is to be understood that by this approval, the undersigned do not necessarily endorse or approve any statement made opinion expressed and conclusion drawn therein but approve the THESIS only for the purpose for which it has been submitted.

Committee on Final Examination for
The Evaluation of Thesis

BOARD OF EXAMINERS

(SIGNATURE OF THE EXAMINER)

(SIGNATURE OF THE SUPERVISOR)

*Only in case the thesis is approved

DECLARATION OF ORIGINALITY AND COMPLIANCE OF ACADEMIC ETHICS

I the undersigned do hereby declare that this thesis contains literature survey and original work done by means a part of my MASTER OF ENGINEERING IN ELECTRONICS AND TELECOMMUNICATION ENGINEERING. All informations in this document have been obtained and presented in accordance with academic rules and ethical conduct. I also declare that as required by these rules and conduct I have fully cited and referenced all materials and results that are not original with this work.

Project Title

"DESIGN AND ANALYSIS OF PROBE-FED CYLINDRICAL DIELECTRIC RESONANTOR ANTENA"

ANUSRI PATRA

Exam Roll No.: M4ETC19003

Registration No.: 140706 of 2017-18

Electronics & Telecommunication Engineering Department,

Jadavpur University, Kolkata-700032, India.

DATE: May, 2019

PLACE: Jadavpur University, Kolkata

_____

(ANUSRI PATRA)

Acknowledgements

The success and final outcome of my thesis required a lot of guidance and assistance from many people and I am extremely fortunate to have got this all along the completion of my thesis work. Whatever I have done is only due to such guidance and assistance and I would not forget to thank them.

First and foremost, I owe my immense gratitude to my project supervisor **Prof. Manotosh Biswas** for his invaluable help and guidance during my dissertation work. I am highly indebted to him for constantly encouraging me by giving his critics on my work. I attribute my master degree to his encouragement and effort, and without him this thesis would not have been completed. No words will suffice in describing his contribution towards the completion of my thesis work.

I sincerely thank **Prof. Sheli Sinha Chaudhuri**, Head of the Department of Electronics & Telecommunication Engineering, Jadavpur University and all the authorities of the institute for providing nice academic environment and adequate infrastructure to carry out the present investigations.

I would like to acknowledge the assistance and co-operation from all my seniors of Microstrip Antenna Laboratory, **Mr. Amartya Banerjee**, **Mr. Suman Pradhan**, **Mrs. Rinki Ghosal** and my friend **Mr. Sayan Sarkar** during the course of experimental works. I really appreciate their precious efforts to keep laboratory environment up-to-date both in terms of equipments and measurement facilities. I would also like to express my heartfelt thankfulness to all my batch mates for helping me whenever I needed them.

Finally, I must express my very profound gratitude to **Anindya Das** and to my parents for providing me with unfailing support and continuous encouragement.

DATE: May, 2019 _____

PLACE: Jadavpur University, Kolkata (ANUSRI PATRA)

Abstract

In modern communication framework, everything is becoming wireless from wired connections. So, to build a smart, useful and cost effective communication in wireless technology, there are requirements of compact and methodical radiators. One of these smart radiators is a dielectric resonator antenna (DRA). DRAs have a very attractive and important feature which is radiated field will absorb almost all the radiated power, because of this it has become popular in the wireless communications field at microwave frequencies. DRAs are very popular in the crucial sectors of a country like defense, military, radar and especially for millimeter wave applications. Due to this flexibility in DRAs, they can be modelled in various shapes as per coverage requirements based on the applications in the wireless communication system.

The principal objective of this thesis is to investigate and design Cylindrical Dielectric Resonator Antenna and study all its parameters such as return loss, radiation patterns, gain, resonant frequency and input impedance. Here, the designed DRA is excited by using coaxial probe feed technique, having advantageous features like, ease of fabrication, low spurious radiation, low cost, etc. The performance characteristics of the proposed antenna are first simulated using Ansoft HFSS software and comparative studies of its various parameters are then discussed by changing the length and position of the probe, varying the dimensions of the antenna i.e. radius and height and by introducing an airgap between DRA and the ground plane. Finally, fabrication of a probe-fed cylindrical DRA is performed with the probe located at the edge of the antenna. It is then evaluated and compared with the simulated results.

Contents

List of Figures

List of Tables

CHAPTER 1

INTRODUCTION

1.1 Preface

One aspect of modern life is a growing dependency on wireless communication systems with a constant increase in demand for cheaper technology or more efficient technology together with more data transmission capability. Consequently this market place is expanding rapidly and will continue to do so for the foreseeable future. Existent wireless communication systems integrate multiple services with high speed transmission data. Nevertheless telecommunication companies must constantly wider the use of different frequency bands required to incorporate high speed transmission data processing. Enhancement in wireless communication systems technology requires novel and better elements able to support the different applications. One of the key elements is the antenna technology able to keep the systems on working accordingly with the oncoming new services and applications.

Over the past two decades, two classes of antennas, i.e. a microstrip patch antenna and a dielectric resonator antenna, have been investigated for modern wireless applications. For millimeter-wave applications, various solutions have been proposed for conventional low-gain antennas based on monopoles, dipoles, and connecting antennas. These antennas are small in size, light in weight and low in cost and can be easily integrated into the chip. However, until advanced design solutions are adopted, based on the integration of suitable dielectric superstrates or lens structures, these antennas tend to suffer from reduced radiation efficiency and narrow impedance bandwidth due to the influence of silicon substrate materials. Thus, dielectric resonator antennas (DRA) have appeared, since they are promising candidates for replacing traditional radiating elements at high frequencies, especially for applications on millimeter waves and beyond. This is mainly due to the fact that DRAs do not suffer from losses due to conduction and are characterized by high radiation efficiency with proper excitation.

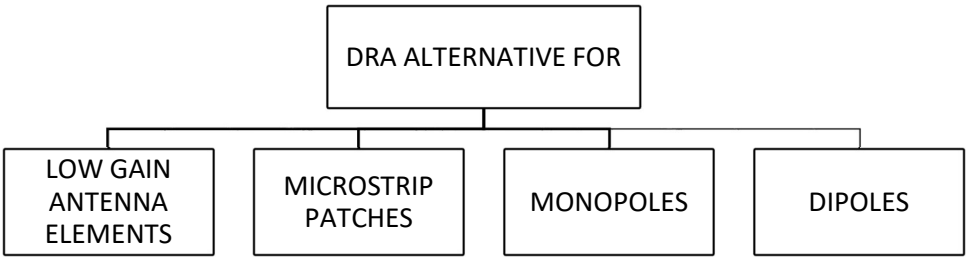

Fig. 1.1: DRA as an alternative for traditional low gain antenna elements

To date, there are more than 800 publications and more than two dozen issue patents,[1] entailing the dielectric resonator antenna (DRA) technology. In the past few years, the first two books on dielectric resonator antennas have also been released. These studies have shown that the antenna of the dielectric resonator is a versatile, efficient radiator, the design flexibility of which makes it an attractive alternative to traditional low-gain antennas (as shown in Fig. 1.1).

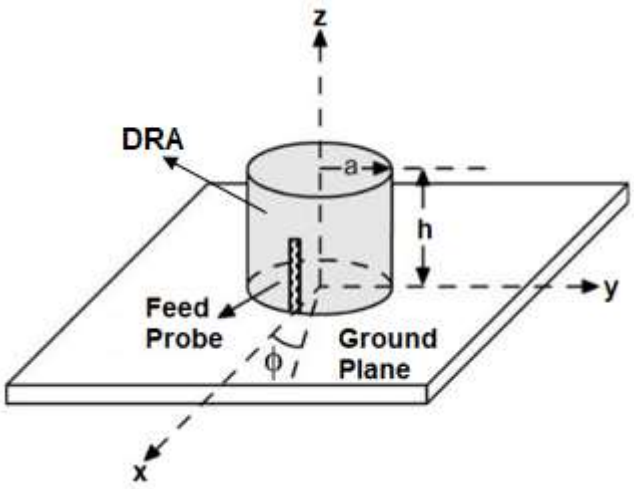

Fig. 1.2: Geometry of Dielectric resonator antenna

DRA is a resonant antenna, made of a dielectric ceramic material with a high dielectric constant (from about 6 to 100) and with high Q factor (between 20 and 2000), mounted on a grounded surface and excited by a coaxial probe, slot coupling or microstrip line in the ground plane. Currently, DRAs are made of plastic (polyvinyl chloride (PVC)). Radio waves are introduced into the inside of the resonator material from the transmitter circuit and bounce back

and forth between the resonator walls, forming standing waves. The walls of the resonator are partially transparent to radio waves, allowing the radio power to radiate into space.

The antenna was first suggested by Robert Richtmyer in 1939. In 1982, Long et al. completed the first design and testing of antennas with a dielectric resonator taking into account the model with leakage from the waveguide, assuming the model of the magnetic conductor of the dielectric surface.

Various DRA geometries are possible, such as rectangular, cylindrical, hemispherical, round, triangular, etc. The DRA resonant frequency is a function of the size, shape, and relative permittivity of the material.

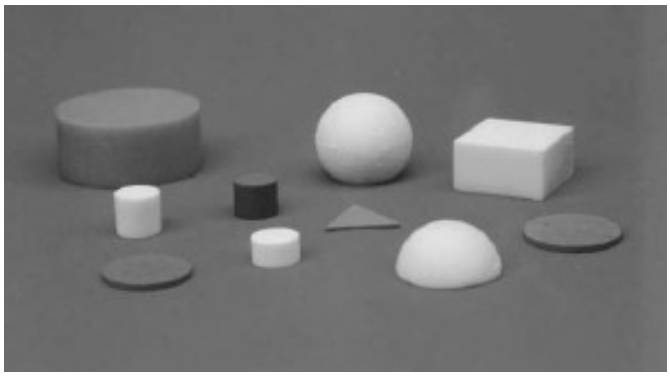

Fig 1.3: Different shapes of DRA

1.2 Dielectric Resonator Antenna Characteristics

DRA exhibits the following striking characteristics:

a) A wide range of dielectric constants (ε_r = 2.1 – 100) are used in DRAs that allows the designer to have control over the physical size of the DRA and its bandwidth.

b) The dimension of the DRA is of the order of $\frac{\lambda_o}{\sqrt{\varepsilon_r}}$ with $\lambda_0 = c/f_0$ being the free-space wavelength at the resonant frequency f_0 and where ε_r denotes the relative permittivity of the resonator material. As compared to traditional metallic antennas whose size is proportional to λ_0, DRAs are characterized by a smaller form factor especially when a material with high dielectric constant (ε_r) is selected for the design.

c) Due to the absence of conducting material, there is no inherent conductor loss and hence, this leads to high radiation efficiency. This characteristic makes them very suitable for applications at very high frequencies, such as in the range from 30GHz to 300GHz. whereas at these frequencies, traditional metal fabricated antennas suffer from high conductor losses.

d) DRAs can be excited using various feeding techniques which is useful in different applications and for array integration.

e) DRAs can have large impedance bandwidth if the dimensions of the resonator and the material dielectric constant are chosen properly.

f) DRAs offer simple coupling schemes to nearly all transmission lines used at microwave and mm-wave frequencies. This makes them suitable for integration into different planer technologies. The coupling between a DRA and the planer transmission line can easily be registered by changing the position of the DRA, so it can be easily optimized experimentally.

g) DRAs can be excited by various modes, many of which emit a radiation pattern, similar to a short electric or magnetic dipole, creating a broadband or omnidirectional radiation pattern for different coverage requirements.

1.3 Problems with Microstrip Patch Antenna (MPA)

a) It has inherently narrow impedance bandwidth associated with tolerance problem
b) Low radiation efficiency due to dielectric losses and conductor losses.
c) Low gain (nearly 6dB), polarization purity is difficult to achieve.
d) Spurious feed radiation exists (surface waves, strips, etc)
e) Higher level of cross polarization radiation.
f) Extraneous radiation from feeds and junctions.
g) Microstrip Patch Antennas have low dielectric strength, hence have lower power handling capability.

1.4 Advantages of DRA over Microstrip Patch Antenna

DRAs possess attractive features when compared to microstrip patch antennas. Main advantages of DRAs over Microstrip patch antennas are listed below:

a) Much wider Impedance Bandwidth Moreover the operating bandwidth of a DRA can be varied by suitably choosing the permittivity (εr) of the resonator material and its dimensions.
b) DRA has more radiation efficiency compared to microstrip patch antenna because DRA radiates through the whole antenna surface except the grounded part but microstrip patch antenna radiates only through two narrow radiation slots
c) Absence of surface wave and metallic losses.
d) DRAs have high dielectric strength which allows them to handle higher power in a much wider temperature rage.

1.5 Advantages and limitations of DRA

a) DRA possesses lightweight, low volume, and low profile configuration.
b) Depending on the resonator shape (rectangular, cylindrical, hemispherical, etc), various modes can be excited within the DRA. These modes can produce different radiation patterns for various coverage requirements. Also, the Q-factor of some of these modes will depend on the aspect ratio of the DRA, thus allowing one more degree of flexibility in the design.
c) DRAs have been intended to operate over a wide frequency range (1 – 44 GHz) compared to other antennas found in the literature.
d) Due to absence of inherent conductor loss, high radiation efficiency is possible in case of DR antennas.
e) DRAs have high dielectric strength and hence higher power handling capacity. Moreover temperature-stable ceramics allow the antenna to operate over a wide temperature range.
f) Low production cost

g) Many of the existing feeding mechanisms can be used (probes, slots, microstrip lines, dielectric image guides, coplanar waveguide lines, etc) to excite DRAs, making them easy to integrate with existing technologies.
h) Unlike Microstrip antennas, since DRA radiates through the whole antenna surface except the grounded part, it has a much wider impendence bandwidth.
i) Avoidance of surface waves

The problem with dielectric resonator antennas is typical for ceramic materials that are machined to shape from a large block. To excite the antenna with probes, it is necessary to drill the antenna, since it is bounded to the ground plane or substrate. The fabrication of DRA is more complicated and more expensive than printed circuit antennas, especially for array applications. DRA offers a solution for the applications where performance is more significant than cost.

In general, impedance bandwidth of DRA is usually less than 10%. Hence, for the past two decades, various methods have been adopted for improving the bandwidth of DRA. Since the DR element with a high dielectric constant is very sensitive to frequency, when DR is placed in the desired position, there is a high probability of changing the position in microns, which also significantly affects the antenna behaviour. Thus, an automated machine is usually required to place the dielectric resonator. Although there are many materials with different dielectric constants, it is difficult to obtain the required material in ideal shape for integration into the antenna. Another important disadvantage is the proximity of the resonant frequencies of different modes. Therefore, it is very important to know the resonant frequency and nature of the field pattern, not only for the desired mode of operation (usually) but also for other undesirable modes.

1.6 Dielectric Resonator Antenna Performance

The performance of an antenna is determined from the required specifications which are directly related to its application i.e. the frequency of operation, radiation pattern, gain and efficiency, beam-width (main lobe), minor lobes, radiation resistance and overall efficiency, input impedance, bandwidth and polarization (linearly, elliptically or circularly).[2]

The DRA performance involves high efficiency, wide bandwidth, no excitation of surface waves, high radiation efficiency, low dissipation loss, zero inherent conduction loss and a consistent radiation pattern, high power capability and a high speed rate.

1.6.1 Resonant Frequency

The resonance frequency is the frequency for which the dielectric resonator antenna delivers the best performance i.e. the S_{11} reaches the lowers value within the frequency band. The resonance frequency is recognized as one of the main considerations in dielectric resonator antenna design. The resonant frequency effectively determines the DRA characteristics. The resonant frequency indicates the operational modes in a DRA and is used to calculate and design the required DRA piece. The resonant frequency of a DRA is a function its size, shape and dielectric constant parameters. [3] For example, resonant frequency of cylindrical DRA is

$$f_{dom} = \frac{1}{2\pi a\sqrt{\mu\epsilon}}\sqrt{X_{11}'^2 + \left(\frac{\pi a}{2h}\right)^2} \quad \text{------ (1.1)}$$

where a is the radius, h is the height and ε is the dielectric constant.

1.6.2 Input Impedance

It is defined as the ratio of input voltage to input current. Mathematically,

$$Z_a = R_a + J(X_a + X_F) \quad \text{--------- (1.2)}$$

where, Z_a = Antenna impedance , R_a = radiation resistance, resistive part represents losses in the antenna, X_a = reactive part results from fields surrounding the antenna and X_F = probe reactance

1.6.3 Radiation Q factor

All the matter has the tendency to resonate at a certain frequency. The operation of some electronic devices base their performance on the principle of resonance i.e. resonators, filters, dielectric resonator and dielectric resonator antennas [4]. Energy storage and energy release is the basis of the resonance principle. Resonance is observed when an object is vibrating / oscillating, when receiving energy from an external source. The type of energy that makes an object oscillates being a function of the nature of the object, which has the tendency to free the energy being received. The relationship which describes how the energy is release from the object is called the quality factor and is represented as Q.

In a device specially designed to resonate or to oscillate is given certain value of Q factor. The Q factor describes how much external energy is stored in relation to how much of that energy is released. Devices with a high Q factor releases low levels of energy, while a lower Q factor releases more energy. As the Q factor is lowered the energy released increases.

$$Q = \frac{\sqrt{(VSWR-\ )}}{VSWR(BW)} \qquad \text{---------- (1.3)}$$

Equation 1.2 defines the Q factor in terms of the VSWRS (e.g. VSWR ≤ 2.00) and bandwidth (BW). In this relationship it is clear that as the BW increases the Q value decreases.

1.6.4 Bandwidth

The frequency range within which the performance characteristics of the antenna maintain certain level with respect to the specified performance characteristics, e.g., 90%, is referred to as antenna bandwidth. Thus antenna bandwidth is the range of frequencies where the antenna exhibits the optimum performance. The bandwidth is defined in terms of the limit frequencies i.e. the lower frequency and the higher frequency. The limit frequencies represent the boundaries of the BWs achieved for DRA design. The lower and higher frequencies are chosen in relation to the associated S_{11} (e.g. $|S_{11}| \leq$ -10 dB). The bandwidth can be defined in terms of the lower/higher frequencies and central frequency i.e. f_1, f_2 and f_c respectively; refer to Equation 1.4 and 1.5. [4]

$$BW = \frac{(f_2 - f_1)}{f_c} \qquad \text{--------- (1.4)}$$

$$f_c = \frac{f_2 + f_1}{2} \qquad \text{---------- (1.5)}$$

VSWR is chosen as the parameter for bandwidth considerations and this bandwidth is called the impedance bandwidth. The range of frequencies over which VSWR< 2 is chosen as the bandwidth of operation.

$$\text{Percentage Bandwidth} = \frac{1}{\sqrt{VSWR-1}.Q_T} = \frac{1}{\sqrt{2}.Q_T} \qquad \text{------- (1.6)}$$

The low frequency characteristic of a DRA design can be affected by the methods used in the assembly process, i.e. the use of adhesives, the environment, the measurement equipment and the fabrication process [5]. The adhesives have a dielectric constant that can influence the antenna in the electric field. If the adhesive layer has a different dielectric constant than the DRA, it can modify the operating frequency, up or down. Additionally the performance of the antenna could degrade by the influence of other radiations in the environment and the use of measuring equipment incorrectly calibrated [6]. It was proved that at the lower frequency degradation was due to a C-slot radiation [7].

1.6.5 Antenna Efficiency

The antenna efficiency, e, is the measure of an antenna's capability to convert the input power to the radiated power. A highly efficient antenna emits most of the power present at the input of the antenna. A low efficient antenna has most of the power absorbed as losses inside the antenna, or is reflected from an impedance mismatch. The antenna efficiency e_o is the result of many losses -- reflection mismatch, conduction or joule heating, dielectric losses etc.

Generally, the overall antenna radiation efficiency can be stated as

$$e_o = e_r . e_c . e_d \text{--------- (1.7)}$$

where, e_o = total efficiency

e_r = reflection efficiency

e_c = conduction efficiency

e_d = dielectric efficiency

1.6.6 Directivity

Antenna directivity is a parameter that measures the degree to which emitted radiation is concentrated in one direction. It measures the power density radiated by an antenna in the direction of its strongest emission, compared to the power density radiated by an ideal isotropic radiator (which radiates uniformly in all directions), radiating the same amount of power.

1.6.7 Gain

This is another useful measure describing the performance of the antenna. Although antenna gain is closely related to directivity, it is a measure of the antenna efficiency as well as its directivity.

$$\text{Gain} = \text{Antenna Efficiency } (\eta) \times \text{Directivity (D)} \text{ ------ (1.8)}$$

An antenna gain (in a given direction) is defined as "the ratio of the intensity in a given direction to the intensity of the radiation, which would have been obtained if the power received by the antenna were radiated isotropically" [8]. The radiation intensity corresponding to the isotropically radiated power is equal to the power received by the antenna divided by 4π. In equation form this can be expressed as

$$\text{Gain} = 4\pi \frac{Radiated\ Intensity}{Total\ input(accepted)power} \quad \text{------- (1.9)}$$

Generally, we deal with the relative gain, which is defined as the ratio of the power gain in a given direction with the gain of the reference antenna in a reference direction.

1.6.8 Radiation Pattern

The radiation pattern is a graphical representation of the geometric distribution of the radiated power over the entire space. It is typically expressed in the spherical coordinates as a function of space coordinates and is independent of distance. Radiation properties include power flux density, radiation intensity, field strength, directivity, phase or polarization. A radiation pattern usually consists of a mainbeam, one or a few near sidelobes adjacent to the main beam and many far sidelobes further away from the mainbeam.

The DRAs are in the classification of low gain antennas, as they are characterized to have a natural broad radiation pattern without any performance enhancement being introduced [9]. The radiation pattern is the area of influence of the energy radiating from the antenna. It has two components the electric field components (E) and the magnetic field components (H). The orientation of the E field is in elevation and the H field has azimuth orientation [10][11]. It had been reported that a DRA has omnidirectional characteristics in the E field and quasi-omnidirectional in the H field "with a half power beam width" [10].

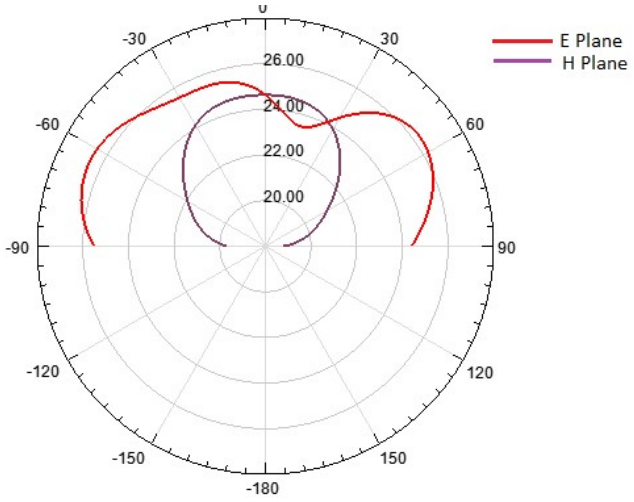

Fig. 1.4: Radiation Pattern

One factor that affects radiation pattern is the cross polarization. By reducing the cross polarization it is possible to get an improvement in the radiation pattern [12]. It was found that by using a strip as the feeding mechanism, the cross polarization level was reduced and the co-polarization radiation pattern was improved [13].

The radiation pattern can be changed using other shapes and exciting different resonant modes for that shape, in this way it is possible to obtain different "types of radiation pattern" as every mode creates a different kind of radiation pattern [14][15][16]. It was reported that a gap in the DRA design hardly affects the radiation patterns. The radiation patterns can be created by adding the effect of two different modes whilst they are excited in the DRA [15].

In a study about the effect of the ground plane in the radiation pattern by using an antenna design composed by a slot and a DRA, it was shown that the region of the radiation pattern corresponding to the slot, were more dramatically affected by changes in the ground plane size, than in the part of radiation pattern relating to the DRA [17]. It was reported that the radiation pattern was modified by making changes in the slot, modifying the slot position and the slot shape [18]. It was reported a reduction of the back radiation pattern of a DRA by placing below the ground plane of the antenna a "radial quarter-wavelength metallic annular disc [19]. It was reported that the radiation pattern depend of the excited mode and the cross polarization level which increases at higher frequencies [20].

By exciting the $TM_{01\delta}$ mode inside the DRA it is possible to obtain an omni-directional radiation pattern [19]. It was found that the omni-directional radiation pattern is appropriate for the application in the WLAN mobile communications field [21].

1.6.9 Half power beam width

The half power beamwidth (HPBW) or beamwidth, is the angle between the two directions of a two-dimensional radiation pattern at which the power gains are one-half of the peak gain. Its value depends on the shape of the reflector, the method of illumination, and other factors. With decreasing beam width, the sidelobe increases and vice versa. In addition, the antenna beamwidth is also used to describe the resolution of the antenna to distinguish between two adjacent radiating sources or radar targets. [8]

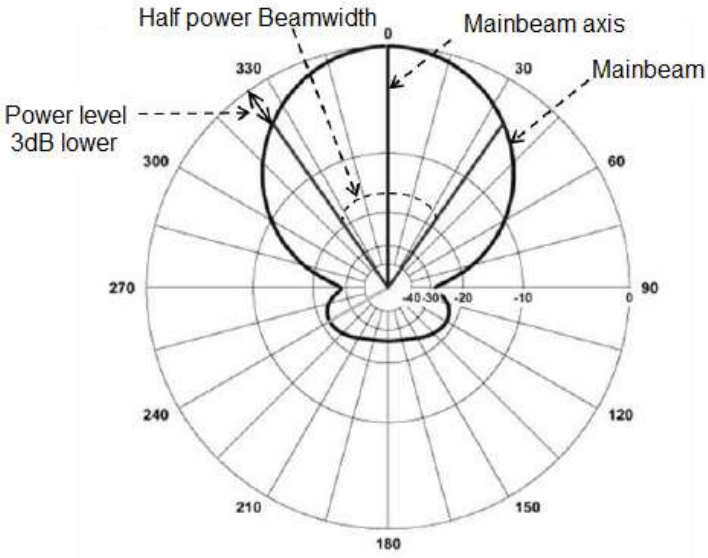

Fig.1.5: Antenna beam and HPBW

1.6.10 Polarization

The antenna polarization refers to the polarization of the far-field EM wave generated by the antenna, while the polarization of EM wave refers to its orientation of the electric-field. Polarization is important because the receiving antenna must have the same polarization as the transmitting antenna in order to maximize the received power. The EM wave can be linearly, circularly or elliptically polarized. For a linearly polarized EM wave, the direction of its electric field is constant with respect to the direction of the wave propagation. For an elliptically polarized EM wave, the direction of its electric field rotates with respect to the direction of the wave

propagation. Circular polarization is a special case of elliptical polarization where the major and minor axes of the rotation are the same. [22]

1.7 Thesis Motivation

The growing demand for wireless applications in the microwave range has motivated the research enthusiasts to study and research on high-performance antennas that exhibit high bandwidth, better radiation properties and low metal loss with small sizes. In this scenario, DRA is preferred over other traditional low gain antennas and microstrip antennas. DRA is a practical choice for the above applications due to many inherent features, such as small size, cost effectiveness and no metallic loss. In recent years, successive researches have resulted in DRAs which offers a much wider bandwidth to achieve wideband response which will achieve high data rates for aiding more information. The consolidation of the DRA into a wireless communication system; the operating bandwidth, volume and the size of the DRA need to be evaluated carefully. Looking into the advantages of using Cylindrical Dielectric Resonator Antenna and its advancements in various applications, the present study attempts to explore the design and fabrication of a Cylindrical Dielectric Resonator Antenna and analyze its different characteristics through theoretical and experimental studies.

1.8 Organization of the Thesis

This thesis is composed of 5 chapters –

Chapter 1: This chapter has summarized a short review of the importance of the Dielectric Resonator antennas and its performance. While the fundamental characteristics of the DRA are not fully researched, it is difficult to fully utilize their most important aspects to design efficient and high-performance antennas. Hence, this chapter also briefs the general characteristics of DRAs, problems with microstrip patch antennas and its advantages over it, advantages and limitations of DRAs and finally the basics of antenna parameters used in antenna measurements such as resonant frequency, Q factor, gain, directivity, radiation pattern, bandwidth, input impedance, antenna

efficiency etc. At the end, the motivation and the chapter wise arrangement of the thesis is comprised in summary.

Chapter 2: This chapter describes the historical background of dielectric resonator antenna and also the developments that have taken place over the years. It also dedicates the advancements in the field of cylindrical dielectric resonator antennas until today.

Chapter 3: This Chapter presents the theoretical details of the Cylindrical DRA including its radiating modes yielding typical resonant frequencies and radiation patterns. This chapter also depicts the basic theory behind the various feeding or excitation techniques for DRA. Their advantages and disadvantages are discussed in brief. Various bandwidth enhancement techniques are explained thereafter. Finally, it describes the various methods or analysis for analytical evaluation of DRAs and MATLAB simulated results of various parameters of cylindrical DRA.

Chapter 4: This chapter introduces Ansoft HFSS software and describes each step in the process of setting up a general simulation in Ansoft HFSS. A detailed description of the simulation of the DRA structure, which includes drawing the geometry, assigning materials, setting up the boundaries and setting up the solution, is presented in this chapter. Then, various simulations are performed to examine different parameters of cylindrical dielectric resonator antenna and their effect on input impedance, resonant frequency, gain and radiation patterns.

Chapter 5: This chapter presents a new antenna simulation introducing air-gap between the ground plane and DRA to increase DRA performance in bandwidth. Simulation results obtained using Ansoft HFSS, the simulation results (return loss, input impedance, resonant frequency, gain, radiation patterns, etc.) have been analysed.

Chapter 6: This chapter presents design and fabrication of a probe-fed cylindrical DRA and its characteristics like return loss, input impedance and radiation patterns are measured and then compared with the simulated results.

Chapter 7: This chapter concludes the work done in this thesis and provides a brief discussion on the future scope of the dielectric resonator antenna.

References

[1] A. Petosa, *Dielectric resonator antenna handbook*. Artech House Publishers., 2007.

[2] L. V. Blake, *Antennas*. John Wiley & Sons Inc., 1966.

[3] R. K. Gangwar, S. P. Singh, and D. Kumar, "A MODIFIED FRACTAL RECTANGULAR CURVE DIELECTRIC RESONATOR ANTENNA FOR WIMAX APPLICATION," *Prog. Electromagn. Res. C*, vol. 12, pp. 37–51, 2010.

[4] D. M. Pozar, *Microwave engineering*. Wiley, 2012.

[5] M. S. M. Aras, M. K. A. Rahim, A. Asrokin, and M. Z. A. Abdul Aziz, "Dielectric resonator antenna (DRA) for wireless application," in *2008 IEEE International RF and Microwave Conference*, 2008, pp. 454–458.

[6] Z.-B. Weng, X.-M. Wang, Y.-C. Jiao, and F.-S. Zhang, "CPW-fed dielectric resonator antenna for ultra-wideband applications," *Microw. Opt. Technol. Lett.*, vol. 52, no. 12, pp. 2709–2712, Dec. 2010.

[7] Hua-Ming Chen, Yang-Kai Wang, Yi-Fang Lin, Shih-Chieh Lin, and Shan-Cheng Pan, "A Compact Dual-Band Dielectric Resonator Antenna Using a Parasitic Slot," *IEEE Antennas Wirel. Propag. Lett.*, vol. 8, pp. 173–176, 2009.

[8] C. A. Balanis, *Antenna Theog Analysis and Design*. John Wiley & Sons, Inc., New York., 1982.

[9] M. F. Ain *et al.*, "A NOVEL 5.8 GHz HIGH GAIN ARRAY DIELECTRIC RESONATOR ANTENNA," *Prog. Electromagn. Res. C*, vol. 15, pp. 201–210, 2010.

[10] A. A. Abumazwed and A. Sebak, "Compact DRA for broadband wireless applications," in *2009 IEEE Antennas and Propagation Society International Symposium*, 2009, pp. 1–4.

[11] A. R. Abumazwed, A., Ahmed, O., & Sebak, "Broadband half-cylindrical DRA for future WLAN applications.," in *In 2009 3rd European Conference on Antennas and Propagation, IEEE.*, 2009, pp. 389–392.

[12] A. S. Al-Zoubi and A. A. Kishk, "Wide band strip-fed rectangular dielectric resonator antenna with improved radiation patterns," in *2009 IEEE Antennas and Propagation Society International Symposium*, 2009, pp. 1–4.

[13] M. M. Morsy, M. R. Khan, and F. J. Harackiewicz, "Ultra wideband hybrid dielectric resonator antenna (DRA) with parasitic ring," in *2010 IEEE International Conference on Wireless Information Technology and Systems*, 2010, pp. 1–4.

[14] Yih-Chien Chen, Shi-Li Yao, and Kuei-Chien Chen, "Dual band hybrid CPW fed planar monopole/dielectric resonator antenna," in *2009 IEEE 9th Malaysia International Conference on Communications (MICC)*, 2009, pp. 37–40.

[15] Tze-Hsuan Chang and Jean-Fu Kiang, "Bandwidth Broadening of Dielectric Resonator Antenna by Merging Adjacent Bands," *IEEE Trans. Antennas Propag.*, vol. 57, no. 10, pp. 3316–3320, Oct. 2009.

[16] T.-H. Chang and J.-F. Kiang, "Sectorial-Beam Dielectric Resonator Antenna for WiMAX With Bent Ground Plane," *IEEE Trans. Antennas Propag.*, vol. 57, no. 2, pp. 563–567, Feb. 2009.

[17] Y. Ding and K. W. Leung, "On the Dual-Band DRA-Slot Hybrid Antenna," *IEEE Trans. Antennas Propag.*, vol. 57, no. 3, pp. 624–630, Mar. 2009.

[18] C. Gopakumar and K. T. Mathew, "A Wideband Microstrip-Line-Fed Isosceles Trapezoidal Dielectric Resonator Antenna with Modified Ground Plane," *Prog. Electromagn. Res. C*, vol. 16, pp. 127–136, 2010.

[19] L. K. Hady, A. A. Kishk, and D. Kajfez, "Dual band dielectric resonator antenna for GPS and WLAN applications," in *2008 Asia-Pacific Microwave Conference*, 2008, pp. 1–4.

[20] M. N. Jazi and T. A. Denidni, "Ultra wideband dielectric resonator antenna with band rejection," in *2010 IEEE Antennas and Propagation Society International Symposium*, 2010, pp. 1–4.

[21] M. F. Ain *et al.*, "3.5 GHz rectangular dielectric resonator antenna," in *2008 IEEE International RF and Microwave Conference*, 2008, pp. 189–191.

[22] L. K. W. Luk, K. M., *Dielectric Resonator Antennas*. Research Studies Press Ltd., Hertfordshire, England, UK., 2003.

CHAPTER 2

LITERATURE REVIEW

2.1 Introduction

In this chapter some important works on the field of dielectric resonator antenna are discussed. Different aspects and applications of cylindrical dielectric resonator antenna and the advancements happening in it are referenced.

2.2 Historical Development of Dielectric Resonator Antenna

In middle era of 1900s, R.D. Richmyer disclosed that non metallized dielectric objects are able to perform like metallic cavities which is named as dielectric resonators (DRs). Until 1960s, no practical applications were found as the appropriate dielectric compounds were not much available. Formerly, the dielectric resonators were widely used in microwave circuits, such as filter and oscillators due to its high Q-factor, usually between 50 and 500, but can also be as high as 10,000. Extraordinary progress and efforts have been experienced in DR filter technology from the end of 1960's. In 1980, amplification of the radiation resistance using high permittivity of DRs of short electric probes and loops was first suggested by Sager and Tisi. Even though it was brought to light many years ago that open DRs radiate [2-4], DRs as an antenna were not popularly used until the native article about cylindrical dielectric resonator antenna (CDRA) [5] was published in 1983. After the discovery, it was noticed that the interest in frequency domain was gradually reaching to the millimeter and nearly millimeter bands (100-300 GHz) for many systems. At these frequency bands, the conductor loss of metallic antenna becomes notable, and the antenna efficiency is significantly minimized. On the other hand, the only loss for a DRA arises due to the imperfection in dielectric material, reasonably, which may be very small. After considering the cylindrical DRA [5], Long et al. eventually inspected rectangular [6] and hemispherical [7] DRA which paved the base for further research on DRA. From then, theoretical and experimental research have been attested by many researcher enthusiasts on DRAs of different shapes like triangular [8], spherical-

cap [9] and cylindrical-ring [10-11] etc. Their explorations revealed that DRA may be considered as promising substitutes to traditional low-gain antennas.

Since the invention of DRA till mid-1990s, huge amount of research work was emphasized on analyzing various excitation modes of simple-form dielectric resonators, studying various feed mechanisms and determining the input impedance, quality factor and directivity pattern analytically as well as numerically. Three research groups executed much of this work: one headed by Kishk, Glisson and Juncker, another by Luke and Lueng, and the remaining one by Mongia. Much of this early work on the characteristics of DRA with simple forms was summarized in a widely cited article published by Mongia and Bhartier in 1994 where it was suggested to standardize the nomenclature of modes used to describe DRA. They also presented some simple equations to predict the resonance frequency and quality factor for numerous modes of different DRA shapes.

In 1990s, emphasis was given in tuning linear and planar arrays of DRA. Simple two-element arrays to complex planar phased arrays of over 300 elements with electronic phase-steering capabilities were reported in a number of publications. Research was continued in the fields of compact designs, miniaturization techniques, low-profile designs, circular polarization and multiband-wideband designs and antennas with hybrid designs. Newer research fields comprises of enhanced gain techniques, tunable DRAs, finite-ground-plane effects, patterns which reconfigurable, designing in ultra-wideband, polarization agility and dual-function designs (used both as a resonator and as an antenna).

The use of magneto dielectrics, electromagnetic bandgap (EBG) structures and liquids is also being explored to increase DRA performance. A substantial amount of the recent publications includes designing DRA for specific applications, such as integration into mobile handsets for IMT- 2000 and WLAN applications; use in cellular base-station antennas; UWB applications ; radar applications; breast-cancer imaging; RFID; spatial power combining; direction finding; and all-dielectric wireless receivers.

Many techniques were suggested to increase the bandwidth of dielectric resonator antennas, such as stacking multiple DRs, using coplanar parasitic strips, annular DRAs, multiple resonance techniques. A novel wide band structure of antenna consists of a rectangular dielectric resonator

with coplanar waveguide, fed by inductive slot was also discovered. Various fedd mechanisms o DRAs were also investigated, such as coaxial feed, microstripline feed, aperture coupling, conformal-strip, dielectric image guide feed etc. Recently, a dual function DRA filter (DRAF) that combines the DRA and DRF were reported in 2008 and sot fed wideband dielectric resonator for wireless application has been proposed in 2010 that enables the DRA for practical use.

Lim and Leung were the firt ones to discover transparent glass type DRA of 3D and 2D type. [12] Borosilicate Crown Glass transparent hemispherical DRAs was proposed in the field of optics. In [13], the researchers proposed a dual function glass DRA with omnidirectional hollow rectangular glass as a light cover. Glass Swan Antenna, made of crystal and glasswares (K-9 glass), is a type of DRA was fabricated by K. W. Leung [14]. This kind of DRA is used wireless applications, sensor designs and medical applications.

Succeeding wireless communication systems require reconfigurablantenna systems for improving multifunctionality, signal quality, diversity gain and possible integration of various systems [15]. Recently, there exists some research articles mentioning frequency reconfigurable DRAs, using different frequency methods like controlling the dimension of parasitic strips and slots, altering the height of colloidal dispersion and varying the differential feed by varactors [16-21]. But, there exist very few mechanism of polarization or pattern reconfiguration of DRA.

2.3 Advancements of Cylindrical Dielectric Resonator Antenna

The DRA, introduced by Long, has many useful features, such as light weight, small size with high gain and adaptability in desired forms and feeding mechanism. Many existing wireless applications and others that have emerged require such qualities which are fulfilled by DRA characteristics. So DRA is well convenient for WLAN/Wi-MAX application systems. Among all the elementary shapes of DRA, cylindrical shape is well recognize one due to its constricted surface area, omnidirectional far-field pattern and easy availability in market.

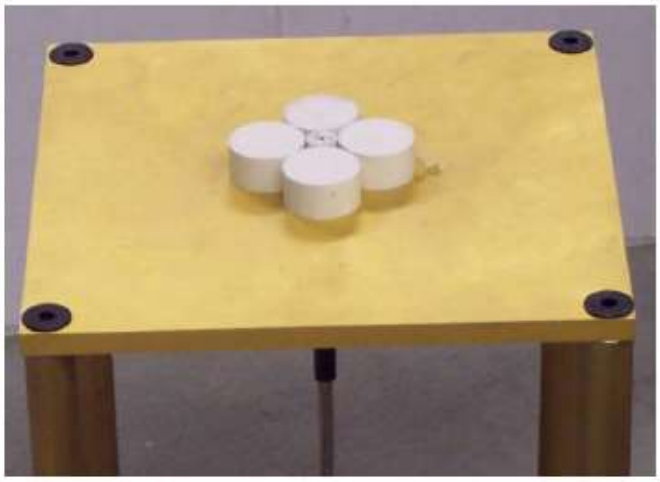

Fig. 2.1: A four-element Cylindrical DRA for wideband monopole like radiation

A 3D polar plot which gives the measure of relative field's strength emitted by antenna at different angles is called a radiation pattern. The radiation pattern can be improved when excited in TM_{11} mode, by decreasing the dimensions of the ground plane as well as back lobe level by fixing the antenna in topless cylindrical cavity [22]. Additionally, encapsulating the cylinder by a quarter-wavelength choke and by using circular conducting ring residing on top of dielectric material can facilitate improvements [23-24]. The impact of air gap between the perfect conductor ground plane and dielectric resonator antenna is very crucial. It can severely affect the input impedance and resonance frequency of antenna. To show severity, comparison of 2 cylindrical dielectric resonator antenna designs were made with same air gap of 0.05mm and hg value of 0.0 but different dielectric constants of 22 and 8.9, the frequency at which the input reactance passes through zero was shifted from 4.4 GHz for an $\varepsilon_r = 8.9$ antenna to 4.75 GHz for an $\varepsilon_r = 22$ [25].

The antenna bandwidth predicts the frequency range where antenna efficiency and performance does not retards as a result of impedance mismatch. Therefore it is very crucial to have a wide bandwidth, though resonant antenna exhibits pure resistive feed-point impedance at a particular frequency, numerous applications require antennas operating at broad frequency range. Studies show that cylindrical DRA operating in HEM mode gives very efficient suitable parameters like high bandwidth and better wideband performance. Hence it was very useful to numerally model the HEM modes. The numerical modelling of more enhanced flushed-mounted cylindrical dielectric resonator antenna was proposed using cylindrical conducting cavity. Moment method

can be used to couple the integral equations and complex resonant frequencies for numerical modelling of HEM modes with low resonance frequencies [26]. In [27], bandwidth enhancement of split cylindrical DRA is performed. “An antenna having radius = 2.25cm, height = 3.9cm, probe radius = 0.0118cm, zf = 15.8mm, r = 12, and with different wire lengths.” Variation the wire length changes the return loss and indicates that an optimized probe length of 18mm delivers a bandwidth of about 22%, operating in either HEM_{11} or HEM_{12} modes. Analyzing the results at different values of specific resonator and excitation probe parameters, the broadband performance has been optimized and increased to 35%.

Also, the coaxial probe fed cylindrical DRA gives more efficient results as bandwidth increases by 94% compared to conventional DRA with the use of metamaterial super substrate and also the use of this material enhances the peak gain of antenna by 103% experimentally [28]. Metamaterials are materials which when coupled with artificial structures are capable of generating electromagnetic properties that cannot be otherwise obtained naturally [29]. The symmetrical broadside radiation pattern can also be converted to directive radiation pattern using metamaterial in both H and E planes [28].

Directivity is also a fundamental antenna parameter. It is a measure of how 'directional' an antenna's radiation pattern is. The antenna radiating in all directions with same strength is proved to have a zero directionality having directivity equal to 1db or 0db. To enhance the directivity, single element circular slot aperture cylindrical DRA was coupled with a box shaped reflector. Results show that the directivity increases upto 53% i.e. from 5dbi to 7 .5dbi [30-33]. By replacing box reflector with a flat reflector, we can still enhance the directivity [34-35]. But parabolic reflectors are more efficient as it also enhances the gain by 240% in comparison with reflectorless single element CDRA [36-37].

With the advancement, multiport Cylindrical DRAs were developed. In [38-39], eight port cylindrical dielectric resonator antenna was investigated for MIMO (Multiple Input Multiple Output) applications. It was found to be more effective than the previously made four port structure. Overall height of antenna as well as ground plane was reduced by 37% and 44% simultaneously. It also delivers improved radiation performance along with 30% more bandwidth.

In [40-42], an annular column loaded wideband cylindrical DRA is named as LCDRA. It comprises of two components i.e. the inner small cylindrical dielectric and loaded concentric column dielectric. Coaxial probe is used to feed power into the antenna. It was excited with four modes, i.e. $TM_{01\delta}$, $TM_{02\delta}$, $TM_{03\delta}$ and $TM_{04\delta}$ modes, providing a bandwidth of 56% (3.14 GHz to 5.56 GHz). The experiment results were in good accordance with the simulated ones. Considering dimensions, gain and bandwidth, the LCDRA can offer outstanding performance for broadband applications.

The purpose of multiband antenna antenna is to operate on different frequencies which can be achieved by making some part to operate in one frequency band and rest part in another frequency band. In [46], the partially enclosed cylindrical DRA is designed for multi band antennas. The resonator is excited with the vertical monopole. More accurate impedance matching and improved -10db radiation bandwidth is achieved using this single pole design. This type of antenna operating in several bands can effectively be changed into a linear planar antenna array and circular polarization can also be achieved by exciting this antenna with two mono poles instead of one monopole.

Accessible different techniques available in to create multiband/dual-band characteristics in DRA: (i) originate the higher order modes along with fundamental mode in DRA [47]; (ii) combination of DRA and other resonating assemblies (hybrid radiator) [48-49]; (iii) combining dielectric resonator antenna with parasitic strip [50]. Fang et.al. suggested a dual-band circularly polarized cylindrical dielectric resonator antenna. 3-dB antenna radiation bandwidth of above mentioned cylindrical dielectric resonator antenna is around 12.4% and 7.4 % in lower and upper frequency band respectively. They achieved CP characteristics in CDRA with the help of complex feeding structure i.e. quadrature coupler which increase its fabrication complexity [51]. To mitigate the limitation of complex feeding network, Ngan et al. suggested chamfered dielectric resonator antenna. However, chamfered dielectric resonator antenna minimized the feed complexity but the proposed antenna had underwent a narrow 3-dB antenna radiation bandwidth (~ 5.2% and 1.4 % in lower and upper frequency band) [52].

In [53], a wideband DRA with high gain, working in hybrid $HEM_{11\delta}$ mode is developed. This antenna is a cylindrical DR that is partially surrounded with a transparent dielectric superstate and retreated by a single side metal coated dielectric reflector plane. The reflector is used for

intensifying the gain and the superstrate is devoted for integrating two resonance bands to acquire a single wideband. The DR is fed by microstripline feed aperture coupling method and works in X-band (7.12 - 8.29 GHz). Bandwidth of 15.18% with 11.34 dBi peak gain is achieved. The different design phases, like stand-alone DRA, DRA with superstratum, DRA with reflector and DRA with superstratum and reflector plane with respect to bandwidth and gain properties, are properly estimated.

In this connection, a substantially feasible antenna with a cylindrical dielectric resonator with a high gain and broadband characteristics was investigated in [54]. To excite a cylindrical resonator, a simple aperture-coupling method with a microstrip feed is used, which is located above a square aperture made in the center of the ground plane. The top portion of the DR remains open for radiation without interference. To reduce unnecessary back radiation, the underside of the substrate of the ground plane is covered with a one-sided copper-coated dielectric reflector ($1.35\lambda_0 \times 1.35\lambda_0 \times 0.04\lambda_0$) at a short distance of 4 mm air gap. This helps to increase the gain by 101.48% compared to the 17.14% impedance band. The influence of the reflector on the bandwidth, gain and pattern is analyzed. The measured peak gains are 10.84 and 10.45 dB at a resonant frequency of 7.3 and 8.08 GHz.

In [55], a compact DRA was proposed for use in ultra-wideband car communications. Two cylindrical DR are positioned asymmetrically relative to the center of the offset rectangular slot coupling through which they are excited. Optimization of design parameters leads to a bandwidth of 21%, (ranging from 5.9 to 7.32 GHz in the lower band) and 53% (ranging from 8.72 to 15 GHz in the upper band). The maximum gain achieved is 12 dBi.

In future, following the above discussed advancements in cylindrical DRA, novel techniques to improve antenna efficiency and performance can be expected come in the limelight.

References

[1] T. D. Iveland, "Dielectric resonator filters for application in microwave integrated circuits," *IEEE Trans. Microwave Theory Tech.*, vol. 19, no. 7, pp. 643-652, Jul. 1971.

[2] R. D. Richtmyer, "Dielectric Resonators," *J. Appl. Phys*., vol. 10, pp. 391-398, June 1939

[3] M. Gastine, L. Courtois and J. L. Dormann, "Electromagnetic resonances of free dielectric spheres," *IEEE Trans. Microwave Theory Tech*., vol. 15, pp. 694-700, Dec. 1967

[4] O. Sager and F. Tisi, "On eigenmodes and forced resonance-modes of dielectric spheres," *Proc. IEEE*, pp. 1593-1594, Sept. 1968

[5] Long, S. A., M. W. McAllister, and L. C. Shen, "The resonant cylindrical dielectric cavity antenna," *IEEE Transactions on Antennas and Propagation*, Vol. AP -31, 406–412, 1983.

[6] M. W. McAllister, S. A. Long and G. L. Conway, "Rectangular dielectric resonator antenna", *Electron. Lett*., vol. 19, pp. 218-219, Mar. 1983

[7] M. W. McAllister and S. A. Long, "Resonant hemispherical dielectric antenna", *Electron. Lett*., vol. 20, pp. 657-659, Aug. 1984

[8] A. Ittipiboon, R. K. Mongia, Y. M. M. Antar, P. Bhartia and M. Cuhaci, "Aperture-fed rectangular and triangular dielectric resonators for use as magnetic dipole antennas," *Electron. Lett*., vol. 29, pp. 2001-2002, Nov.1993

[9] K. W. Leung, K. M. Luk and E. K. N Yung, "Spherical cap dielectric resonator antenna using aperture coupling" *Electron. Lett*., vol. 30, No.17, pp. 1366-1367, Aug. 1994

[10] R. K. Mongia, A. Ittipiboon, P. Bhartia and M. Cuhaci, "Electric monopole antenna using a dielectric ring resonator," *Electron. Lett*., vol.29, pp. 1530-1531, Aug. 1993

[11] K. W. Leung, K. Y. Chow, K. M. Luk and E. K. N. Yung, "Excitation of dielectric resonator antenna using a soldered-through probe," *Electron. Lett*., vol. 33, pp. 349 - 350, Feb. 1997

[12] E. H. Lim and K. W. Leung, "Transparent dielectric resonator antennas for optical applications," *IEEE Trans. Antennas Propag.,* vol. 58, no. 4, pp. 1054-1059, Apr. 2010.

[13] Leung, K., X. Fang, Y. Pan , E. Lim, K. Luk, and H. Chan, "Dual-Function Radiating Glass for Antennas and Light Covers – Part II: Dual-Band Glass Dielectric Resonator Antennas," *IEEE Transactions on Antennas and Propagation,* Vol. 61, No. 2, pp. 587-597, August 2012.

[14] K. W. Leung, E. H. Lim and X. S. Fang, "Dielectric resonator antennas: From the basic to aesthetic," *Proceedings of the IEEE ,* vol. 100, no. 7, pp. 2181-2193, Jul, 2012.

[15] L. H. Trinh, F. Ferrero, L. Lizzi, R. Staraj, and J.-M. Ribero, "Reconfigurable antenna for future spectrum reallocations in 5G communications," *IEEE Antennas Wireless Propag. Lett*., vol. 15, pp. 1297_1300, 2016.

[16] G. H. Huff, D. L. Rolando, P. Walters, and J. McDonald, "A frequency reconfigurable dielectric resonator antenna using colloidal dispersions," *IEEE Antennas Wireless Propag. Lett*., vol. 9, pp. 288_290, 2010.

[17] C. X. Hao, B. Li, K. W. Leung, and X. Q. Sheng, "Frequency-tunable differentially fed rectangular dielectric resonator antennas," *IEEE Antennas Wireless Propag. Lett.*, vol. 10, pp. 884_887, 2011.

[18] J. Desjardins, D. A. McNamara, S. Thirakoune, and A. Petosa, "Electronically frequency-reconfigurable rectangular dielectric resonator antennas," *IEEE Trans. Antennas Propag*., vol. 60, no. 6, pp. 2997_3002, Jun. 2012.

[19] J.-B. Yan and J. T. Bernhard, "Implementation of a frequency-agile MIMO dielectric resonator antenna," *IEEE Trans. Antennas Propag*., vol. 61, no. 7, pp. 3434_3441, Jul. 2013.

[20] T. Apperley and M. Okoniewski, "An air-gap-based frequency switching method for the dielectric resonator antenna," *IEEE Antennas Wireless Propag. Lett*., vol. 13, pp. 455_458, 2014.

[21] S. Danesh, S. K. A. Rahim, M. Abedian, and M. R. Hamid, "A compact frequency-reconfigurable dielectric resonator antenna for LTE/WWAN and WLAN applications," *IEEE Antennas Wireless Propag. Lett.*, vol. 14, pp. 486_489, 2015.

[22] Kishk, A.A., Auda, H.A.; Ahn, B.C. "Accurat e prediction of radiation patterns of dielectric resonator antennas", *Electronics Letters* (Volume: 23, Issue: 25)

[23] Kishk, A.A., Auda, H.A.; Ahn, B.C. "Radiation characteristics of cylindrical dielectric resonator antennas", Southeastcon '88, IEEE Conference Proceedings, pages: 556 – 560

[24] Kishk, A.A., Elsherbeni, A.Z. "Cylindrical dielectric cavity antenna loaded by a beam forming ring", *Antennas and Propagation Society International Symposium*, June 1988. AP-S. Digest, 820 - 823 vol.2.

[25] G.P. Junker, A.A. Kishk, A.W. Glisson and D. Kajfez "Effect of air gap on cylindrical dielectric resonator antenna operating in TM or mode", *ELECTRONICS LETTERS* 20th January 1994 Vol. 30 No. 2

[26] Glisson, A.W., "Analysis of a dielectric resonator antenna in a cylindrical conducting cavity: HEM modes", *Microwaves, Antennas and Propagation, IEE Proceedings* (Volume: 141, Issue: 1), Feb 1994

[27] A. A. Kishk, A. W. Glisson and G. P. Junker, "BANDWIDTH ENHANCEMENT FOR SPLIT CYLINDRICAL DIELECTRIC RESONATOR ANTENNAS," *Progress In Electromagnetics Research*, PIER 33, 97–118, 2001

[28] Bhagirath Sahu- Pankaj tripathi- S.P.Singh, "Investigation on Cylindrical Dielectric Resonator Antenna with Metamaterial Superstrate", *Springer Science+Business Media New York,* May 2015.

[29] Yuandan Dong, Itoh, T., "Metamaterial-Based Antennas," *Proceedings of the IEEE* (Volume: 100, Issue: 7) 2012, Page(s): (2271 – 2285).

[30] Ali, S.M.,Zakariya, M.A. ; Baharudin, Z. ; Md Khir, M.H. ; Baba, A.A. ; Adz, J.J. "Aperture coupled Cylindrical Dielectric Resonator Antenna design with box shaped reflector" *Wireless Technology and Applications (ISWTA), 2013 IEEE Symposium* on Sept. 2013. Page(s):167 – 171
.
[31] A. Petosa, Dielectric Resonator Antenna Handbook. Norwood, MA: Artech House, 2007.

[32] A. Petosa, et al., "Recent advances in dielectric-resonator antenna technology," *Antennas and Propagation Magazine, IEEE*, vol. 40, pp. 35-48, 1998.

[33] Y. M. M. Antar and Z. Fan, "Theoretical investigation of aperture coupled rectangular dielectric resonator antenna," *Microwaves, Antennas and Propagation, IEE Proceedings*-, vol. 143, pp. 113-118, 1996. (Pubitemid 126763889)

[34] Ali, S.M.,Zakariya, M.A. ; Baharudin, Z. ; Adz, J.J. "Aperture coupled Dielectric Resonator Antenna design with flat reflector" *Business Engineering and Industrial Applications Colloquium (BEIAC), 2013 IEEE*, Page(s):135 – 139.

[35] Nasimuddin and Esselle, KP, "Antennas with dielectric resonators and surface mounted short horns for high gain and large bandwidth," *Microwave, Antennas & Propagation, IET*, vol. 1, no. 3, pp.723-728 June 2007.
[36] Ali, S.M.,Zakariya, M.A.; Baharudin, Z ; Adz, J.J. "Parabolic reflector fed by Cylindrical Dielectric Resonator Antenna with high gain", *Intelligent and Advanced Systems (ICIAS), 2014 5th International Conference* on, June 2014, Page(s):1 – 6.

[37] S. A. Malekabadi, et al., "Circular polarized cylindrical dielectric resonator antenna using a single probe feed," in *Microwave and Millimeter Wave Technology, 2008. ICMMT 2008. International Conference* on, pp. 1098-1101, 2008.

[38] Johnstone, J.C.,Podilchak, S.K. ; CLENET, M. ; Antar, Y.M.M. "A compact cylindrical dielectric resonator antenna for MIMO applications" *Antennas and Propagation Society International Symposium (APSURSI), 2014 IEEE*, July 2014, Page(s):1938 – 1939.

[39] G. Massie, M. Caillet, M. Cl¿¿net, and Y. M. M. Antar, "A new wideband circularly polarized hybrid dielectric resonator antenna," *Antennas and Wireless Propagation Letters, IEEE*, vol. 9, pp. 347-350, 2010.

[40] Yan He, Yi Lin, Changjiang Deng, Zhenghe Feng, " Annular Column Loaded Cylindrical Dielectric Resonator Antenna for Wideband Conical Radiation", DOI 10.1109/TAP.2015.2480096, *IEEE Transactions on Antennas and Propagation.*

[41] A. A. Kishk, X. Zhang, A.W. Glisson, and D. Kajfez, "Numerical analysis of stacked dielectric resonator antennas excited by a coaxial probe for wide-band applications," *IEEE Trans. Antennas Propag*., vol. 51, no. 8 pp. 1996–2006, Aug. 2003.

[42] Huang and A. A. Kish. "Compact wideband multi-layer cylindrical dielectric resonator antennas." *Microwave, Antennas Propag., IET*, vol. 1, pp.998 -1005, 2007.

[43] K. M. Luk and K. W. Leung, "Dielectric Resonator Antennas," Eds. Baldock, U.K.: Research Studies Press, 2003.

[44] E. H. Lim and K. W. Leung, "Transparent dielectric resonator antenna for optical applications," *IEEE Trans. Antennas Propag.*, vol. 58, no. 4, pp. 1054-1059, Apr. 2010.

[45] Yuxiang Sun, Xiaosheng Fang, and Kwok Wa Leung, "Wideband Two-Layer Transparent Cylindrical Dielectric Resonator Antenna Used as a Light Cover" 978-1-4799-6281-5/15/$31.00 ©2015 *IEEE*

[46] Konstantinos Pliakostathis, Dariush Mirshekar-Syahkal, "Partially Enclosed Cylindrical Dielectric Resonator (DR) for Multiband Antennas", 978-1-4799-7815-1/15/$31.00 ©2015 IEEE.

[47] Guha, D., P. Gupta and C. Kumar, "Dual Band Cylindrical Dielectric Resonator Antenna employing HE11δ and HE12δ mode excited by new composite structure," *IEEE Transaction on Antennas and Propagation*, Vol. 63, No.1, 433-438, Jan. 2015.

[48] Din, Y. and K.W. Leung, "On the Dual-Band DRA-Slot Hybrid Antenna," *IEEE Transaction on Antennas and Propagation*, Vol. 57, No.3, 624-630, Mar. 2009.

[49] Li, Y.F., H.M. Chen and C.H. Lin, "Compact Dual-Band Hybrid Dielectric Resonator Antenna With Radiating Slot," *IEEE Antenna and Wireless Propagation Letters*, Vol. 8, 6–9, 2009.

[50] Chen, H.M., Y.K. Wang, Y.F. Lin, S.C. Lin and S.C. Pan, "A Compact Dual-Band Dielectric Resonator Antenna Using a Parasitic Slot," *IEEE Antenna and Wireless Propagation Letters*, Vol.8, 173–176, 2009.

[51] Fang, X.S. and K.W. Leung, "Linear-/Circular-Polarization Designs of Dual-/Wide-Band Cylindrical Dielectric Resonator Antennas," *IEEE Transaction on Antennas and Propagation*, Vol. 60, No.6, 2662-2671, Jun. 2012.

[52] Ngan, H.S., X.S. Fang, and K.W. Leung, "Design of dual-band circularly polarized dielectric resonator antenna using a high-order mode," *in Proc. IEEE-APS APWC*, 424–427, 2012.

[53] S. K. K. Dash, T. Khan, B. K. Kanaujia, and N. Nasimuddin. "Wideband Cylindrical Dielectric Resonator Antenna Operating in HEM11δ Mode with Improved Gain: A Study of Superstrate and Reflector Plane," *International Journal of Antennas and Propagation*, vol. 2017, Article ID 2414619, 11 pages, 2017.

[54] S. K. K. Dash, T. Khan, B. K. Kanaujia, Yahia M.M. Antar, "Gain improvement of cylindrical dielectric resonator antenna using flat reflector plane: a new approach", *Microwave, Antennas Propag., IET*, vol. 11 Iss. 11, pp.1622 -1628, 2017

[55] C.-E. Zebiri, M. Lashab, D. Sayad, I. T. E. Elfergani, K. H. Sayidmarie, F. Benabdelaziz, R. A. Abd-Alhameed, J. Rodriguez, and J. M. Noras, "Offset Aperture-Coupled Double-Cylinder Dielectric Resonator Antenna with Extended Wideband," *IEEE Transaction on Antennas and Propagation*, Vol. 65, No.10, Oct. 2017.

CHAPTER 3

CYLINDRICAL DIELECTRIC RESONATOR ANTENNA BACKGROUND

3.1 Introduction

DRA can be assessed with respect to its form and modes of excitation. The electromagnetic near fields inside the resonating body are the main bases of understanding the far-field radiation patterns, thus helping in realizing the general antenna characteristics. Despite the fact that many shapes are available for the DRA, the best among them is that it is either easily accessible or easily cut, polished and molded. Due to this, a cylindrical shape was selected and studied in this dissertation. Cylindrical DRA has advantages over hemispherical and rectangular DRA. It offers diverse design possibilities, where the radius to height ratio dictates the resonance frequency and quality factor. Here, fabrication is much simpler, and several modes can be excited, resulting in broadside or omnidirectional radiation patterns.

Various DRA subclasses in cylindrical form are electric monopole, sectored cylindrical DRA, disk-loaded cylindrical DRA, split-cylindrical DRA, cylindrical-ring DRA and ring DRAs, conical DRAs, elliptical DRA. Ring DRA provides improved impedance bandwidth. Cylindrical

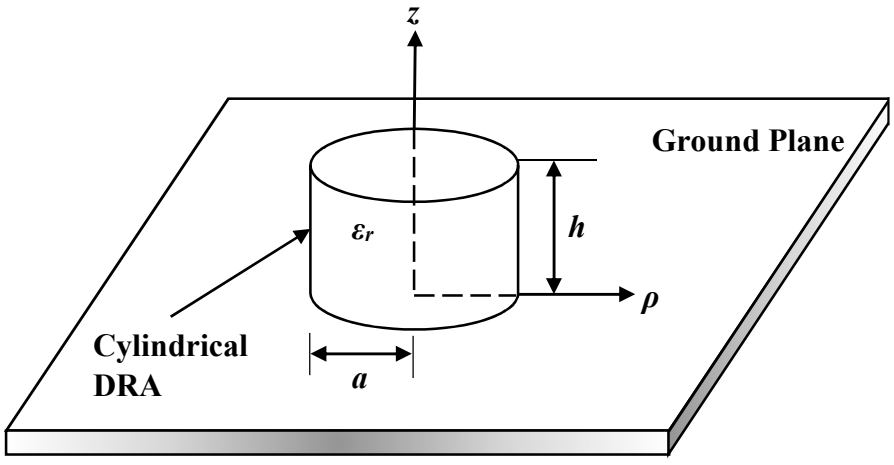

Fig. 3.1: The geometry of the cylindrical DRA

DRs are used in circuit applications, filters, and oscillators and mainly in microstrip technology, where resonant waveguide cavities are not very practical. Figure 3.1 illustrates the geometry of the cylindrical dielectric resonator antenna.

It comprises of a dielectric material of height 'h', radius 'a' and dielectric constant 'ε_r'. This shape provides one more degree of freedom more than hemispherical shape because it has aspect ratio a/h, which determines k_0a and the Q-factor for a given dielectric constant [1].

3.2 Resonant Modes

Whatever may be the profile of the DRA that is cylindrical, rectangular and hemispherical, ultimately it is evaluated with respect to its resonant modes, near-field distribution inside the resonator, far-field radiation into the space, resonant frequency and impedance bandwidth. The resonant modes are generally classified into two categories such as *Transverse Electric (TE) and Transverse Magnetic(TM).* Both TE & TM must refer to a coordinate axis. For instance if TE is considered, it represents that the electric field component vanishes in the direction of propagation while it becomes Transverse (perpendicular) to it [2]-[3]. For cylindrical DRA, it is suggested to make a mode analysis on the basis of cavity resonant model in which outer surfaces of the cavity are approximated by perfect magnetic walls so that eigen function expansion for the fields can be utilized.

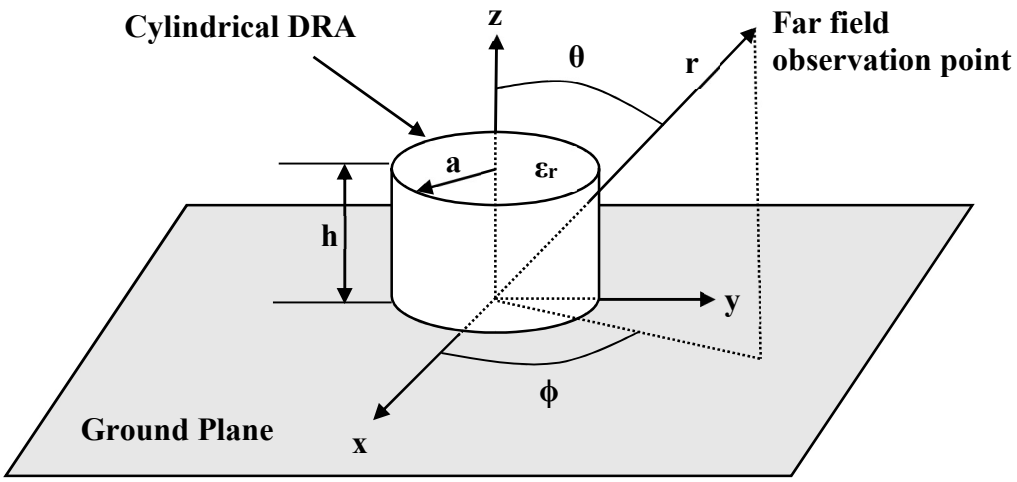

Fig. 3.2: Cylindrical DRA positioned on the ground plane

An isolated cylindrical DRA with radius "a" and height "h" on a large ground plane supports three distinct modes that is TE (to z), TM (to z) and hybrid. TE ($E_z = 0$) and TM ($H_z = 0$) are axially symmetric and have no φ variation while hybrid modes do have. At higher frequencies, pure transverse electric or pure transverse magnetic fields behaviour does not exist distinctively. So they are termed as hybrid electromagnetic fields and are represented by HEM, the lowest of them is HEM_{11} [3] .These fields are φ dependent and can be categorised into further two groups HE (if E_z component is dominant) and EH (if H_z component is dominant). However, for practical purposes only TE, TM and HEM_{11} are mostly considered. To identify the field variations along azimuth (φ), radial (r) and axial (z) usually three indices that is npm are used such as TE_{npm} or TM_{npm}. The 1st index represents the no. of full period field variations in azimuthal direction, the 2nd index indicates the no. of radial variations while 3rd index specifies that the dielectric resonator is shorter than half wave length which is rarely used and hence for most of the cases it is omitted. The field description then depends upon just first two indexes n & p. When 1st index is zero, the electromagnetic field is circularly symmetric and seems in the form of concentric circles when viewed form the cross section side.

3.2.1 Theoretical Formulation - Resonant Frequencies

The geometry of the DRA is shown in Fig. 3.3 using standard cylindrical coordinates. The feed probe is temporarily ignored, i.e., the cylinder is considered uniform. Image theory can be immediately applied and the ground plane can be replaced by an imaged portion of the cylinder extending to z = *-d;* the isolated cylinder is now analyzed with an implied boundary condition of zero $\boldsymbol{E_\rho}$ and $\boldsymbol{E_\phi}$ at z = 0.

An approximate solution for the fields inside such a cylinder can be obtained by assuming that the surfaces are perfect magnetic conductors. For such a cavity, wave functions transverse electric (TE) and transverse magnetic (TM) to z may be postulated as:

$$\varphi_{TM_{npm}} = J_n\left(\frac{X_{np}}{a}\rho\right)\begin{pmatrix}\sin(n\emptyset)\\ \cos(n\emptyset)\end{pmatrix} sin\left[\frac{(2m+1)\pi z}{2h}\right] \quad \text{------ (3.1)}$$

$$\varphi_{TM_{npm}} = J_n\left(\frac{X'_{np}}{a}\rho\right)\begin{pmatrix}\sin(n\emptyset)\\ \cos(n\emptyset)\end{pmatrix} cos\left[\frac{(2m+1)\pi z}{2h}\right] \quad \text{------ (3.2)}$$

Where J_n is the Bessel function of the first kind,

$J_n(X_{np}) = 0, J_n'(X_{np}') = 0,$

n = 1, 2, 3, ---, p = 1, 2, 3, ---, m = 0, 1, 2, -----

The separation equation $k_\rho' + k_z^2 = k^2 = \omega^2\mu\epsilon$ leads to an expression for the resonant frequency of the npm mode.

$$f_{npm} = \frac{1}{2\pi a\sqrt{\mu\epsilon}}\sqrt{\left\{\frac{X_{np}'}{X_{np}'^2}\right\} + \left[\frac{\pi a}{2h}(2m+1)\right]^2} \quad \text{--------- (3.3)}$$

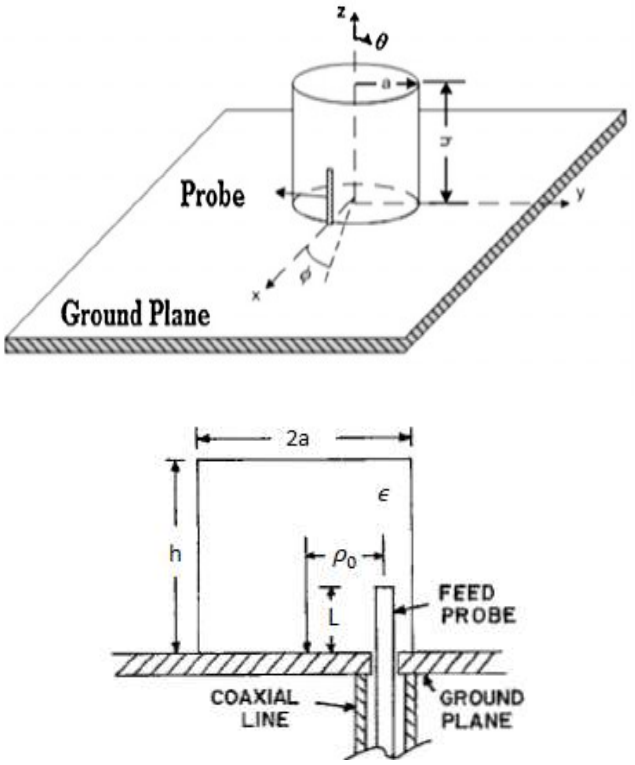

Fig. 3.3: Antenna Geometry and feed configuration

The dominant mode is the one which has the lowest resonant frequency.

This occurs for m = 0, n = 1, p =1: $X_{11}' = 1.841$.

$$f_{dom} = \frac{1}{2\pi a\sqrt{\mu\epsilon}}\sqrt{X_{11}'^2 + \left(\frac{\pi a}{2h}\right)^2}$$

Practically Important Modes:

From application point of view, some typical modes are categorized as;

In open space dielectric resonator acts as a radiator either radiating broadside radiation patterns employing $TE_{01\delta}$ mode or HEM_{11} mode while monopole like radiation patterns (endfire) using TM_{01} mode. As per need of a typical radiation pattern, any of the modes can be excited using a suitable feeding mechanism.

$TE_{01\delta}$ mode:

Usually this mode is excited in split-cylindrical shape for which the design formula is given in equations (3.4) and (3.5)

$$fr_{TE01}(GHz) = \frac{30(k_0 a)}{2\pi a(cm)} \quad \text{--------- (3.4)}$$

$$k_0 a = \frac{2.327}{\sqrt{\varepsilon_{r+1}}}\left\{1 + 0.212\frac{a}{h} - 0.008\left(\frac{a}{h}\right)^2\right\} \quad \text{---------- (3.5)}$$

TM_{110} (HEM_{11}) mode:

Its simplified design formula is given by the equation (3.6) as:

$$fr_{TM110} = \frac{c}{2\pi a\sqrt{\varepsilon_r}}\sqrt{(1.841)^2 + \left(\frac{\pi a}{2h}\right)^2} \quad \text{---------- (3.6)}$$

TM_{01} mode:

Its simplified design formula is given by equations (3.7) & (3.8) such as:

$$fr_{TM01}(GHz) = \frac{30(k_0 a)}{2\pi a(cm)} \quad \text{---------- (3.7)}$$

$$k_0 a = \frac{\sqrt{(3.83)^2 + \left(\frac{\pi a}{2h}\right)^2}}{\sqrt{\varepsilon_r + 2}} \quad \text{---------- (3.8)}$$

The resonant frequency associated to each mode is briefed in the example of Table 3.1

Table 3.1: Different modes and frequencies for ε_r = 10, if a = 13 mm and h = 26 mm

NO.	MODES	FREQUENCY
1	TE_{01}	2.84 GHz
2	TM_{110} (HEM_{11})	2.32 GHz
3	TM_{01}	4.14 GHz

3.2.2 Equivalent Magnetic Surface Currents for the Dominant Mode

The wave function of the dominant mode is:

$$\psi_{TM_{110}} = \psi = J_1\left(\frac{X'_{11}\rho}{a}\right)\cos\phi\cos\frac{z\pi}{2h}$$

The $\cos\phi$ term, rather than $\sin\phi$, survives due to the feed position at $\phi = 0$. In anticipation of calculating the far-field patters, tangential electric fields on the surface are determined using:

$$E_\phi = \frac{1}{j\omega\epsilon\rho}\frac{\partial^2\psi}{\partial\phi\partial z}\,, E_z = \frac{1}{j\omega\epsilon}\left(\frac{\partial^2}{\partial z^2} + K^2\right)\psi\,, E_\rho = \frac{1}{j\omega\epsilon}\frac{\partial^2\psi}{\partial\rho\partial z}$$

Applying $\vec{M} = \vec{E}\times\hat{n}$, where $\hat{n}$ is a unit normal pointing out of the dielectric, the following equivalent currents are found (primed coordinates are used to indicate the source).

Sides:

$$M_{z'} = \frac{\pi}{2j\omega\epsilon ad}J_1(X'_{11})\sin\phi'\sin\frac{\pi z'}{2h}$$

And

$$M_{\phi'} = \frac{1}{j\omega\epsilon}\left(\frac{X'_{11}}{a}\right)^2 J_1(X'_{11})\cos\phi'^{\cos\frac{\pi z'}{2h}}$$

Top-bottom:

$$M_{\phi'} = \frac{\pi X'_{11}}{j2\omega\epsilon ah}J'_1\left(\frac{X'_{11}\rho'}{a}\right)\cos\phi'$$

And

$$M_{\rho'} = \frac{\pi}{j2\omega\epsilon h\rho'}J_1\left(\frac{X'_{11}\rho'}{a}\right)\sin\phi'$$

3.2.3 Calculation of Far-Field Patterns

The above currents are considered the sources for the far-field radiation. Since the radiation fields will be expressed in spherical coordinates (r, θ, ϕ), the source currents are transformed:

$$M_\theta = M_{\rho'} \cos\theta \cos(\phi - \phi') + M_{\phi'} \cos\theta \sin(\phi - \phi') - M_{z'} \sin\theta$$

$$M_\phi = -M_{\rho'} \sin(\phi - \phi') + M_{\phi'} \cos(\phi - \phi')$$

Electric vector potentials are then calculated:

$$F_\theta = \frac{e^{-jk_0 r}}{4\pi r} \iiint M_\theta e^{jk_0[\rho' \sin\theta \cos(\phi - \phi') + z' \cos\theta]} \rho' d\rho' d\phi' dz$$

$$F_\phi = \frac{e^{-jk_0 r}}{4\pi r} \iiint M_\phi e^{jk_0[\rho' \sin\theta \cos(\phi - \phi') + z' \cos\theta]} \rho' d\rho' d\phi' dz$$

Where $k_0 = \omega\sqrt{\mu_0 \epsilon_0}$ (the free space wavenumber).

Summing the individual contributions to M_θ and M_ϕ, and integrating results in

$$F_\theta = C_1\{I_2 - I_1 - 0.5k_p(I_3 + I_4 - I_5 - I_6) + 1.16k_0 \sin\theta J_1(k_0 a \sin\theta) D_1 - 0.581k_\rho^2 a \cdot J_0(k_0 a \sin\theta) + J_2(k_0 a \sin\theta) D_1\}$$

$$F_\phi = C_2\{-I_1 - I_2 - 0.5k_p(I_3 - I_4 - I_5 + I_6) - 0.581k_\rho^2 a[J_0(k_0 a \sin\theta) - J_2(k_0 a \sin\theta)] D_1\}$$

Where,

$$C_1 = \frac{\pi^2}{j\omega\epsilon h} \frac{1}{4\pi r} \sin\phi \cos(k_0 d \cos\theta) \cos\theta$$

$$C_1 = \frac{\pi^2}{j\omega\epsilon h} \frac{1}{4\pi r} \cos\phi \cos(k_0 d \cos\theta)$$

$$D_1 = \left[\frac{\pi^2}{4h^2} - k_0^2 cos^2\theta\right]^{-1}$$

$$k_\rho = \frac{X'_{11}}{a} = \frac{1.841}{a}$$

$$I_1 = \int_0^a J_1(k_\rho \rho') J_0(k_0 \rho' \sin\theta) d\rho'$$

$$I_2 = \int_0^a J_1(k_\rho \rho') J_2(k_0 \rho' \sin\theta) d\rho'$$

$$I_3 = \int_0^a J_0(k_\rho \rho') J_0(k_0 \rho' \sin\theta) \rho' d\rho'$$

$$I_4 = \int_0^a J_0(k_\rho \rho') 2(k_0 \rho' \sin\theta) \rho' d\rho'$$

$$I_5 = \int_0^a J_2(k_\rho \rho') J_0(k_0 \rho' \sin\theta) \rho' d\rho'$$

$$I_6 = \int_0^a J_1(k_\rho \rho') J_2(k_0 \rho' \sin\theta) \rho' d\rho'$$

For the permittivities and aspect ratios under consideration (a/h ≤ 2, $\epsilon_r \geq 5$), the term $k_0 a$ will always be less than two; this allows polynomial approximations for the above Bessel functions to be used, and the integrals are easily evaluated numerically.

In the far-field region, the electric fields are proportional to the vector potential $\vec{F}$: $E_\theta \alpha F_\phi$, and $E_\phi \alpha F_\theta$. The radiation patterns are thus found as a function of the antenna parameters.

3.3 Typical Mode Excitation:

Depending upon the resonant frequency and the required type of radiation pattern such as broadside or end-fire a particular mode is excited. To accomplish it effectively, proper excitation methods are chosen which are mainly driven by:

- Type of the excitation feed.
- Position of the excitation feed.

Take for instance the case of a coaxial probe excite the TM_{110} (HEM_{11}) mode. It is to be placed close to the peripheral boundary of the cylindrical DRA whether embedded inside or poled equidistant outside it to yield corresponding broadside radiation pattern. Now, if the same probe is shifted gradually towards the centre of the DRA, the TM_{110} mode diminishes while $TM_{01\delta}$ emerges to dominate so instead of exhibiting broadside, it presents the end-fire type radiation pattern. On the other hand, if aperture slot is to be employed, it is to be placed at the centre, for generating a broadside radiation pattern while to seek end-fire pattern it is supposed to be shifted to the DRA boundary.

It is important to note that a crucially important factor is the aspect ratio (a/h). It describes that a taller DRA with smaller diameter can yield the same resonance frequency as that of very short in height but very large in diameter however, both structures possess different Q values. According to different permittivity values, there is a limit of (a/h) and beyond it further control of

shape may not be possible. The aspect ratio(a/h) also plays a significant role in determining as if to merge two closely resonating modes to generate *wider -10dB bandwidth or not*.

To make the concept clearer, we consider the near field distributions inside the cylindrical DRAs and their corresponding far field radiation patterns in terms of TE_{01}, TM_{01} and TM_{110} (HEM_{11}) resonant modes [5-7].

Mode TE_{01}:

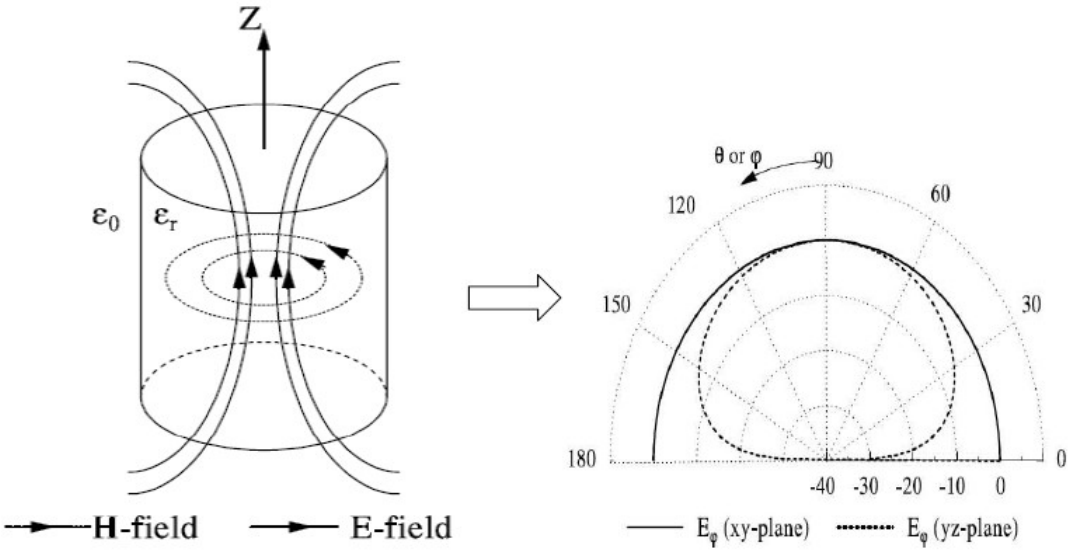

Fig. 3.4: Mode TE_{01} and its broadside far field radiation pattern. [9]

Mode TM_{01}:

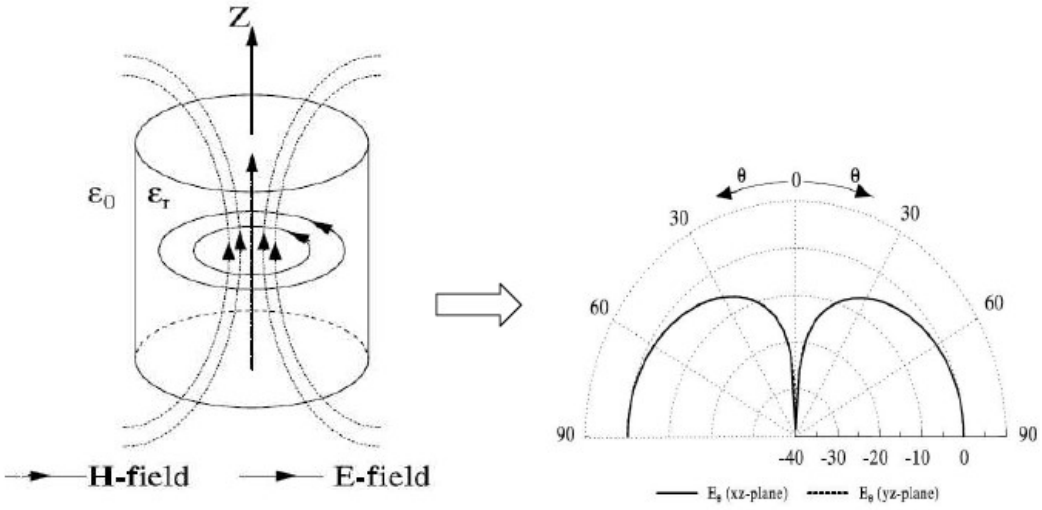

Fig. 3.5: Mode TM_{01} and its monopole like far field radiation pattern. [9]

Mode TM_{110} (HEM_{11}):

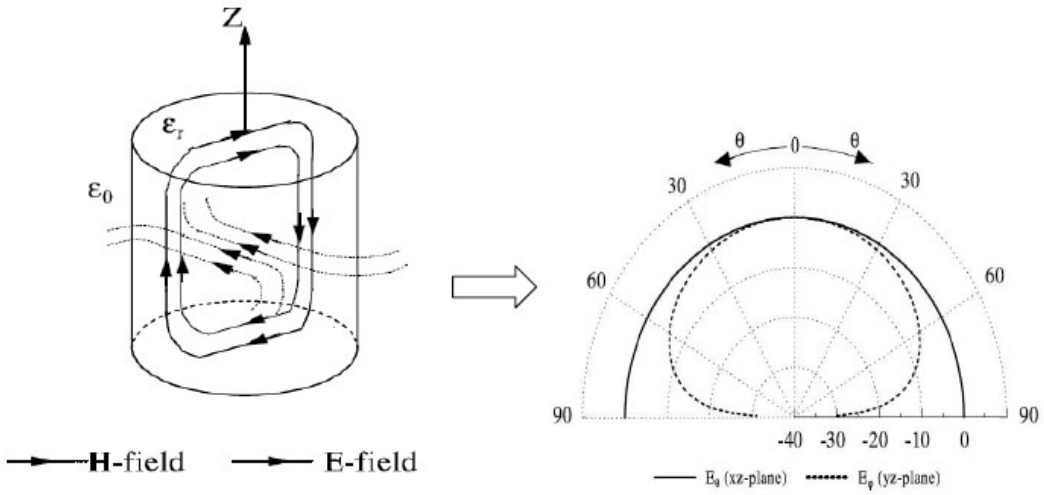

Fig. 3.6: Mode TM_{110} (HEM_{11}) and its broadside far field radiation pattern. [9]

In practice, the excitation source may resonate several modes simultaneously [8]. The field strength for a typical mode depends upon the exactness of the feed location and its operating frequency.

These far field radiation patterns have clear resemblance to other renowned antenna types. The TE_{01} seems like radiation pattern of half wavelength narrow slot on the ground plane and directed to the axis of resonator. The radiation pattern from TM_{01} seems like a quarter wavelength monopole above the ground plane [8]. The HEM_{11} resembles to that of half wavelength narrow slot on the ground plane.

A graphical representation of patterns has been given in Fig3.7 that explains how a gradual transformation in pattern shape takes place at par with the changing locations by an aperture slot under the DRA.

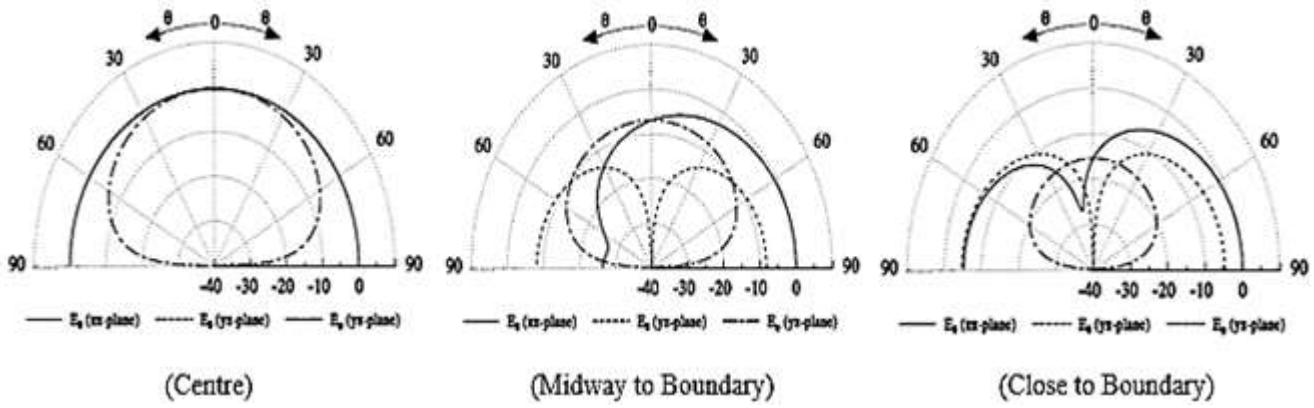

Fig. 3.7: Changing radiation patterns corresponding to different slot positions under DRA.

[9]

It is interesting to observe that when slot is exactly located at the centre the pattern generated is perfectly symmetric with no cross polarization. However, when slot shifts from centre to boundary, the cross polarization grows and ultimately transforms to totally different pattern.

3.4 Feeding Methods

The feeding mechanisms considerably affect the resonance frequency and quality factor of a DRA. Many feeding techniques have been developed. To excite the DRA, input impedance is one of the significant parameters in designing a feed. The feed and location selection both show a significant part in determining which feeding mode. This in turn will determine the input impedance and radiation characteristics of the DRA. The different feeding mechanisms include aperture coupling with a microstrip feedline, coaxial probe, aperture coupling with a coaxial feedline, waveguide coupled aperture, direct microstrip feedline, coplanar feed, soldered through probe, slot line, conformal strip and direct image guide.

3.4.1 Coaxial Probe Feed

Coaxial probe feed is a popular method used to feed a dielectric resonator antenna. The probe may be placed near the DRA or may be inserted in the housing. Optimization of the probe length and position, one can adjust the input impedance of the DRA, therefore, the resonant frequency. The probe can be considered as a vertical electrical current, which is placed to achieve a strong coupling with the DRA, resulting in high radiation efficiency. The level of coupling is optimized by

adjusting the height and diameter of the probe. Depending upon the shape of DRA and probe location, different modes can be excited that is when it is fed axially only TM modes are excited. To be more precise that if TM_{01} mode is to be excited, the feed probe is expected to be located at the centre thus yielding quarter wavelength monopole like far field radiation patterns. On the other side when HEM_{11} (TM_{110}) mode is required, the feed probe is supposed to be located close to the peripheral boundary so as to yield broadside radiation patterns. The benefit of this technique is that the antenna system can be directly connected to a 50Ω circuit without the need for a matching network. Fabrication is easy and it has low spurious radiation. Probes are useful at lower frequencies to cope with the fabrication issues where aperture feeding may not be practical due to the large size of the slot required [9]. However it is equally efficient and result oriented at higher frequencies. For instance compared to slot feed's approximate position in the peripheral area of the cylindrical dielectric resonator antenna, it is simple to locate the probe at its centre when to excite TM_{01} mode. But, the main drawback is that it offers a narrow bandwidth and is hard to simulate, since it is necessary to drill a hole in the substrate and the connector extends beyond the ground plane, which does not make it entirely flat for thick substrates ($h > 0.02\ \lambda_o$). The drilled holes must correspond to the probe dimensions (length and radius), otherwise the effective dielectric permittivity of the resonator will be hampered, which will lead to a shift in the antenna's resonant frequency. In addition, it should be noted that drilling a hole in the dielectric resonator during fabrication is actually complicated and expensive. In addition, for thicker substrates, the increased probe length makes the input impedance more inductive, which leads to matching problems.

A less complicated fabrication is performed by placing the excitation probe at the edge of the dielectric resonator. This technique is cost-effective but results in a smaller coupling to the DR, which eventually affects the antenna radiation characteristics.

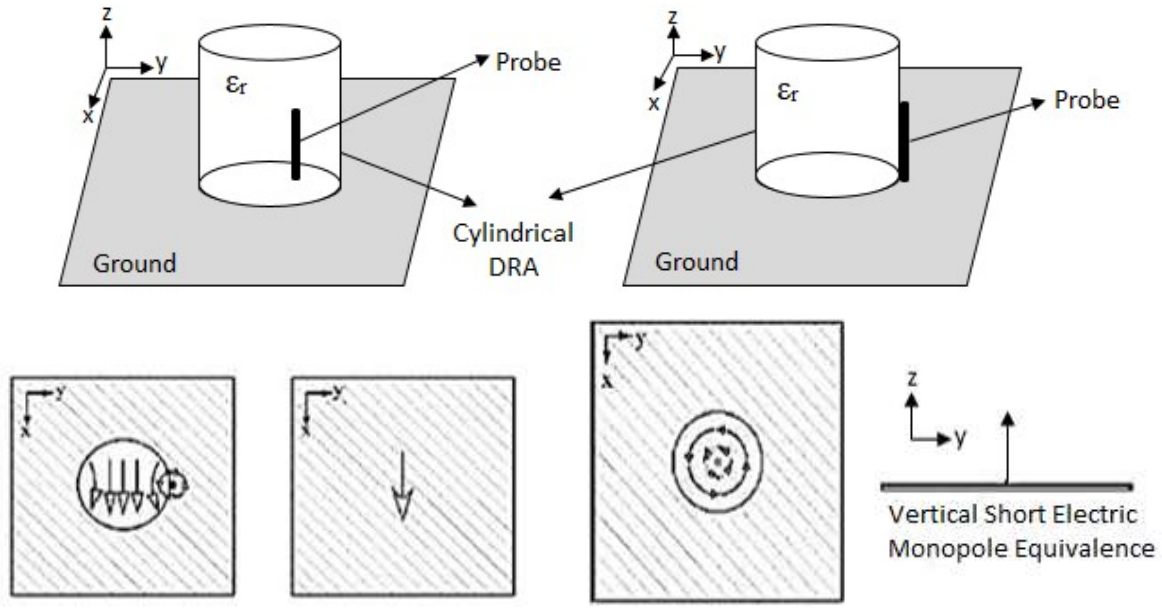

Fig. 3.8: To excite DRA Electric and Magnetic current distributions in monopole. [1]

3.4.2 Slot Aperture

In a slot aperture method, a DRA is excited through a small hole in the ground plane upon which it is placed. The aperture can be of any shape, such as narrow slot, loop, cross, or *C* shape cut in the ground plane, and can be excited by a microstrip line or coaxial feedline beneath the ground plane; some of the shapes are shown in Figure 3.9.

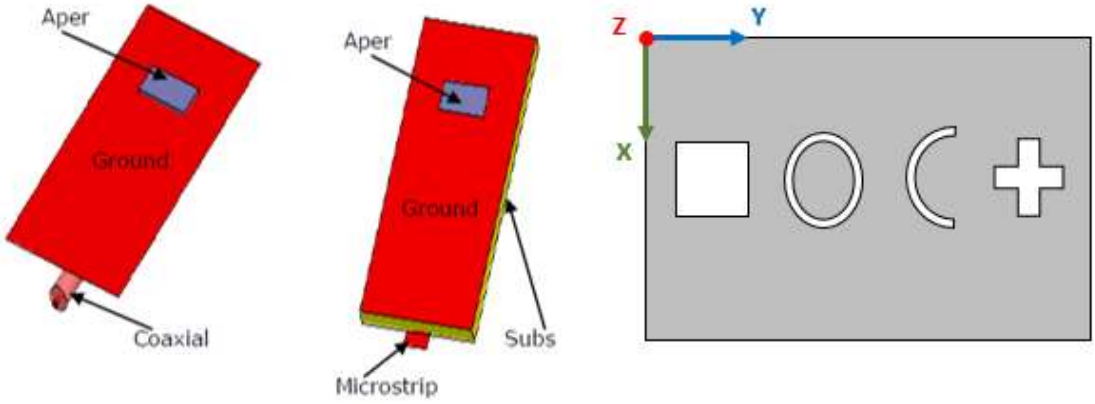

Fig. 3.9: Aperture feeding in various shapes

For HEM_{11} or TM_{110} being the dominant resonant mode, the aperture at the DRA centre behaves like magnetic current flowing parallel to its length and as a result excites the magnetic fields in the DRA body causing broadside radiation pattern in the far field. It is depicted in Figure 3.10. The slot is fed by microstrip line because it is easy to etch on the substrate and to seek impedance matching. The benefit of this method is that it has the feed positioned below the ground plane, separating the radiating aperture from any unwanted coupling or spurious radiation from the feed that cause distortion and degrade the pattern shape, thus enhancing the polarization purity of the DRA.

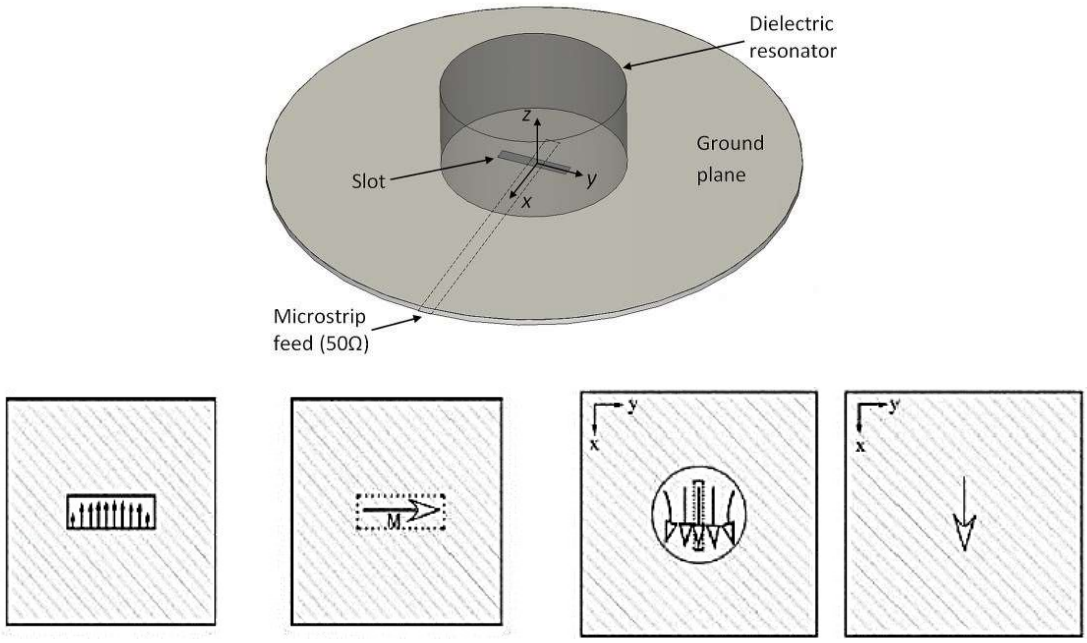

Fig. 3.10: Electric and Magnetic field distributions in slots. [9]

Moreover, this technique is applicable for integrating DRAs with printed feed structures. The coupling level can be optimized by moving the antenna with respect to the slot. Typically, a high dielectric material is used for the substrate, while a thick dielectric constant is used for the upper portion of the dielectric resonator to optimize the radiation from the antenna. The main disadvantage of this feeding method lies in the difficulty in manufacturing because of several layers, which also increases the thickness of the antenna. This method also offers narrow bandwidth (up to 21%). [9] Another disadvantage is that the slot length should be around $\lambda / 2$, which is difficult to implement at lower frequencies while maintaining the size of the DRA compact. This

technique is particularly recommended for high frequency designs requiring highest level of precision and etching accuracy.

3.4.3 Microstrip Line Feed

PDirect and Proximity couplings to microstrip lines are amongst the simplest methods. Here, a microstrip line printed on the same substrate feeds a Dielectric Resonator which can be placed directly above the microstrip line or near the dielectric substrate. Figure 3.11 shows some of the probe shapes that have been used for feeding. The microstrip coupling excites magnetic fields in the DRA to create a short horizontal magnetic dipole level. The level of coupling can be improved by lateral arrangement of the DRA relative to the microstrip line and an increase in the relative dielectric constant of the DRA. [9]. It is a common conclusion that for low value of dielectric

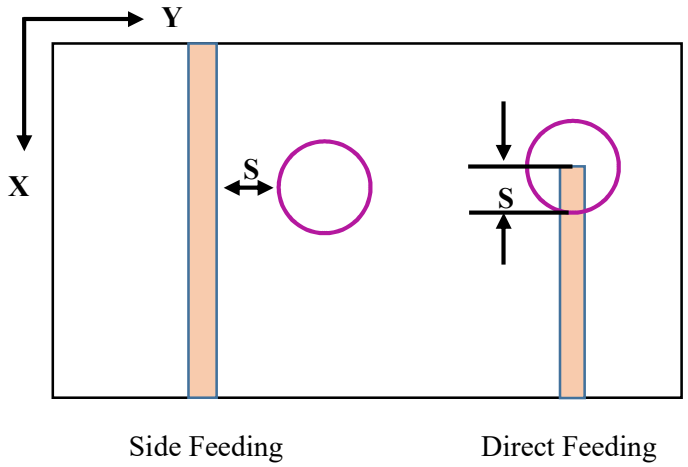

Fig. 3.11 Microstrip line feeding of various shapes

constant, minimum energy is coupled. However, with increase in its value other limitations are encountered particularly at higher frequencies further reduction in size can cause fabrication process too sensitive and that may introduce faulty results. Similarly the consequence reduction in impedance bandwidth can limit its wideband applications.

For lower permittivity values (necessary for DRAs requiring wide bandwidth), the coupling is usually very small. Thus, in order to have an acceptable radiation efficiency, an array of DRAs is required. Microstrip lines can be used as a series feed for a linear DRA array, provided that and ease of modeling along with impedance matching. However, as the thickness of the used dielectric

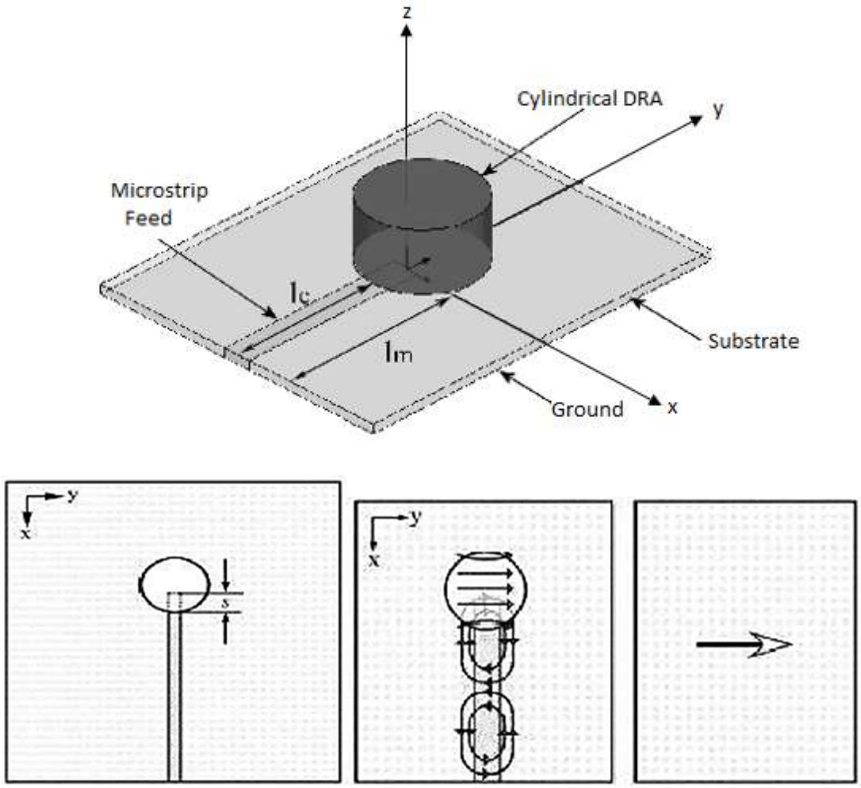

Fig. 3.12: Electric and Magnetic field distributions in proximity coupling. [9]

substrate increases, surface waves and spurious feed radiation also increase, which inhibits antenna bandwidth. [1]. One of the disadvantages of this method is that the polarization of the array is determined by the orientation of the microstrip line, for example, the direction of the magnetic fields in the DRA will be parallel to the microstrip line. [9], [10]. Another disadvantage enough elements are used. This is a simple feed technique because it offers ease of manufacture of this method is that the feeding line is not separated from the DR, which can affect the the DRA radiation performance. Additionally, when placing the dielectric resonator directly above the transmission line, an unwanted air gap is formed between the resonator and the substrate. The behaviour of the coupling fields can be observed from the Fig.: 3.12.

3.4.4 Dielectric Image Guide

Dielectric image guide is one of the popular feeding technique in DRAs, shown in Fig 3.13. Dielectric image guide offers several advantages compared to microstrip at millimeter-wave frequency, as they do not suffer seriously from conductor losses. The dielectric image guide

couples the energy to the DRA that is located in its proximity. Since in case of microstrip lines, the amount of coupling to DRA is normally very small, especially in DRAs having lower permittivity values, even it can be possible to enhance the amount of coupling by operating the guide nearer to cut-off frequencies. Hence the dielectric image guide is the best utilized series feed to any linear array present in a DRA. [10]

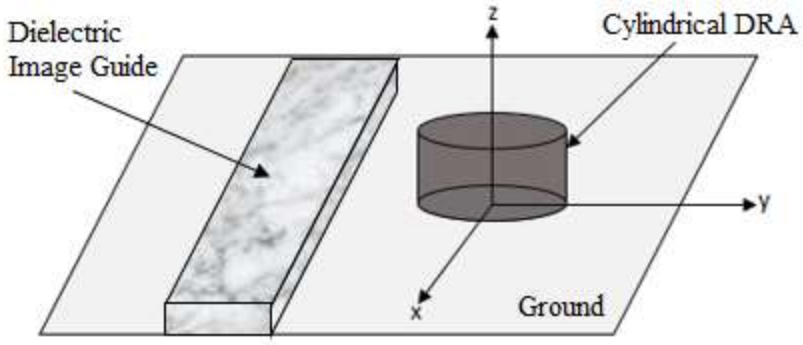

Fig. 3.13: Dielectric Image Guide Fed DRA

3.4.5 Coplanar Waveguide Feed

The coplanar waveguide feed was first cited in [11], where a cylindrical DRA is excited by a coplanar waveguide (CPW) circular-loop network. Fig. 3.14 shows some of the coplanar shapes that have been used for feeding. The feed lines of the DRs using the coplanar waveguide seem very promising because it enables easy feeding.

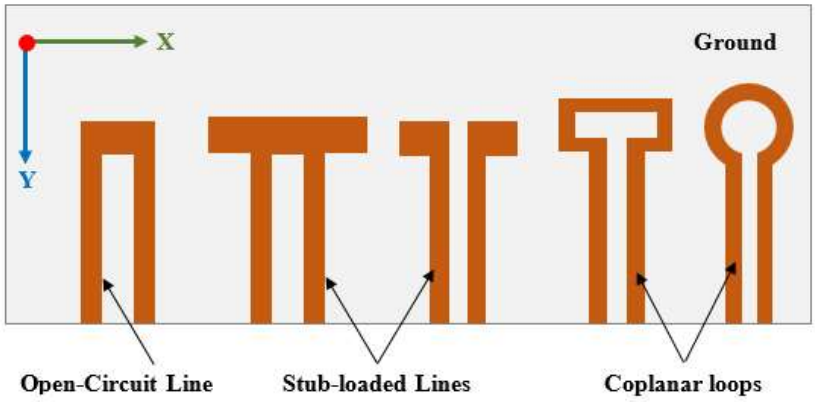

Fig. 3.14: Coplanar feeding of various shapes

The prime benefit of the CPW excitation is the position of the coupling slot which is below the DR can be altered to optimize the DRA performance. The coplanar loop efficiently couples energy to the DRA. The coupling level and desired mode excitation can be obtained by gradually sliding the DR element over the loop [11-14]. Impedance tuning can be done by adding stubs, slots, or loops at the end of the coplanar line. By shifting the loop from the edge to the centre one can yield required resonance frequency and radiation patterns, i.e. one can couple into either the $HE_{11\delta}$ mode or the TE_{011} mode of the cylindrical DRA [1], [9]. One such arrangement with field distribution is shown in fig. 3.15. The circular loop network can be substituted by a capacitive slot as well as by an inductive slot. It has been seen that capacitive slot provides an additional resonance which results in a dual-band behavior, with two resonances associated with the DR and the feeding slot itself, respectively. CPW feeding structures are widely used for millimeter-wave applications especially where the DRA is integrated in a system on chip (SoC). As a matter of fact, by using CPW transmission lines, it is possible to achieve high antenna efficiency since the ground plane separates the dielectric resonator from the lossy silicon substrate.

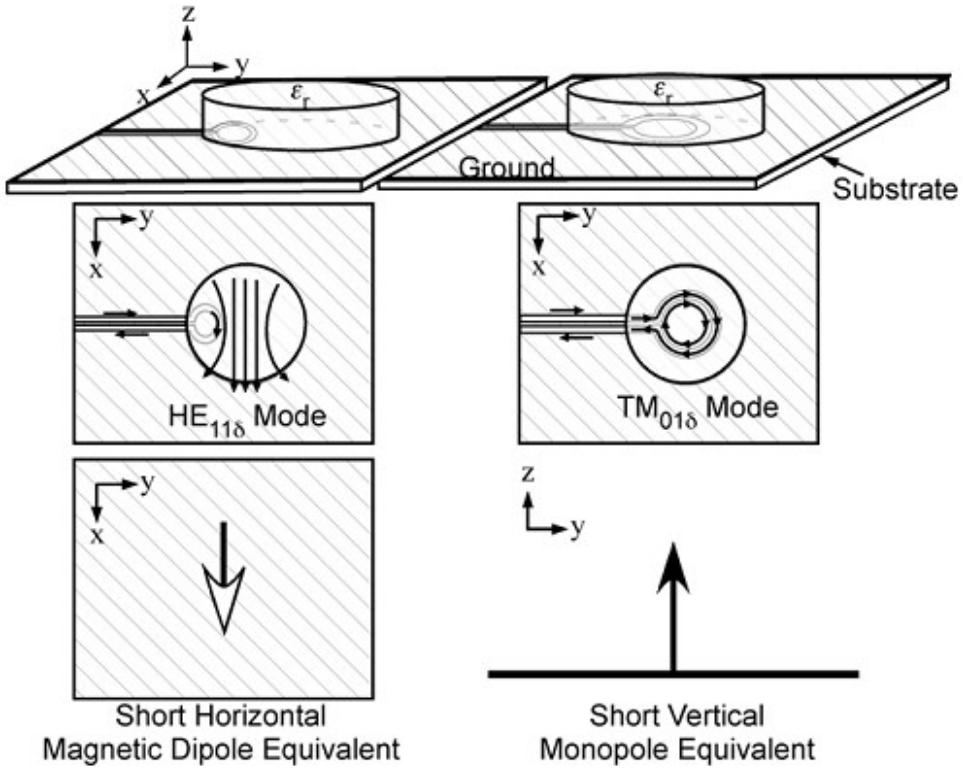

Fig. 3.15: Coplanar Waveguide Fed Cylindrical DRA

Co-planar waveguide (CPW) feeding technique is also referred as planar strip line feeding. CPW feeding technique more advantageous compared to other feeding techniques, because it has the following attractive features. They are

- Lower radiation leakage
- Less dispersion than microstrip lines
- Active devices can be mounted on top of the circuit like on microstrip.
- It can provide extremely high frequency response (100 GHz or more). Since connecting to CPW does not involve or require any parasitic discontinuities in the ground plane [9].

In addition, the CPW has lower loss than the microstrip line. One important application is that a fibre optics system can be integrated with the slot antenna. Recently, different types of CPW-fed slot antennas have been designed for wideband applications, achieving 50% bandwidth in a multi-slot design and 60% and width by optimizing a tuning stub. As with microstrip line excitation, slot antennas excited by coplanar waveguides also have bidirectional radiation characteristics [15].

3.5 Bandwidth Enhancement Techniques of DRAs

The most attractive feature of Dielectric Resonator antennas is Bandwidth Enhancement. By choosing proper structure for DRAs we can easily enhance the bandwidth. The various techniques used in Bandwidth Enhancement by using DRAs as listed below [1].

- Optimizing the feeding mechanisms and the DRA parameters.
- Changing the shape of DRAs.
- Use of modified feed geometries (stub matching).
- Making use of Stacked Dielectric Resonators in DRA designs.
- Introducing air gap between the ground plane and Dielectric Resonator.
- Reducing the permittivity of Dielectric Resonator.
- Use of coplanar parasitic strip coupled with different resonators.

Recently, the stacked method is used to increase the Bandwidth of DRAs.

3.5.1 Stacked Method

The method of utilizing multiple DRAs for the enhancement of bandwidth requires stacking DRAs on the top each other. In many cases it is evident that required results are not achieved with a single element DRA. As an example, a high gain, directional pattern can never be in synchronous with a single DRA of any shape. In these applications, a DRA with proper element positioning and feed arrangement can be used to produce desired specifications.

This technology offers the advantage that each DRA can be independently tuned for either broadband or dual band performance. Figure 3.16 manifests a cylindrical stacked dielectric resonator antenna. The stacked DRA arrangement contains two cylindrical discs of various materials vertically stacked, on each other, placed above a ground plane. Lower DRA is excited by a probe feed and the upper DRA is electromagnetically coupled, where the cylindrical DRA has radius (a), height (h) and relative dielectric permittivity (ε_r) [1].

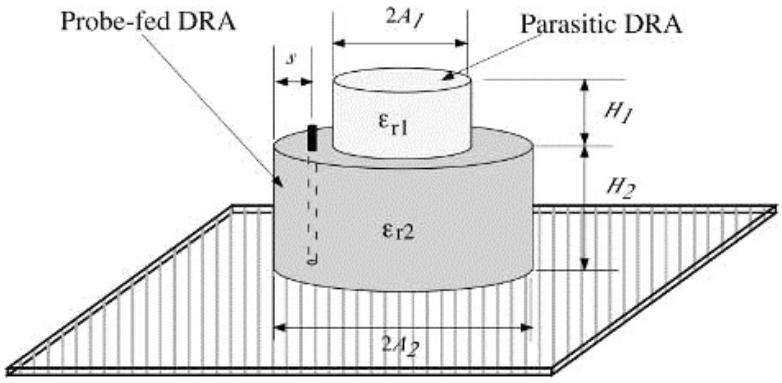

Fig. 3.16: Geometry of stacked cylindrical DRAs

Air gaps can also be introduced in between DRAs to enhance the impedance bandwidth. The main disadvantage of this configuration is that the DRA geometry is not very low profile; however, they may still be suitable for array applications [1].

3.5.2 Coplanar Parasitic Method

Another method of enhancing the impedance bandwidth for a cylindrical DRA is by adding a parasitic coplanar strip, loaded coplanar with the 50Ω microstripline feed. The antenna offers bandwidth as high as 17.33% at a centre frequency of 2.77 GHz, as a result of the enhanced coupling produced by the coplanar strip. At an optimum strip position and dimensions, dual

radiating modes are excited in close proximity to form a linearly polarized, wider impedance bandwidth. [23]

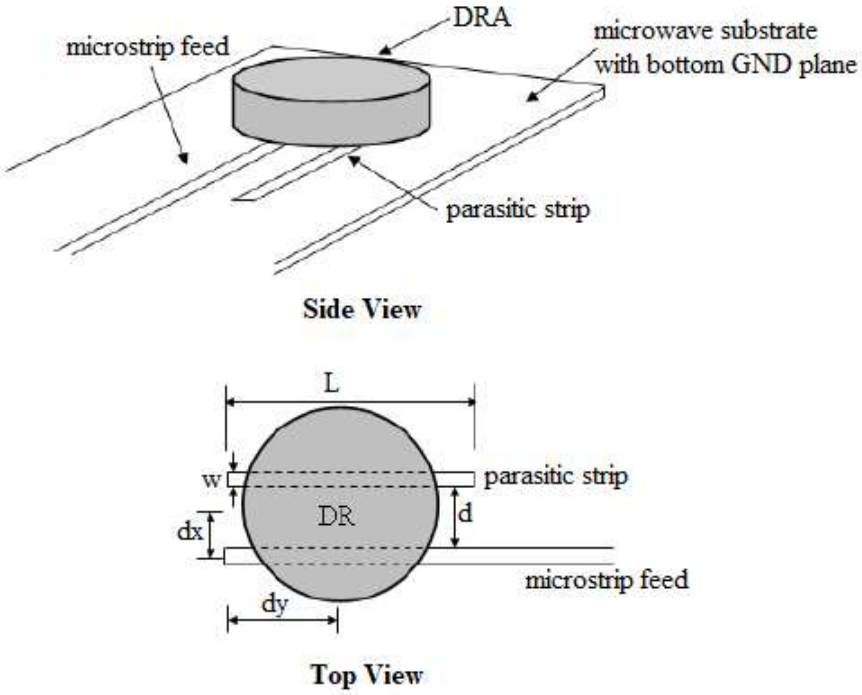

Fig. 3.17: Configuration of microstrip line fed cylindrical DRA using coplanar parasitic strip

3.5.3 Annular DRA

For a cylindrical DRA, the central section is removed to form an angular ring and the probe is placed at the centre as shown in Fig. 3.17. The design approach carried out by Shum and Luk [24] is based on dielectric ring resonators of very high permittivity. The air gap between the DRA and the ground plane is used to enhance the bandwidth.

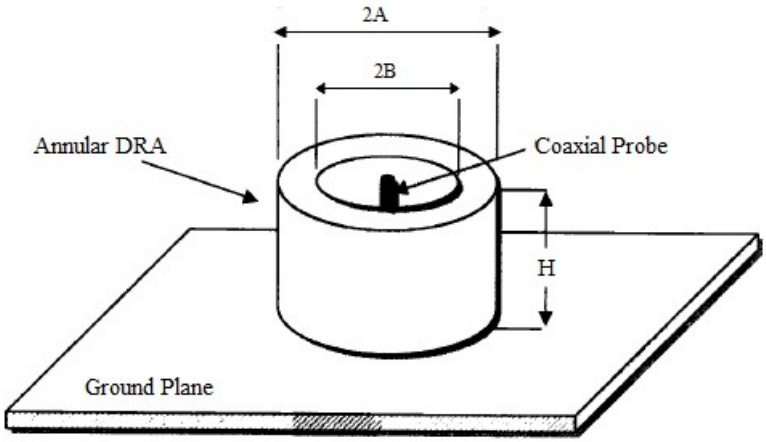

Fig.: 3.17: Probe Fed Annular DRA

3.6 Analytical Evaluation of Dielectric Resonator Antenna

In design technology, input impedance is the most dominant parameter which is a feed to excite the DRA. Input impedance as a function of frequency is to estimate the bandwidth of operation and for complementing the antenna to the circuit. It is sad to relate that there are no elementary closed-form expressions for the prediction of the input impedance of the DRA when excited by a particular feed and severe analytical. Some of the techniques are mentioned below that have been used to anticipate the input impedance for DRAs excited by the different feeds [9].

3.6.1 Green's function analysis

For a probe-fed DRA, the input impedance (Z_{in}) can be calculated using the following equation:

$$Z_{in} = \frac{-1}{I_o^2}(E.J_s)ds$$

Where, E = Electric fields of the DRA

J_s = Applied source current density on the probe

I_o = Magnitude of the current on the probe

The electric fields of the DRA controlled by the excitation of souce and calculated by using: $(E.J_s)ds$

Here, G represents Green's function for the DRA.

By using some simple assumptions about a single-mode operation and the currents on the probe, the Green‘s function for a hemispherical DRA was first acquired and was then used to anticipate the input impedance of the probe-fed DRA operating in the TE_{111} mode. This technique was also used in a probe–fed hemispherical DRA operating in the TM_{101} mode. The input impedance of conformal strip feeds and aperture feeds can also be surveyed using Green‘s function. The advantage to this technique is the relatively fast computation time required to obtain the input impedance. It is useful method for analysing the effects of altering probe dimensions and probe location and can be used for optimizing the input impedance. The main drawback is its limitation only to hemispherical DRA geometries. For other DRA shapes, different analytical techniques are required [9].

3.6.2 Numerical methods for analyzing DRAs

Numerical methods for analysing DRAs can be categorized into two groups, frequency domain technique and time domain technique. Each category offers advantages for particular antenna geometries [9].

3.6.2.1 Frequency domain analysis

Two common frequency domain techniques that have been used to analyse DRAs are the method of moments (MOM) and the finite element method (FEM). The MOM was first developed for wire or metal antennas of arbitrary shape, but can be extended to include dielectric materials by introducing equivalent currents. The MOM involves discretizing the antenna into a number of small segments and solving for a set of unknown coefficient representing the current on one segment due to a known incident field. Analysis of DRAs is not limited to a hemispherical shape, and the technique can be used to also analyses simple cylindrical and rectangular DRA shapes. Determining the DRA input impedance using the MOM technique will require more computer memory and time than applying Green‘s function. Thus, MOM technique is not convenient tool for optimizing the DRA performance. MOM is used to investigate the effect of the air gaps and calculate internal field pattern of various modes of cylindrical DRAs [1], [9].

FEM (Finite Element Method) can be used to analyze a DRA of any shape. Like MOM, it includes the sampling of geometry, but while in MOM only the ground plane requires segmentation, the entire volume surrounding the DRA must also be sampled in FEM, which

increases the computational size of the problem. The advantage of FEM is that it does not require the formulation of equivalent currents and, thus, can be easily applied to arbitrary shapes. Another advantage of FEM is its availability as commercial software, which provides graphical user interfaces to simplify the geometric definition of the problem. FEM is used to determine the effect of the finite ground plane on the DRA radiation pattern [1], [9], [16]

3.6.2.2 Time domain analysis

There are two time domain techniques that have been applied to analysing DRAs are the finite difference time domain (FDTD) method and the transmission line method (TLM). These techniques require the entire volume around the DRA to be discretized and thus can be memory and time intensive. In it, wideband pulse used to excite the DRA, and by transforming the solution into the frequency domain, the input impedance can be determined over a wide frequency range. For frequency domain techniques, the problem would have to be re-simulated at each frequency of interest and finding the impedance response over a broad frequency range could be very time consuming. With the frequency domain methods, the time domain methods are good tools for analysing the performance of a given DRA geometry, but are less useful for optimizing the performance of DRAs. FDTD is used to calculate circular polarization patterns of cross-shaped DRAs and input impedance of slot-fed rectangular DRA. Transmission line method used to calculate input impedance of microstrip-fed multi-segment DRAs [1], [9].

3.7 MATLAB Simulated Results

The impact of the geometrical parameters of a cylindrical DRA (radius and height) as well as of the relative dielectric constant (ε_r) on the resonant frequency is investigated by the MATLAB programs. Resonant frequency as a function of the DRA's radius and height are being obtained based on formulations. The dielectric constant used to calculate the resonant frequencies is set to $\varepsilon_r = 10$. It is indicated from the simulated graphs that the resonant frequency decreases by increasing either the radius or the height or both of them simultaneously. The programs and simulated results are given below:

3.7.1 MATLAB Program 1

```
clear all;
close all;
% parameter definition
c = 3*10^11;
Er = 10;
x11 = 1.841;
a = 10:10:100;
h = 35;
% resonant frequency equation;
for i=1:length(a)
  fr(i)=(c/(2*pi*a(i)*sqrt(Er)))*sqrt(x11^2+((pi*a(i))/(2*h))^2);
end
subplot(1,1,1);
plot(a,fr);
title('plot a vs fr when a is varying');
xlabel('Radius (mm)');
ylabel('Resonant Frequency (GHz)');
```

3.7.2 MATLAB Program 2

```
clear all;
close all;
% parameter definition
c = 3*10^11;
Er = 10;
x11 = 1.841;
a = 13;
h = 10:10:100;
% resonant frequency equation;
for i=1:length(h)
fr(i)=(c/(2*pi*a*sqrt(Er)))*sqrt(x11^2+((pi*a)/(2*h(i)))^2);
end
subplot(1,1,1);
plot(h,fr);
title('plot h vs fr when h is varying');
xlabel('Height (mm)');
ylabel('Resonant Frequency (GHz)');
```

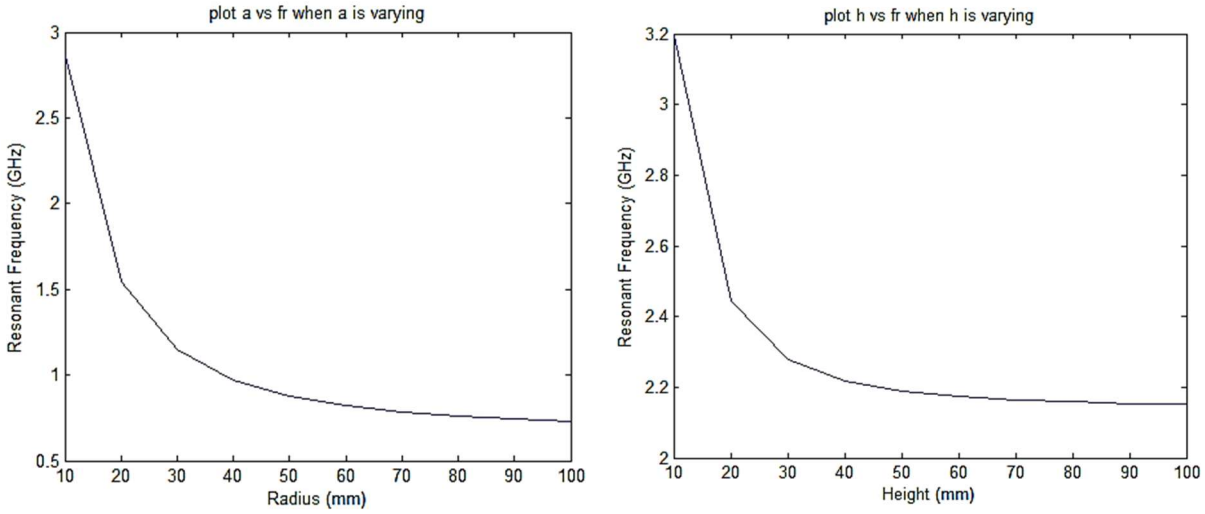

(a) (b)

Fig. 3.19: Resonant frequency versus (a) radius and height (b) of a cylindrical DRA with relative permitivity $\varepsilon_r = 10$

3.7.3 MATLAB Program 3

```
clear all;
close all;
% parameter definition
c = 3*10^10;
x11 = 1.841;
a = 2.5;
h = 5;
Er = 0:5:100
% resonant frequency equation;
for i=1:length(Er)
fr(i)=(c/(2*pi*a*sqrt(Er(i))))*sqrt(x11^2+((pi*a)/(2*h))^2);
end
subplot(1,1,1);
plot(Er,fr);
title('plot εr vs fr when εr is varying');
xlabel('Relative Dielectric constant(εr)');
ylabel('Resonant Frequency (GHz)');
```

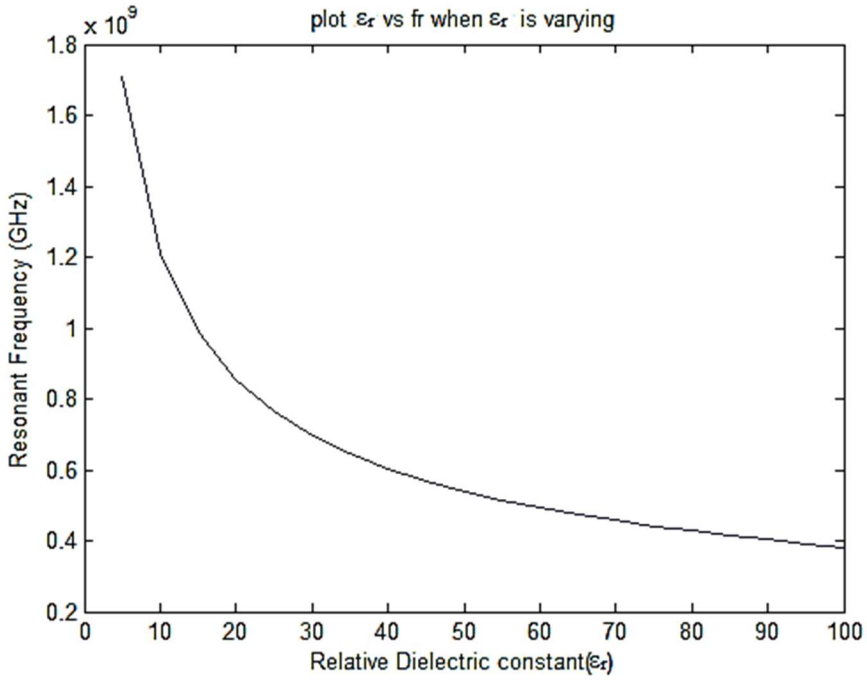

Fig. 3.20: Resonant Frequency of a cylindrical DRA with radius a = 2.5 cm and height h = 5 cm versus relative dielectric constant

Figure 3.20 shows the effect of the relative dielectric constant (ε_r) on the resonant frequency. It is observed that the resonant frequency of the dominant mode decreases with increase in the dielectric constant of the DRA. This behavior is the most important characteristic of the DRA since it allows decreasing the size of the DRA by increasing its dielectric constant. It is to be noted that the impedance bandwidth is inversely proportional to the relative permittivity of the DR. Therefore, the use of materials with high dielectric constant can result in a narrowband antenna behavior.

References

[1] A. Petosa, "Dielectric Resonator Antenna Handbook", Artech House Publishers, 2007.

[2] S.A Long, M.W.McAllister, and L.C .Shen, "The resonant cylindrical dielectric cavity antenna," *IEEE Trans. Antennas Propag*.,Vol. AP-31,no.5,pp.406-412,May 1983.

[3] Darko Kajfez and A. A. Kishk, "Dielectric Resonator Antenna-Possible Candidate for Adaptive Antenna Arrays", University of Mississippi, USA.

[4] H. Y. Yee, "Natural resonant frequencies **of** microwave dielectric resonators," *IEEE Trans. Microwave Theory Tech.***,** vol. MlT-13, p. 256, Mar. 1965.

[5] Y.KOBASHI and S.TANAKA, "Resonant Modes of a Dielectric Rod Resonator Short Circuited at Both Ends by Parallel Conducting Plates", *IEEE Trans. Microwave Theory & Tech.*, 1980, Vol MTT-28 no 10 pp.1077-1085.

[6] D. Kajfez and P. Guillon, Dielectric resonators, Vector Fields, Oxford, Mississippi, 1990.

[7] K. F. Lee. K. M. Luk and P.Y. Tam, "Crosspolarisation characteristics of circular patch antennas", *Electron. Lett*, Vol.28.pp.587-589, 1992.

[8] K. W. Leung. K.M. Luk. K. Y. A. Lai and D. Lin, "Theory and experiment of a coaxial probe fed dielectric resonator antenna", *IEEE Trans. Antennas Propagat*., Vol.41.pp.1390-1398, Oct, 1993.

[9] Kwai- Man Luk and Kwok-Wa Leung; "*Dielectric Resonator Antennas"* City University of Hong Kong Research Studies Press Ltd. Baldock, Hertfordshire, England, 2003.

[10] C. A. Balanis, "Antenna Theory, Analysis and Design" 2nd Edition, John Wiley & Sons, Inc., New York 1982.

[11] R. Kranenberg, S.A Long, J. T. Williams, "Coplanar Waveguide Excitation of Dielectric Resonator Antennas", *IEEE Transactions on Antennas and Propagation*, Vol.39, Jan.1991. pp. 119-122.

[12] C Curry, Novel Size- Reduced Circularly Polarized Antennas", Master's Thesis, Royal Military College, Kingston, Canada, July 2000.

[13] M.S Al Salameh, Y.M.M. Antar, G.Seguin, A. Petosa, " Analysis and Measurement of Compact-Size DRA With CPW Feed", USNC/URSI National Radio Science Meeting,Boston, MA, July 2001,pp,221.

[14] J. P. S. McKenzie, "Dielectric Resonator Antennas Fed by Coplanar Waveguide at Extremely High Frequecy", Master's Thesis, Royal Military College, Kingston.

[15] R. K. Mongia and A. Ittipiboon, “Theoretical and experimental investigations on cylindrical dielectric resonator antennas,” *IEEE Trans. Antennas Propag*., vol. 45, no. 9, pp. 1348-1356, Sep. 1997.

[16] Yuan Gao, Ban-Leong Ooi, Wei-Bin Ewe, and Alexandre P. Popov, “A Compact Wideband Hybrid Dielectric Resonator Antenna”, *IEEE microwave and wireless components letters*, vol. 16, no. 4, April 2006.

[17] Robert E. Collin, “Foundations for Microwave Engineering”, *IEEE Press*, 2001.

[18] Nisha Gupta, S. K. Rout, K. Sivaji, “Characteristics of Cylindrical Dielectric Resonator Antenna” *Microwave Review*, December, 2009.

[19] Kumar, Guha , Antar, Y. M. M.Banerjee , “ A Microstrip line(s) as new feed for exciting a cylindrical DRA with higher order HEM12δ mode”, Antennas and Propagation Society International Symposium (APSU RSI), 2014 , IEEE Page(s):1990 – 1991.

[20] Kaushik Vipul R., Jagruti R. Panchal, “Dielectric resonator antenna and its design parameters-A review,” International Research Journal of Advanced Engineering and Science, Volume 2, Issue 4, pp.128-133, Nov 2017.

[21] A. Petosa, A. Ittipiboon, Y. M. M. Antar, D. Roscoe, and M. Cuhaci, “Recent advances in dielectric-resonator antenna technology,” Antennas & Propagat. Mag., pp. 35–48, June 1998.

[22] S. Keyrouz and D. Caratelli, “Dielectric Resonator Antennas: Basic concepts, Design Guidelines, and Recent Developments at Millimeter-Wave Frequencies”, *International Journal of Antennas and Propagation*, Sept. 2016

[23] A. V. P. Kumar, V. Hamsakutty, J. Yohannan and K. T. Mathew, “Microstripline fed Cylindrical Dielectric Resonator Antenna with a Coplanar Parasitic Strip”, *Progress In Electromagnetics Research,* PIER 60, 143–152, 2006

[24] S. M. Shum and K.M. Luk, "Characteristics of dielectric ring resonator antenna with air gap," *Electron. Lett.,* vol. 30, no. 4, pp. *111-21%,* Feb. 1994.

CHAPTER 4

PARAMETRIC STUDY

4.1 Introduction

About thirty five years ago, experimental studies were conducted to determine the radiation characteristics of cylindrical dielectric resonator antennas [1] residing on a conducting ground plane. These resonators were excited by a coaxial probe extending into the dielectric material through the bottom of the ground plane. One of the conclusions drawn from the experimental studies was that in order to obtain desirable radiation characteristics, the feed probe must be positioned away from the resonator's axis of symmetry and near the outer wall of the dielectric resonator.

In this thesis, coaxial probe excitation is used for feeding the DRA. The main advantage of using probe feed is that, by optimizing length and position of the feeding probe, the input impedance of the DRA can be tuned and, consequently, the resonance frequency can be controlled. The probe can be considered as a vertical electric current that is positioned to achieve strong coupling to the DRA which, in turn, results in high radiation efficiency. The other advantage of this method is that the antenna system can be directly connected to a 50Ω circuit without the need for a matching network. The parametric study is useful because it provides a comprehensive picture of the antenna's characteristics and allows understanding of the influence of the DR geometry parameters on the return loss of the antenna.

4.2 Antenna Design

For this design, the target frequency band is the C band which is from 2 to 4 GHz. In order to achieve this target, the dimensions of the ceramic block must cut for the dominant mode to be commensurate with this requirement. A dielectric constant of 10 with loss tangent (tan δ) = 0.002

was selected based on the available material in the research laboratory. The dimensions for the ceramic block were optimized and analyzed from simulation package. This will ensure the desired mode of the DR is excited. The antenna configuration of the cylindrical DRA is shown in Figure 4.1. The DRA is placed above a conducting ground plane. In the present work, the ground plane size of 5cm×5cm×0.2cm is considered and fed by a coaxial connector. The dimensional parameters of the DRA are radius a=13mm, height h=26mm. The probe is located at a point near the edge of the cylinder. The feed probe is of length l, and radius r =0.63mm. The proposed structure is modelled with finite element solver Ansys HFSS v15.0. By changing the probe height and location, then DRA height and radius, a comparative study of various parameters is performed like input impedance, resonant frequency, gain, radiation patterns etc. The mode of operation and resonant frequency of the dielectric resonator (DR) can be calculated using (1) [1], which shows resonant frequency ~2.32 GHz and also signifies excitation of TM110 mode.

$$fr_{TM110} = \frac{c}{2\pi a\sqrt{\varepsilon_r}}\sqrt{(1.841)^2 + \left(\frac{\pi a}{2d}\right)^2} \quad \text{------ (4.1)}$$

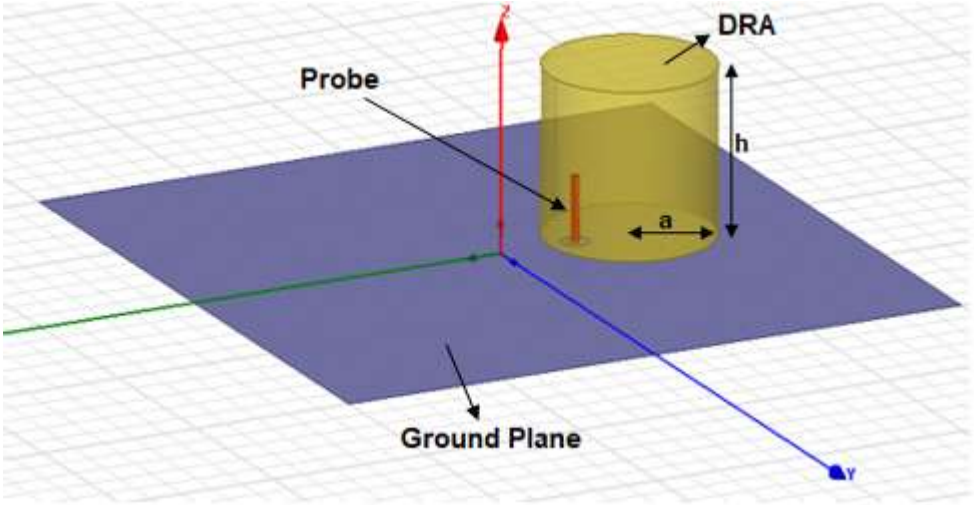

Fig. 4.1: Simulated Dielectric Resonator Antenna Structure

4.3 Simulation Tool and Algorithm -- HFSS

4.3.1 Introduction

HFSS is a high-performance full-wave electromagnetic (EM) field simulator for arbitrary 3D volumetric passive device modelling that takes advantage of the familiar Microsoft Windows graphical user interface. It integrates simulation, visualization, solid modelling, and automation in an easy-to-learn environment where solutions to your 3D EM problems are quickly and accurately obtained. It is an interactive software package for electromagnetic modelling and analyzing 3-D structures.

Ansoft HFSS pioneered the use of the Finite Element Method (FEM), adaptive meshing, and brilliant graphics for giving unique performance and insight to 3D EM problems. FEM is a flexible numerical technique capable of being adapted to problems dealing with complex geometries and material distributions. The finite element method is used to solve partial differential equations describing physical systems, which are generally defined with three spatial variables and a temporal variable Ansoft HFSS can be utilized to determine parameters such as S Parameters, Resonant Frequency, and Fields. The basic mesh element of HFSS is a tetrahedron. This allows us to solve any arbitrary 3D geometry, especially those with complex curves and shapes, in a fraction of the time using other techniques.

The name HFSS stands for High Frequency Structure Simulator. Today, HFSS continues to lead the industry with innovations such as Modes-to-Nodes and Full-Wave Spice. Ansoft HFSS has evolved over a period of years with input from many users and industries. In industry, Ansoft HFSS is the tool of choice for high-productivity research, development, and virtual prototyping.

4.3.2 Process Overview

The first step is to design the geometric model of the structure that is to be analysed. The next step is to assign material characteristics to various drawn objects in the geometric model. Boundaries are then defines for the structure, such as, perfect magnetic or electric conductor, or finite conductivity. A port or a voltage source needs to be defined to excite the structure. This is done as

a part of boundary definitions. Once the structure is completely modelled, the solution is set up. This includes specifying the type of solution to be performed, the frequency at which the adaptive mesh refinement takes place and the convergence criteria. The problem is then solved for the fields associated with the model. Finally, after the completion of the simulation, the solution data is post processed which may include display of far-field plots, S-parameters, impedances and Smith charts.

4.3.3 Flowchart for designing a Project in HFSS

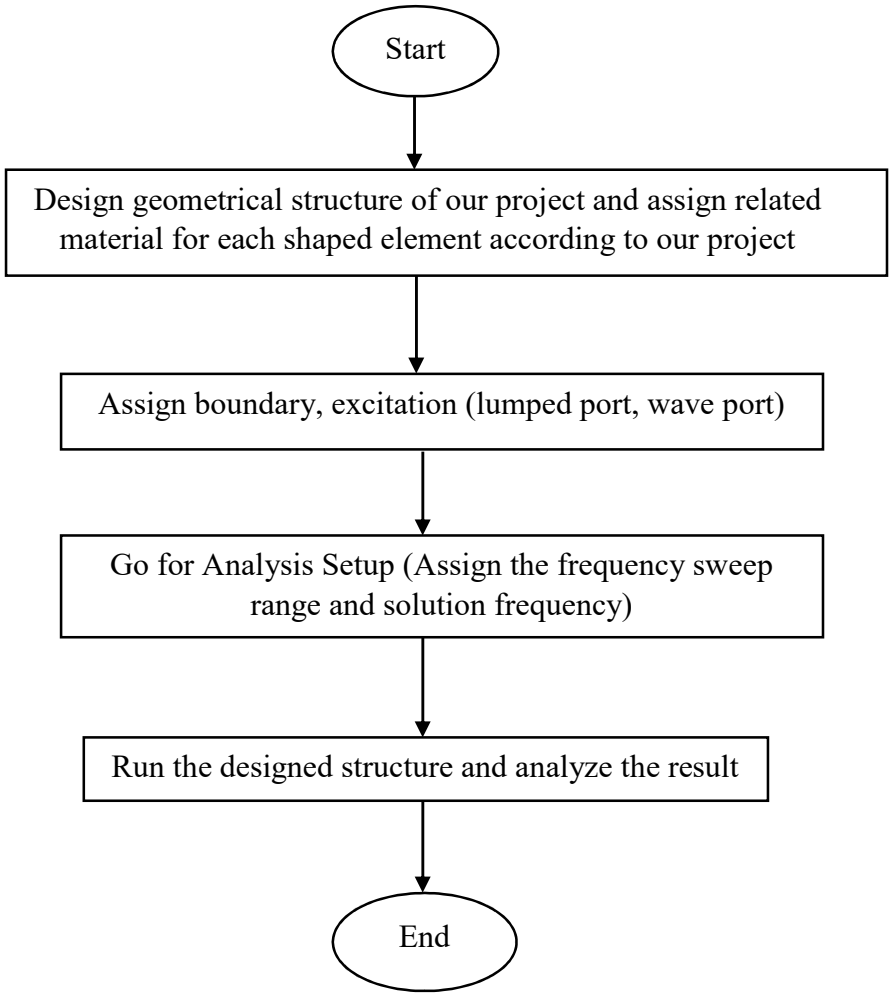

4.3.4 Algorithm for Design a Project in HFSS

1. Start.
2. Open HFSS Software.
3. Insert Geometrical Project design.
4. Assign material for each element of the project.
5. Assign radiation boundary for the Designed structure.
6. Give the excitation (lumped port and wave port) to the Designed structure.
7. Go for the analysis setup (assign frequency sweep range and solution frequency).
8. Run the project and analyzed the results.
9. Stop.

4.3.5 Steps to design the Cylindrical DRA using HFSS Software

1. Create and Save the New Project:

Open new project:-When we will open the software it will automatically open a new project window, just rename as per our requirement (CDRA). It will open the new window which looks like this.

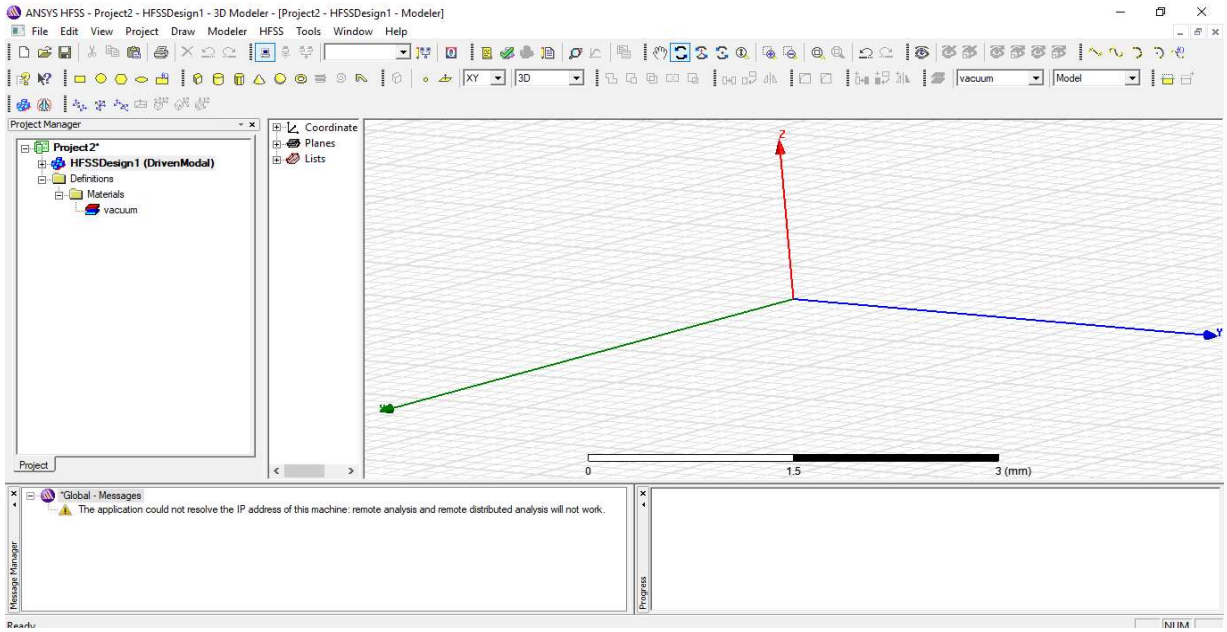

Fig. 4.2: HFSS Window

Elements of HFSS Window:

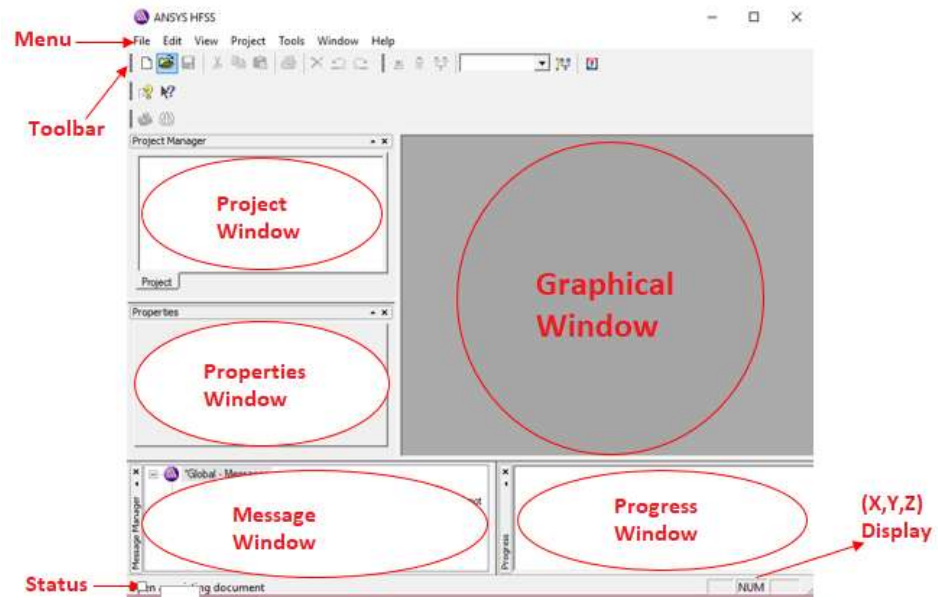

Fig. 4.3: Elements of HFSS

Save the project: Go to file click on "save as" it will save the project where ever we want depend upon our requirement.

2. Set the drawing unit before we start design

Go to modeler in menu and click on units it will one unit window select our required unit normally we select "mm"

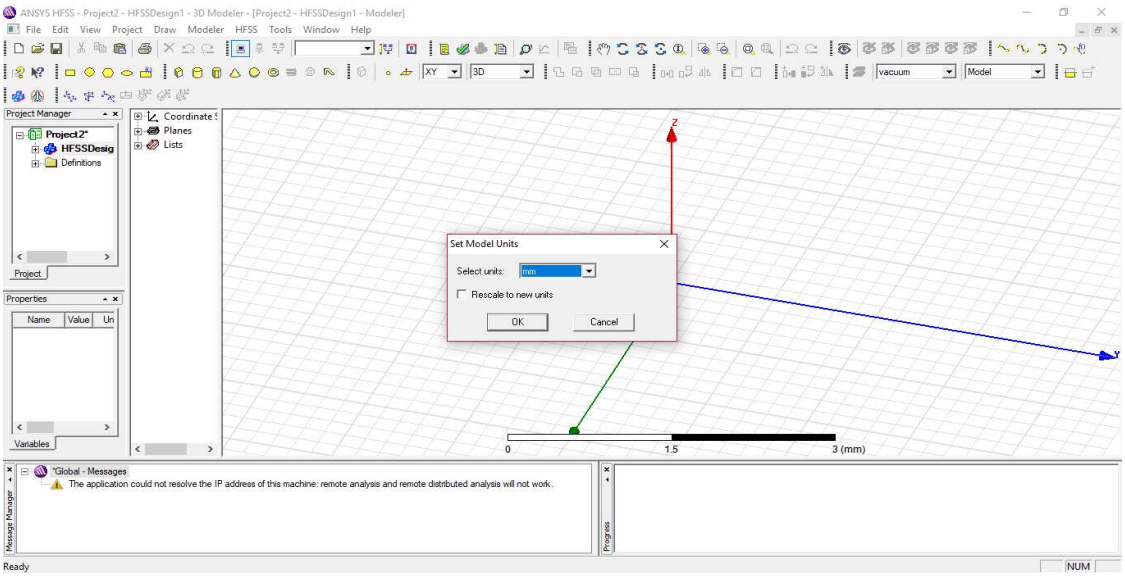

Fig. 4.4: Unit Window

3. *Drawing Different Units*

Take ground plane: For taking ground plane select Draw Box from the toolbar, if it is not available in toolbar than bring cursor to toolbar and by right click on mouse at anywhere in toolbar it will give us list in that click tick on 3D Draw solid. Or go to menu in that click on draw and then click box. Our aim is draw (100×100×2) mm ground plane. We want it should look in center. Change the name of box to ground plane. For that go to history tree in that double click on box1 and change the name as ground. Change the dimension of box. For that go to the history tree and expand ground in that double click on create box. Now we will get one small window in that change position, x size, y size and z size as shown in below. Assign the material for ground. For assigning the material right click on grounded select "pec" material.

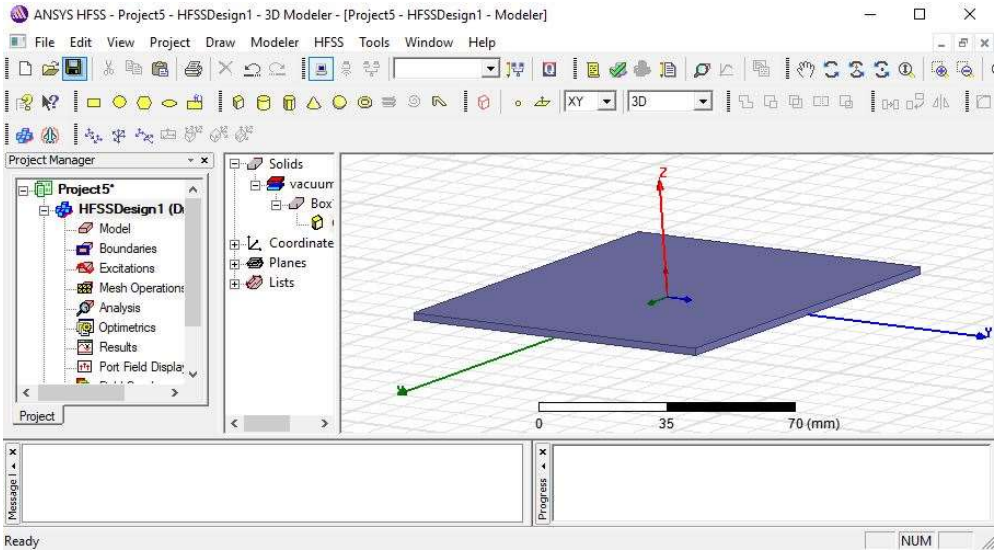

Fig. 4.5: Ground Plane

Designing of Coaxial probe for feeding Cylindrical DRA: For designing of coaxial feed first we will calculate coaxial parameter. Inner Diameter - D1, Outer Diameter - D2, Dielectric material - Teflon, Conductor material – Copper.

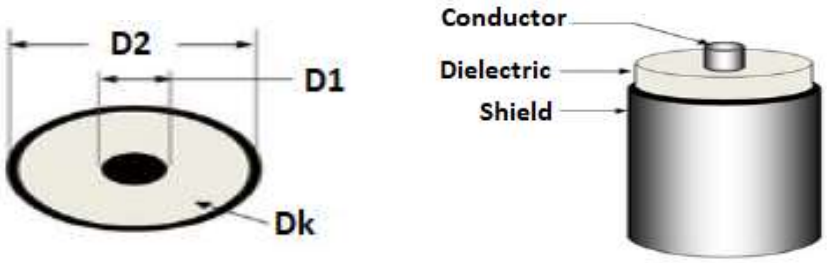

Fig. 4.6: Coaxial Probe

Designing of dielectric part for coaxial probe: Select cylinder dimension of 2.1 mm radius with -5 mm heightened subtract with ground which will create hole of taken cylinder , now again take same dimension cylinder.

How to do subtraction from one shape to other shape: Select both shape from the history tree and perform subtract operation.

Designing of conductor part for coaxial probe: Select one cylinder of 0.63 mm radius and -5 mm height and subtract from dielectric part which will create hole of required dimension. Now again select a cylinder of the same dimensions. Two coaxial probes need to be created, one above and one below the ground plane with same dimensions and position.

Draw cylindrical DRA: Do same as ground for rename and dimensions. Draw cylindrical DRA with dimension of 13×26 mm (Radius×Height) above the coaxial probe and keeping it near the DRA boundary. Assign material for DRA. For that right click on DRA cylinder from history tree and select add new material (dielectric constant is 10).

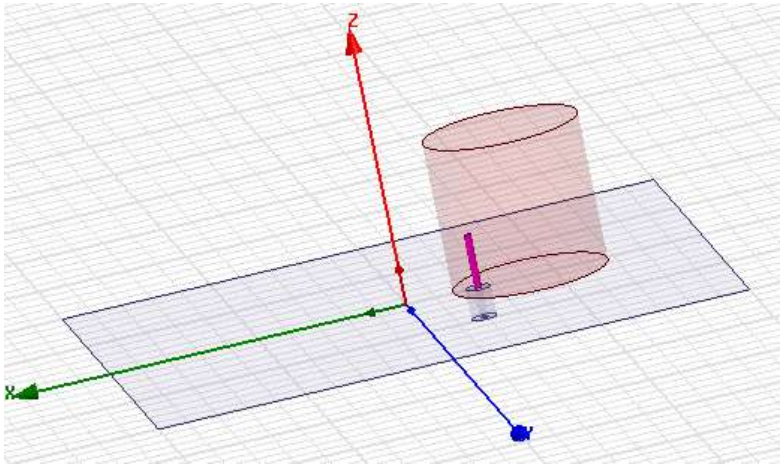

Fig. 4.7: DRA on ground plane fed by coaxial probe

4. Designing of Radiation Boundary and Excitation:

Assigning of port for excitation of coaxial probe: Take one circle to cover the coaxial feed point so that we can assign the port. Assign wave port as excitation, select circle form history tree and right click on that select assign excitation in that again select Wave port.

Designing of radiation box: Take one box dimension of 100 mm x 100 mm x 40 mm which will a vacuum. Assigning the box as radiation box:

- select all of the faces of the Air object except the face at Z = 0 mm
- right click then select faces
- Select the menu item HFSS > Boundaries > Assign> Radiation
- In the radiation boundary window: Name – Rad1, then click OK

Create a Radiation Setup: To define the radiation setup**, s**elect the menu item HFSS > Radiation > Insert Far Field Setup > Infinite Sphere. In the Far Field Radiation Sphere Setup dialog, select the Infinite Sphere Tab

1. **Name**: ff_2d
2. **Phi**: (Start: 0, Stop: 90, Step Size: 90)
3. **Theta**: (Start: -90, Stop: 90, Step Size: 2) then click OK.

5. Analysis Setup

Select the menu item HFSS>analysis setup>add solution setup. In the solution setup window, click the general tab,

- **Solution frequency** = 4 GHz
- **Maximum number of passes** is 20
- **Maximum delta S** is 0.02

6. Adding Frequency Sweep

To add a frequency sweep, select the menu items HFSS>analysis setup>add sweep. Select solution setup: setup1, click ok button then edit sweep window

- **Sweep type**: Fast
- **Frequency setup type**: linear count
- **Start**: 2 GHz
- **Stop**: 4 GHz
- **Count**: 150 click ok button

7. Validation check: Click on validate.

8. Analysis of structure: Click on analysis all.

9. Results: Go to HFSS and click on results tab.

- S11 versus frequency curve: It will show the S11 (dB) versus frequency (GHz) curve.

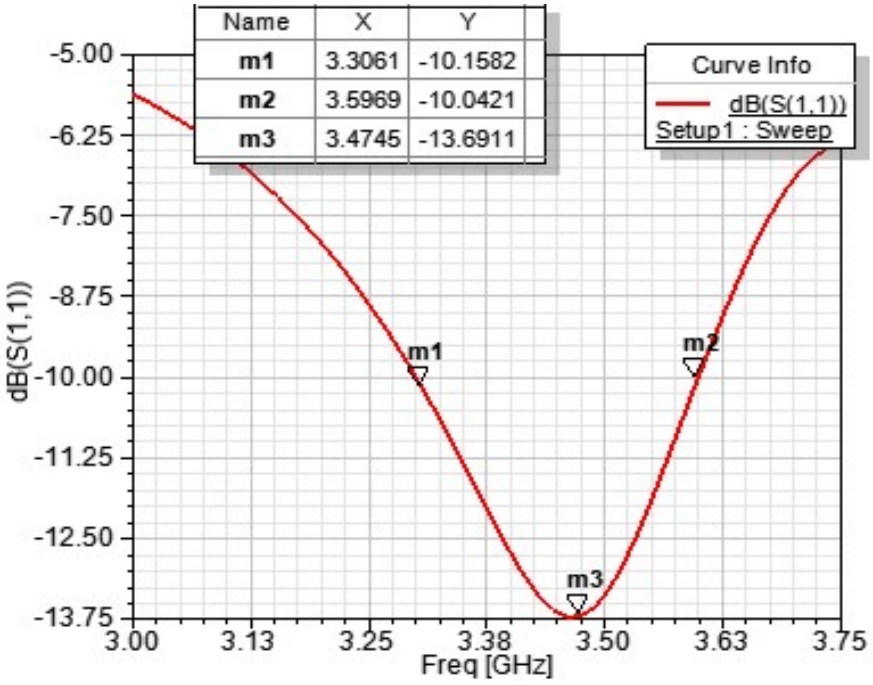

Fig. 4.8: Return Loss and calculation of Bandwidth

Calculation of Resonant Frequency and Bandwidth:

Bandwidth: (m2-m1)/m3 GHz = (3.59-3.30)/3.47 GHz = 0.083 GHz = 83 MHz

Resonant Frequency: m3 GHz = 3.47 GHz

Return Loss: -13.69dB

- Z11 versus frequency curve: It will show the Z11 (dB) versus frequency (GHz) curve. The impedance shows both the real and imaginary parts.

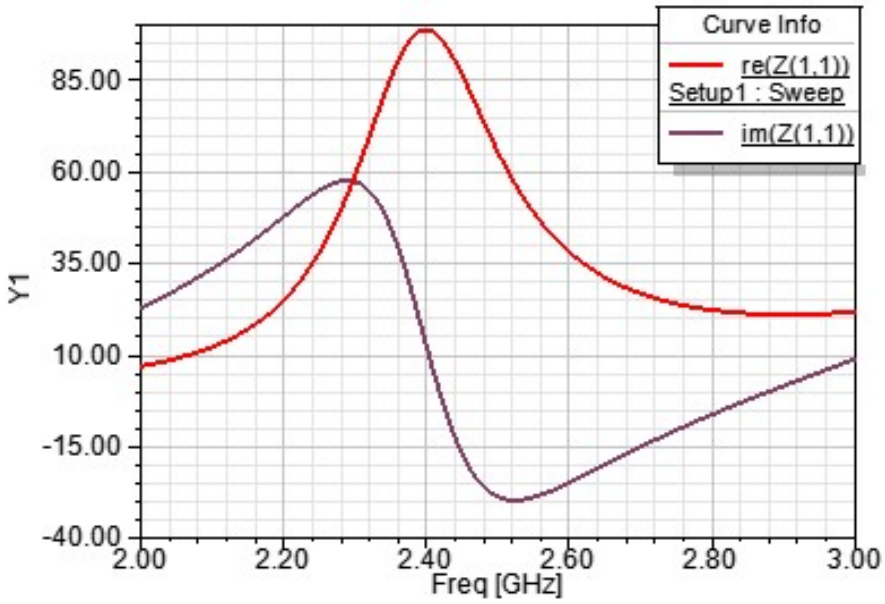

Fig. 4.9: Input Impedance versus Frequency

- Radiation Pattern: Plots electric and magnetic field patterns i.e. E_θ vs θ and E_Φ vs θ at $\Phi=0^\circ$ and 90°

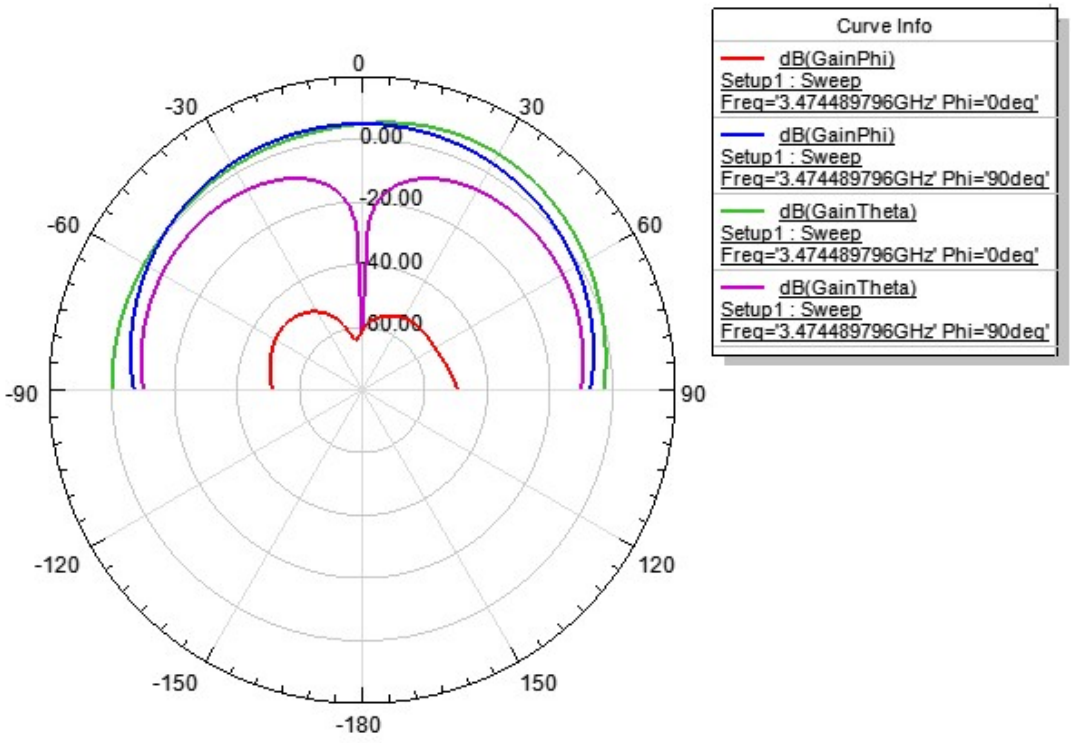

Fig. 4.10: Radiation Pattern Plot

4.4 Results and Discussion

The designed model using HFSS is a cylindrical DRA fed by a coaxial feed. Its specifications are stated above. Now, I will analyze its different characteristics by changing probe height and length and by changing the dimensions of DRA i.e. radius and height. Effect of relative permittivity and introducing air-gaps between DRA and ground plane are also evaluated thereafter.

4.4.1 Effect of variation of Probe Length

Fig. 4.11 shows the plot of input impedance as a function of resonant frequency with the variation of feed probe length, l = 0.30 to 0.65 in (7 to 17 mm). Impedance measurements were taken for a cylinder with radius = 13mm, height = 26cm (a/d = 0.5) and relative permittivity, $\varepsilon_r = 10$. Following the design formula given in equation 3.6, the cylindrical DRA resonant frequency is 2.32 GHz for the above mentioned specifications of the DRA. The probe feed is placed at a point near the edge of the cylinder.

Table 4.1: Table showing variation of Resonant Frequency and Impedance with various probe lengths

Probe Length (in inches)	Simulated Resonant Frequency from Return Loss (S11) (GHz)	Simulated Resonant Frequency from Impedance Plot (GHz)	Re(Z11) At resonance (Ω)
0.30	2.66	2.67	21.56
0.35	2.63	2.64	32.30
0.40	2.60	2.59	46.73
0.45	2.52	2.52	65.13
0.50	2.45	2.45	87.43
0.55	2.35	2.36	110.82
0.60	2.20	2.29	134.74
0.65	2.07	2.20	155.24

It is noticed that as the probe length increases, both the input impedance and input resistance increases (as shown in Fig. 4.11 and Fig. 4.13). This property can be used for impedance matching. On the other hand, resonant frequency decreases (as shown in Fig. 4.14) with the probe length. It is also observed that the measured impedance behavior is a combination of two effects — (a) resonance associated with the dielectric cylinder and (b) feed probe itself. However, since the input

impedance does not change drastically, this is feasible during impedance matching, especially for large ratio of a and h.

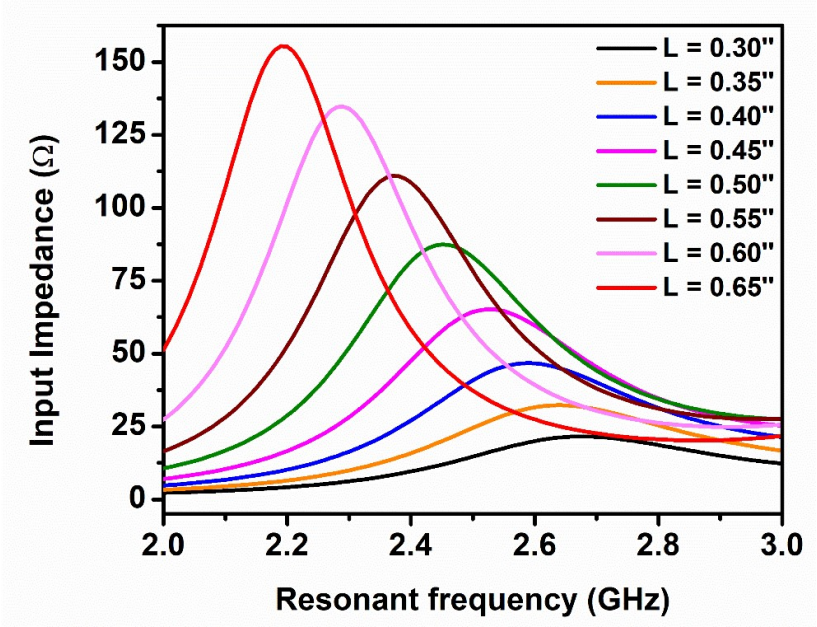

Fig. 4.11 Family of impedance curves for different probe lengths (in inches)

Fig. 4.12 shows the simulated return loss curves for different probe heights, indicating the shift of the operating frequency band towards the lower band and meeting the design goal.

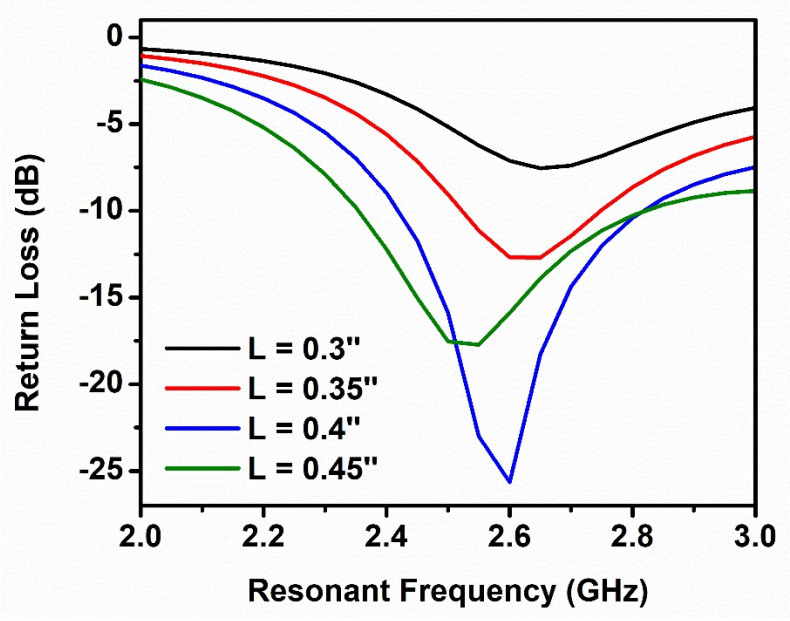

Fig. 4.12: Set of Return Loss curves for different probe heights

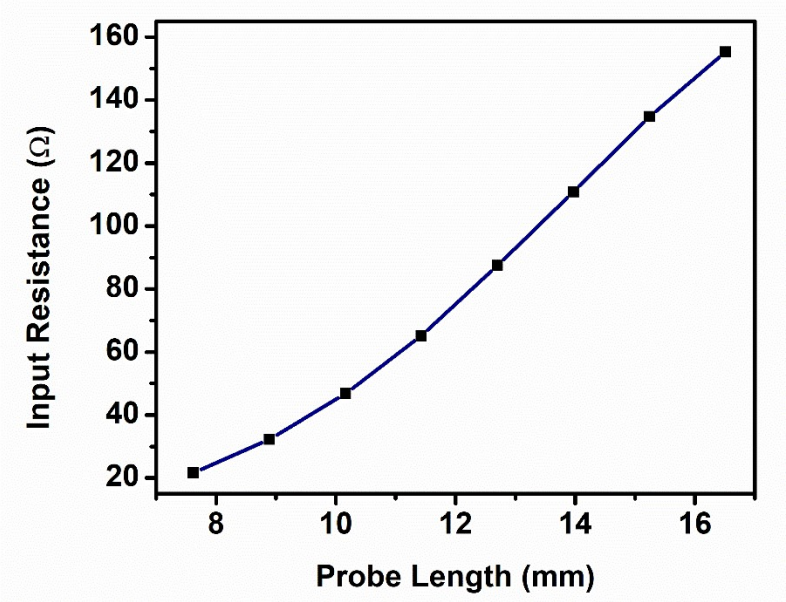

Fig. 4.13: Measured resistance versus variation in probe lengths

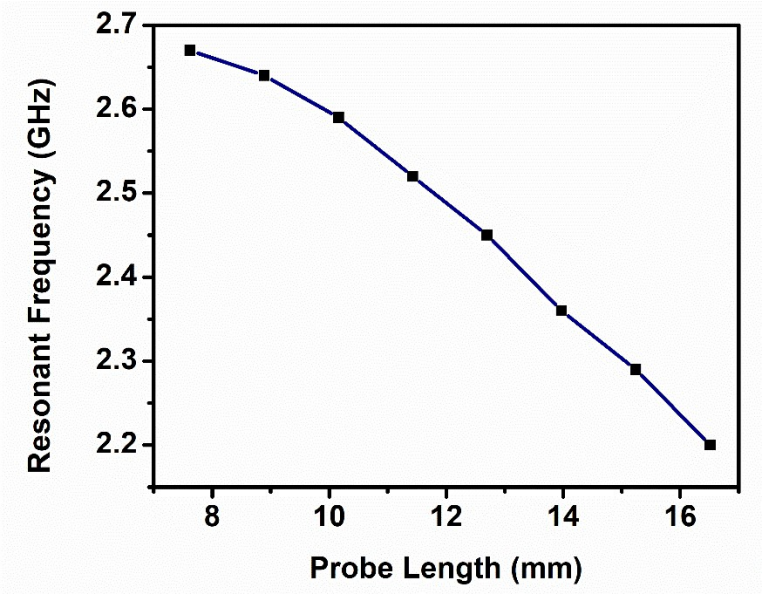

Fig. 4.14: Resonant Frequency versus variation in probe lengths

The far-field radiation patterns of the antenna with the variation of probe length is shown in the Fig 4.15. Figure (a) shows the plot of gain versus theta for H-field when phi is specified to 90˚ (i.e. Coplane) and phi is specified to 0˚ (i.e. Crossplane). Figure (b) shows the plot of gain versus theta for E-field when phi is specified to 0˚ (i.e. Coplane) and phi is specified to 90˚ (i.e. Crossplane). As it is evident from the graphs, there is no as such variation in radiation patterns with the change in probe lengths.

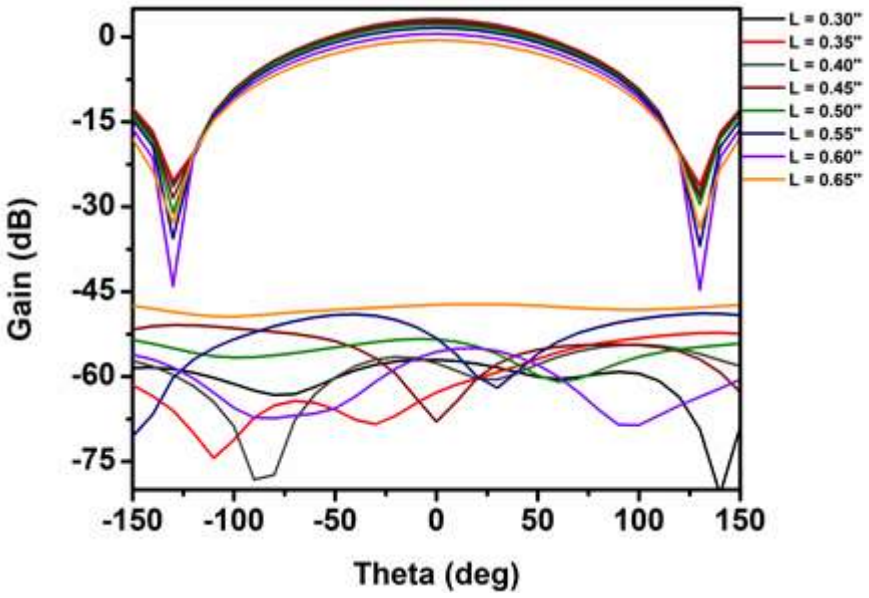

(a)

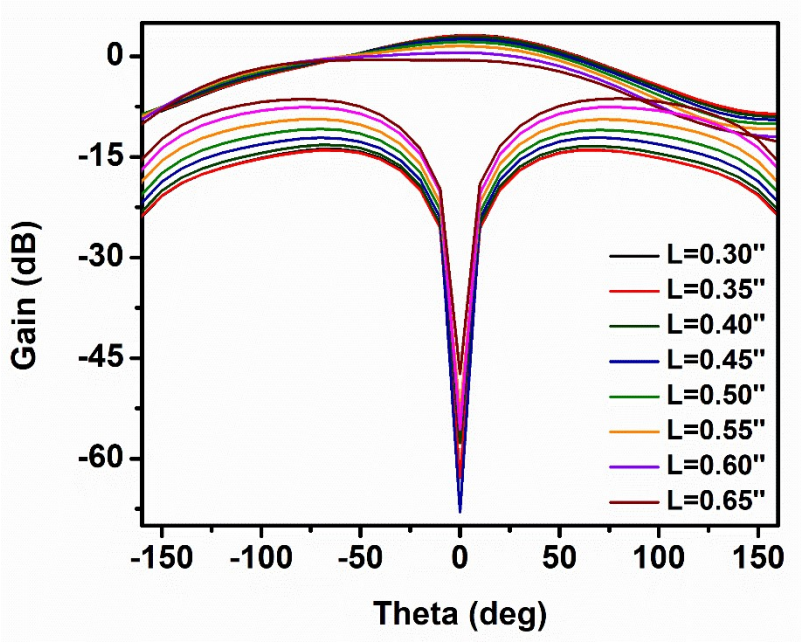

(b)

Fig. 4.15: (a) Gain vs theta for H-field at phi = 90˚ (Coplane) and phi = 0˚ (Crossplane) and (b) Gain vs theta for E-field at phi = 0˚ (Coplane) and phi = 90˚ (Crossplane) with variation in probe heights

4.4.2 Effect of variation of Probe Location

Fig. 4.17 shows the plot of input impedance as a function of resonant frequency with the variation of feed probe location from edge towards centre of the cylinder, i.e. $\rho = 9.8$ to 4.8 mm from centre. Impedance measurements were taken for a cylinder with radius = 13mm, height = 26cm (a/d = 0.5), probe height, l = 11.43mm and relative permittivity, $\varepsilon_r = 10$.

Table 4.2: Table showing variation of Resonant Frequency and Impedance with various probe locations from centre

Probe Position from centre (in mm)	Simulated Resonant Frequency from Return Loss Plot (GHz)	Simulated Resonant Frequency from Imedance Plot (GHz)	Re(Z11) At resonance (Ω)
9.8	2.52	2.52	65.13
8.8	2.55	2.54	63.97
7.8	2.57	2.55	61.00
6.8	2.60	2.57	57.20
5.8	2.65	2.60	52.50
4.8	2.70	2.64	47.42

Fig. 4.16 showing the simulated return loss curves for different probe positions shifting from edge to centre of the DRA, the operating frequency band gradually moves towards the upper band.

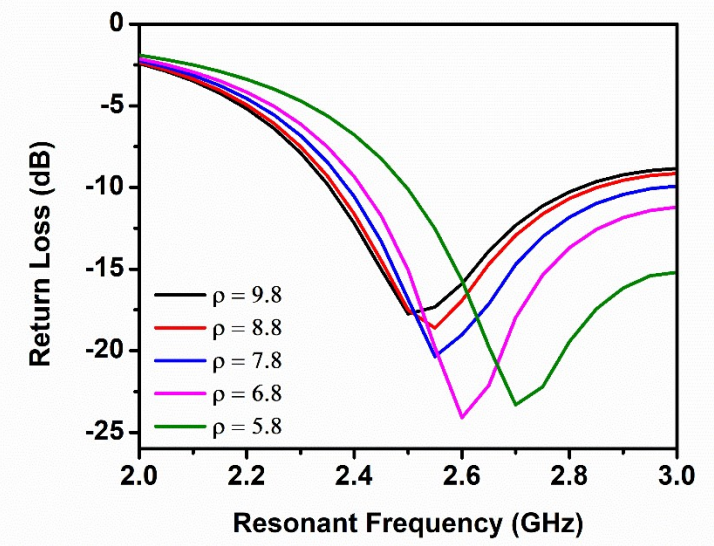

Fig. 4.16: Set of Return Loss curves for different probe positions

It is observed from the simulated graphs that as the position of probe is shifted from edge towards centre of DRA, magnitude of measured impedance decreases (as shown in Fig. 4.18) and resonant frequency increases (as shown in Fig. 4.19).

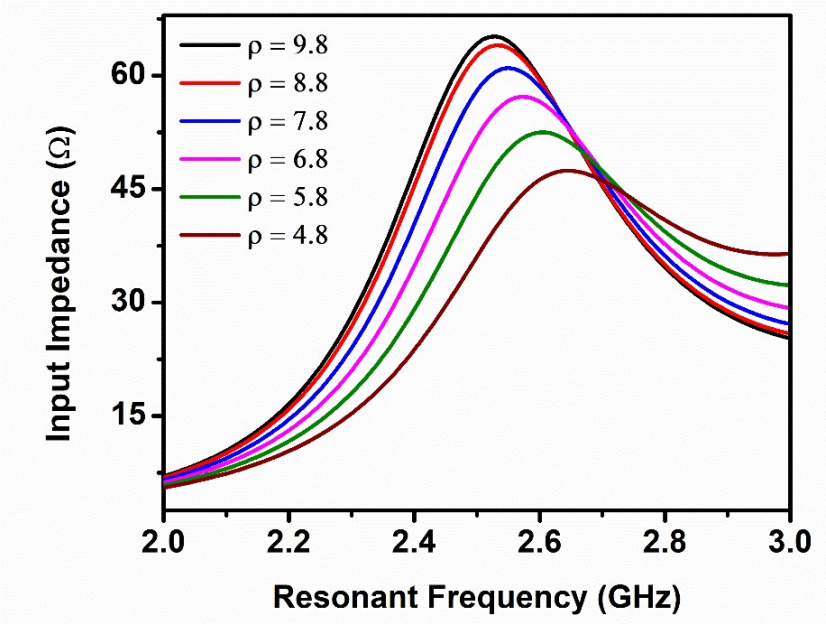

Fig. 4.17: Set of Impedance curves for different probe position changing from edge to center of DRA (in mm)

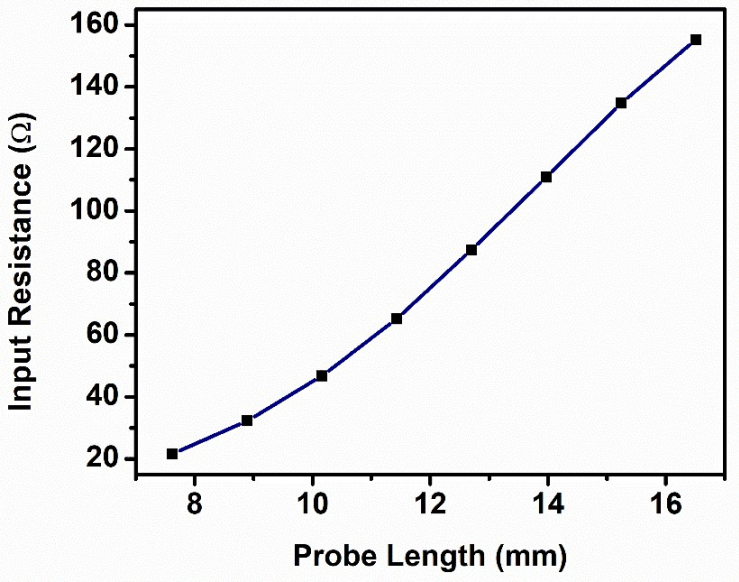

Fig. 4.18: Measured resistance versus variation in probe location within DRA from edge to centre (in mm)

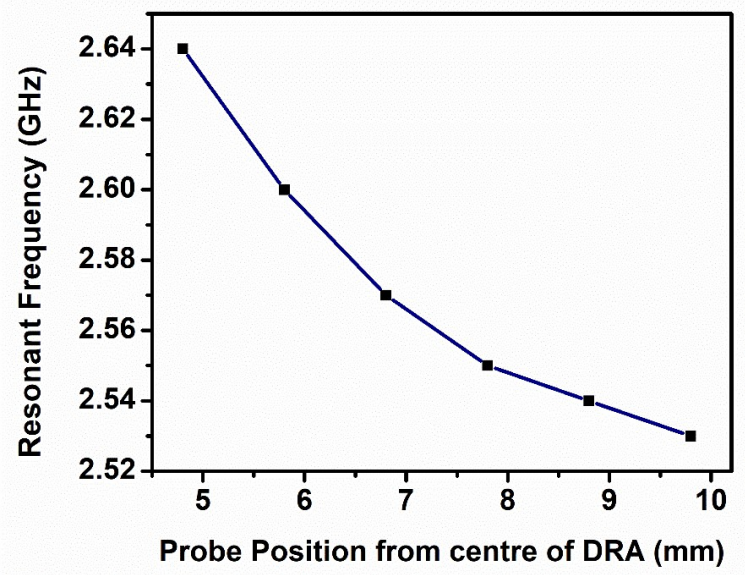

Fig. 4.19: Resonant Frequency vs variation in probe position.

The far-field radiation patterns of the antenna with the variation of probe position is shown in the Fig 4.20. Figure a shows the plot of gain versus theta for H-field when phi is specified to 90˚ (i.e. Coplane) and phi is specified to 0˚ (i.e. Crossplane). Figure b shows the plot of gain versus theta for E-field when phi is specified to 0˚ (i.e. Coplane) and phi is specified to 90˚ (i.e. Crossplane). As it is evident from the graphs, there is no as such variation in radiation patterns with the change in probe location.

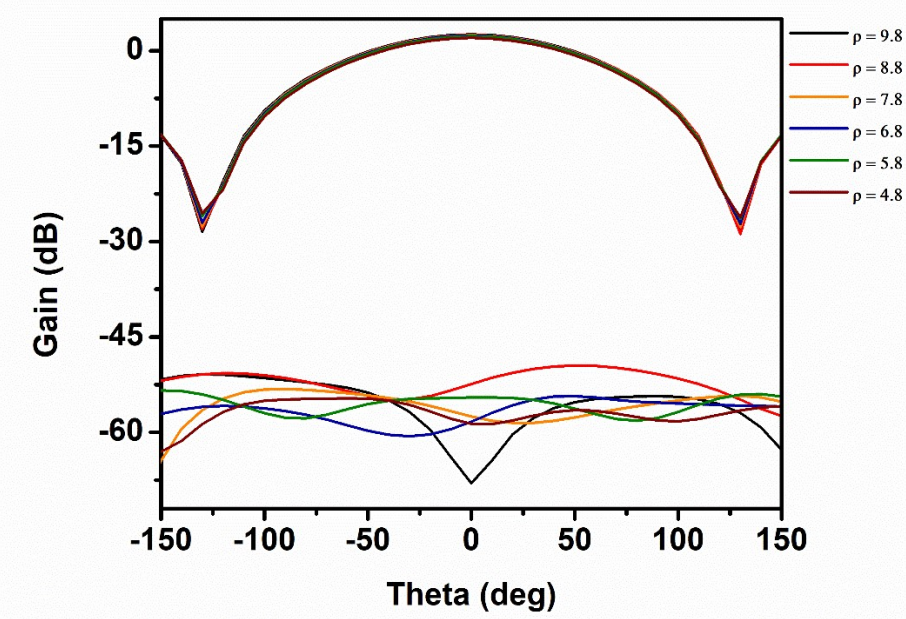

(a)

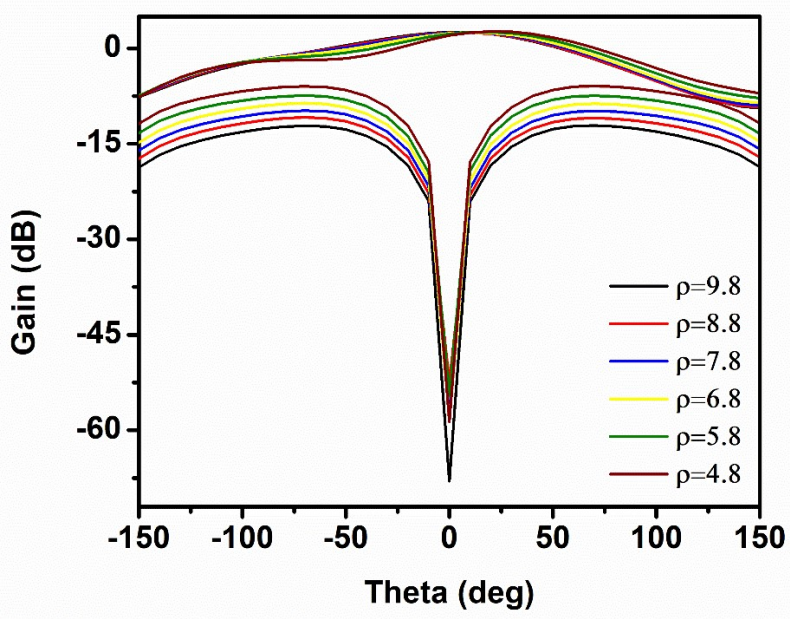

(b)

Fig. 4.20: (a) Gain vs theta for H-field at phi = 90° (Coplane) and phi = 0° (Crossplane) and (b) Gain vs theta for E-field at phi = 0° (Coplane) and phi = 90° (Crossplane) with variation in probe location from edge to centre of DRA

4.4.3 Effect of change of the radius of DRA

Here, the simulated cylinder is of height, h = 26 cm, radius, a which changes from 11mm to 15 mm, probe height, l = 10.16 mm and probe location, ρ = 9.8 mm from centre of DRA. Relative permittivity, ε_r = 10. Fig.4.22 shows the plot of input impedance as a function of resonant frequency with the change in radius of DRA.

Table 4.3: Table showing variation of Resonant Frequency and Impedance with variation in aspect ratio, a/h for change in radius of DRA

Radius (mm)	Height (mm)	a/h	Simulated Resonant Frequency from Return Loss Plot (GHz)	Simulated Resonant Frequency from Imedance Plot (GHz)	Re(Z11) At resonance (Ω)
11	26	0.42	3.44	2.90	72.47
12	26	0.46	3.24	2.75	57.45
13	26	0.5	2.93	2.6	46.73
14	26	0.54	2.36	2.43	38.70
15	26	0.57	2.05	2.30	32.63

Fig. 4.21 shows the simulated return loss curves for different a/h ratio, indicating the shift of the operating frequency band towards the lower band and meeting the design goal.

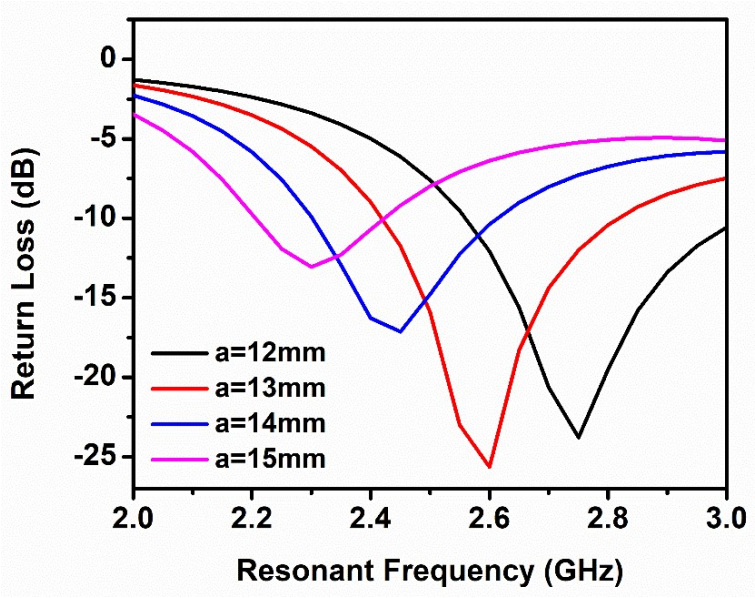

Fig.4.21: Set of Return Loss curves for different values of radius of DRA

It is observed from the simulated graphs that as the radius of DRA changes, i.e., aspect radio increase, magnitude of measured impedance (as shown in Fig. 4.23) as well as resonant frequency decreases (as shown in Fig. 4.24).

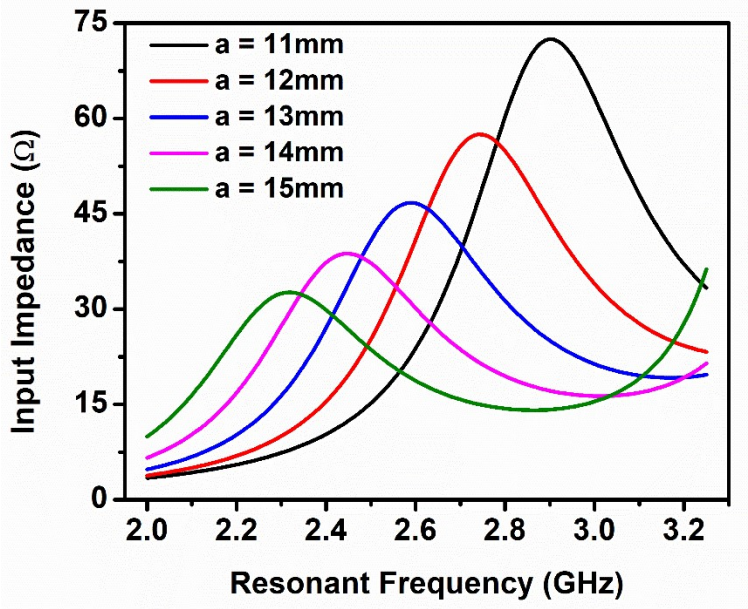

Fig. 4.22: Set of Impedance curves for different values of radius of DRA (in mm)

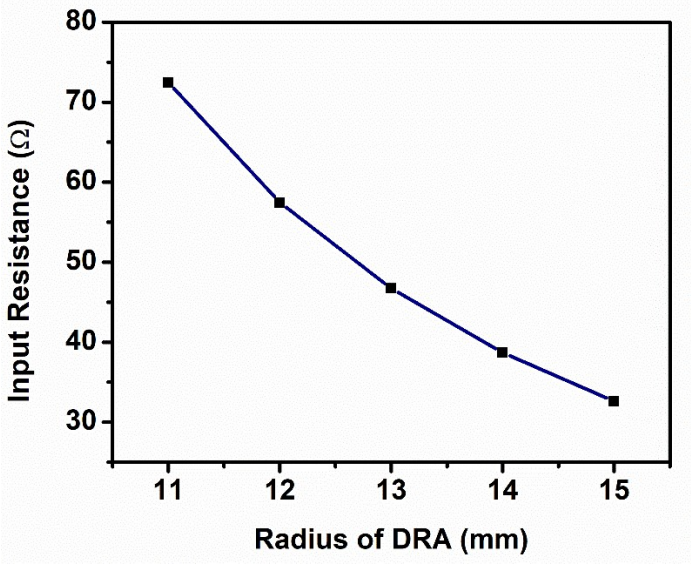

Fig. 4.23: Measured resistance versus change in radius of DRA

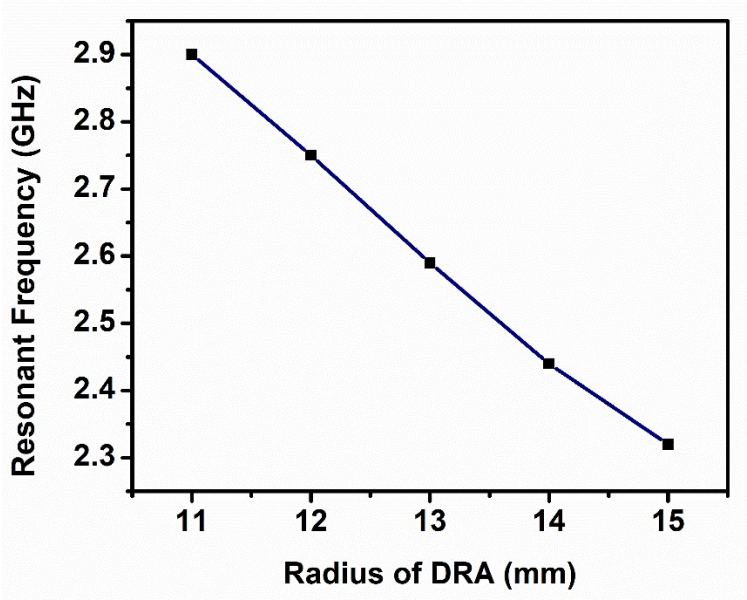

Fig. 4.24: Resonant Frequency versus change in radius of DRA

The far-field radiation patterns of the antenna with change in radius of DRA is shown in the Fig 4.25. Figure a shows the plot of gain versus theta for H-field when phi is specified to 90˚ (i.e. Coplane) and phi is specified to 0˚ (i.e. Crossplane). Figure b shows the plot of gain versus theta for E-field when phi is specified to 0˚ (i.e. Coplane) and phi is specified to 90˚ (i.e. Crossplane). As it is evident from the graphs, there is slight variation in radiation patterns with the change in radius of DRA. From fig. 4.26, we can say that gain decreases with increase in a/h ratio for change in radius of DRA.

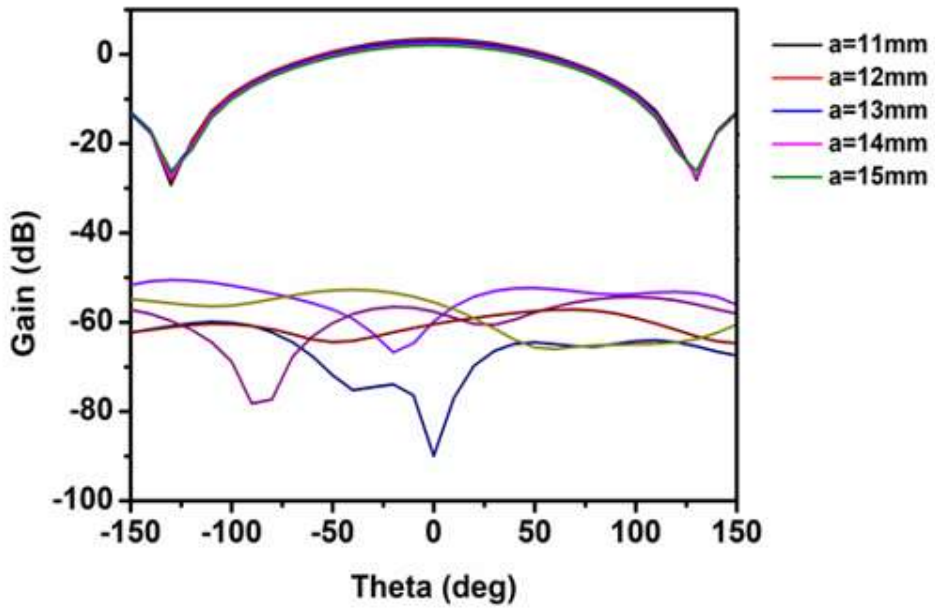

(a)

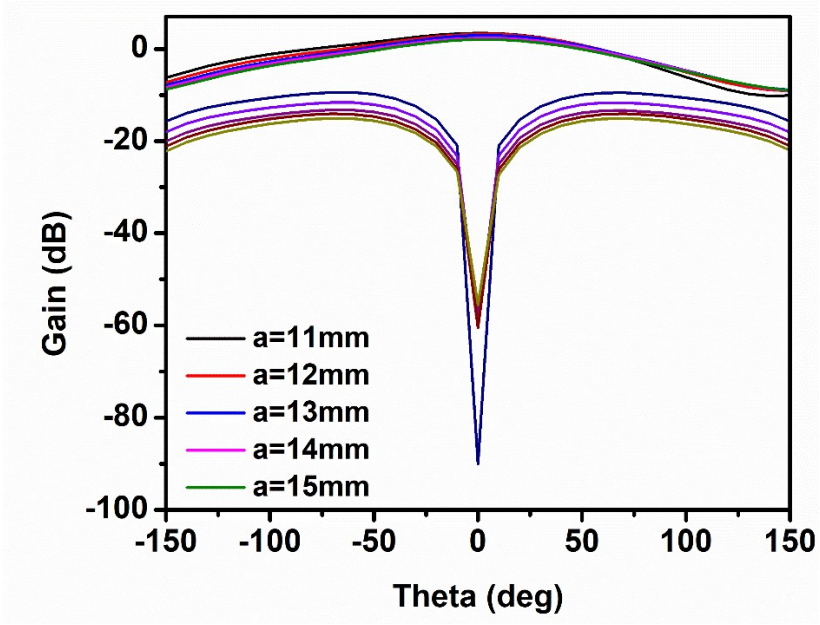

(b)

Fig. 4.25: (a) Gain vs theta for H-field at phi = 90˚ (Coplane) and phi = 0˚ (Crossplane) and (b) Gain vs theta for E-field at phi = 0˚ (Coplane) and phi = 90˚ (Crossplane) with change in radius of DRA

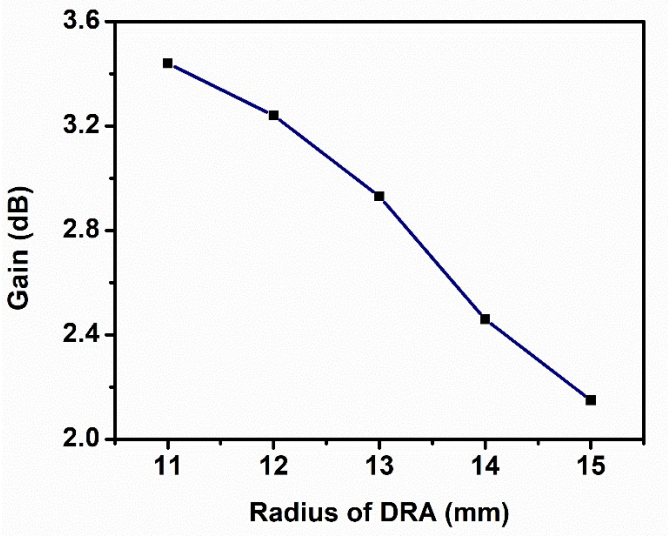

Fig. 4.26: Gain versus change in radius of DRA

4.4.4 Effect of change of the height of DRA

Here, the simulated cylinder is of height, a = 13 mm, height, h which changes from 17mm to 25 mm, probe height, l = 8.89 mm and probe location, ρ = 9.8 mm from centre of DRA. Relative permittivity, $\varepsilon_r = 10$. Fig.4.28 shows the plot of input impedance as a function of resonant frequency with the change in height of DRA.

Table 4.4: Table showing variation of Resonant Frequency and Impedance with variation in aspect ratio, a/h for change in height of DRA

Radius (mm)	Height (mm)	a/h	Simulated Resonant Frequency from Return Loss Plot (GHz)	Simulated Resonant Frequency from Imedance Plot (GHz)	Re(Z11) At resonance (Ω)
13	17	0.76	3.36	2.8	49.18
13	19	0.68	3.27	2.75	44.46
13	21	0.62	3.16	2.7	40.20
13	23	0.56	3.08	2.65	36.66
13	25	0.52	3.02	2.63	33.60

Fig. 4.27 shows the simulated return loss curves for different a/h ratio, indicating the shift of the operating frequency band towards the lower band and meeting the design goal.

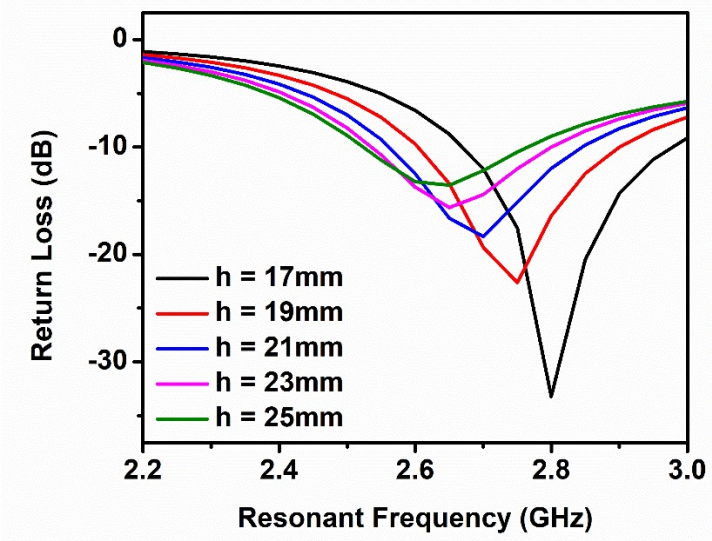

Fig. 4.27: Set of Return Loss curves for different values of height of DRA

It is observed from the simulated graphs that as the height of DRA changes, i.e., aspect radio decreases, magnitude of measured impedance (as shown in Fig. 4.29) as well as resonant frequency decreases (as shown in Fig. 4.30).

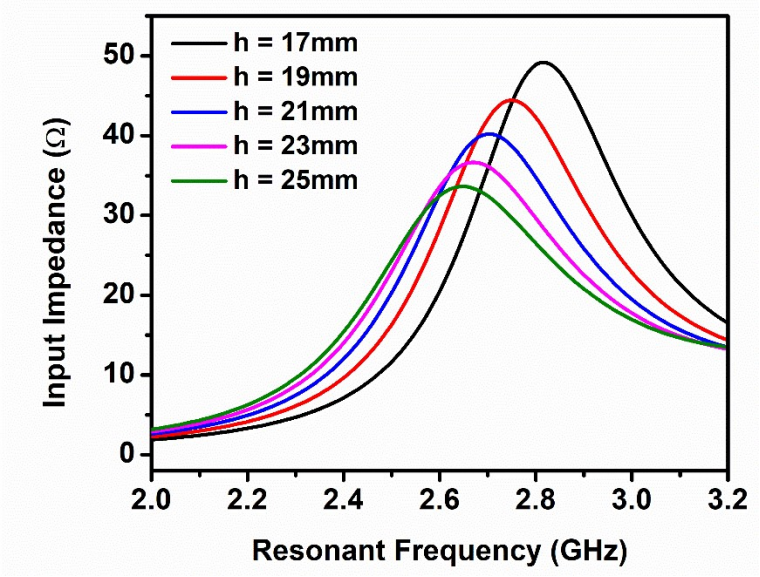

Fig. 4.28: Set of Impedance curves for different values of height of DRA (in mm)

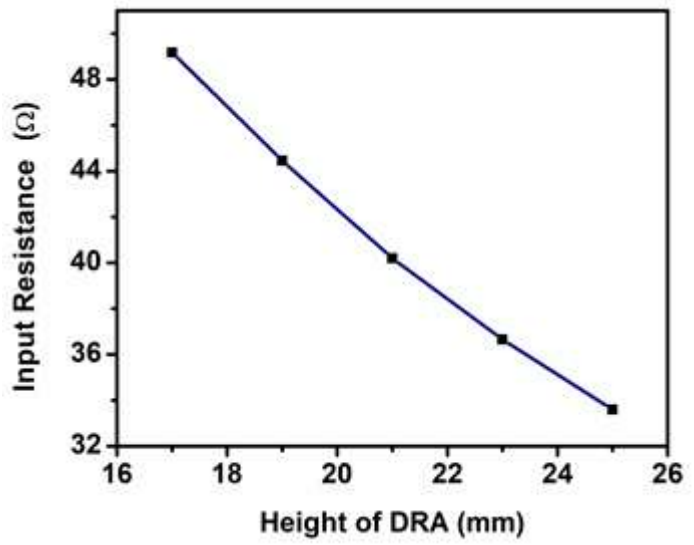

Fig. 4.29: Measured resistance versus change in radius of DRA

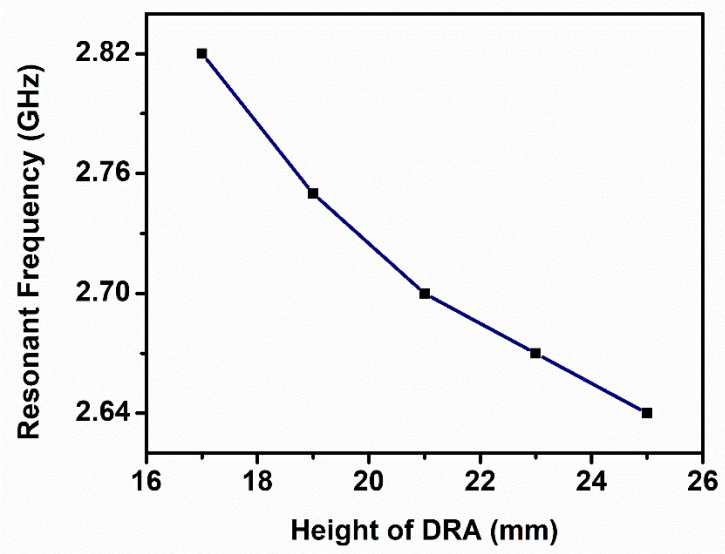

Fig. 4.30: Resonant Frequency versus change in height of DRA

The far-field radiation patterns of the antenna with change in height of DRA is shown in the Fig 4.31. Figure a shows the plot of gain versus theta for H-field when phi is specified to 90˚ (i.e. Coplane) and phi is specified to 0˚ (i.e. Crossplane). Figure b shows the plot of gain versus theta for E-field when phi is specified to 0˚ (i.e. Coplane) and phi is specified to 90˚ (i.e. Crossplane). As it is evident from the graphs, there is slight variation in radiation patterns with the

change in height of DRA. From fig. 4.32, we can say that gain decreases with increase in a/h ratio for change in height of DRA.

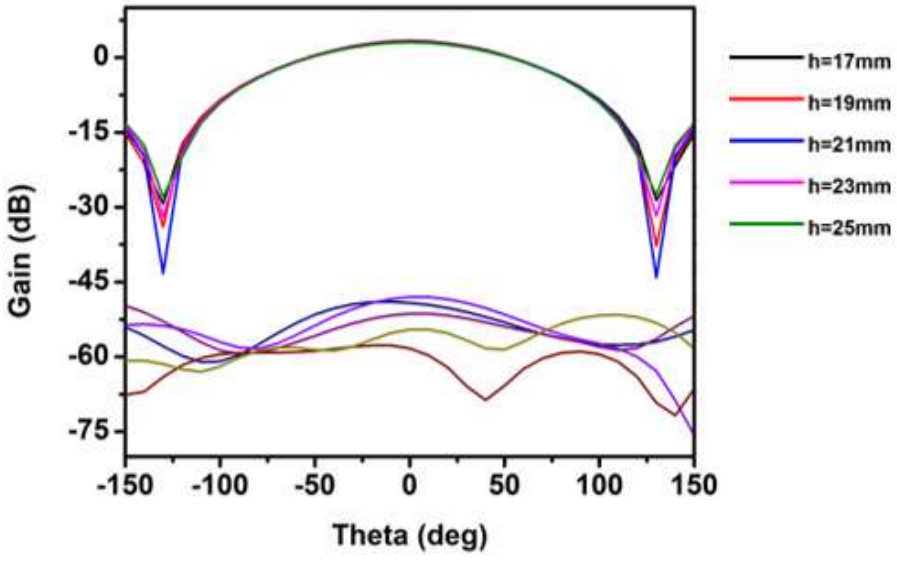

(a)

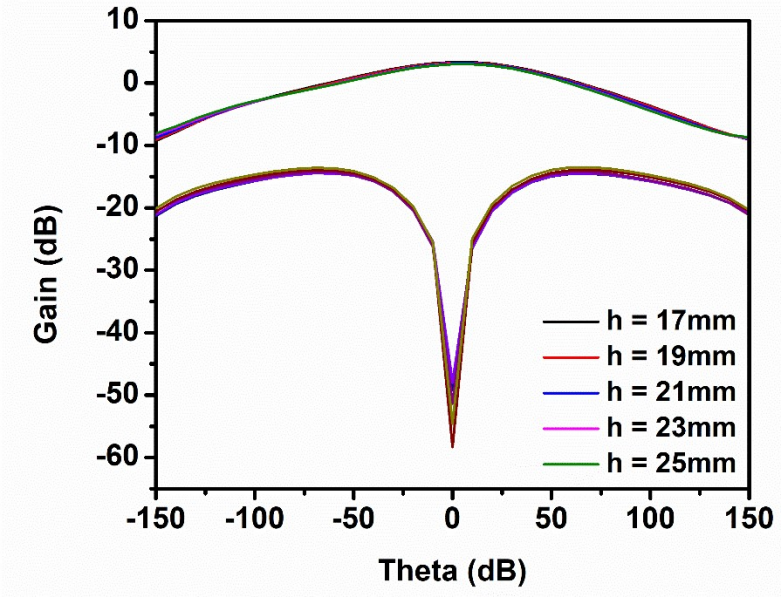

(b)

Fig. 4.31: (a) Gain vs theta for H-field at phi = 90˚ (Coplane) and phi = 0˚ (Crossplane) and (b) Gain vs theta for E-field at phi = 0˚ (Coplane) and phi = 90˚ (Crossplane) with change in height of DRA

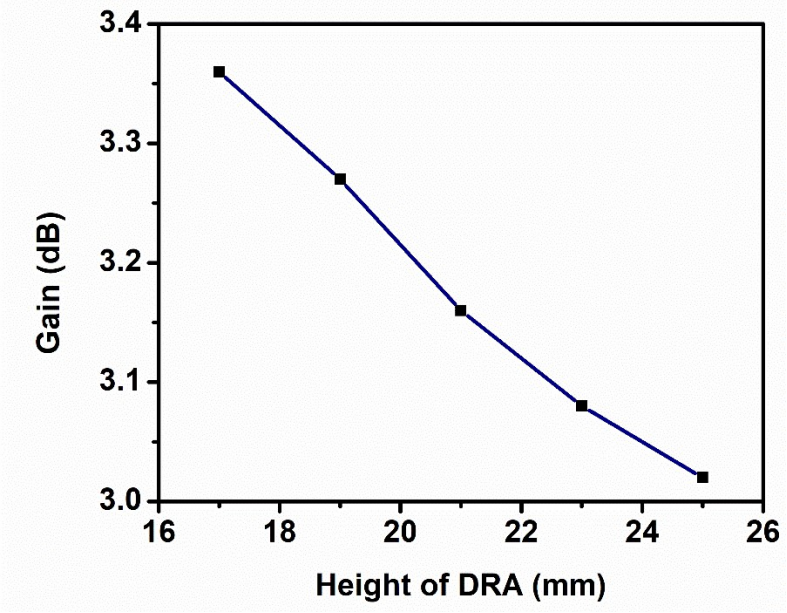

Fig. 4.32: Gain versus change in height of DRA

4.4.5 Effect of change of dielectric constant of DRA

To study the effect of the dielectric constant on the input impedance and resonant frequency, the DRA of height, a = 13 mm, height, h = 26mm, probe height, l = 10 mm and probe location, ρ = 9.8 mm from centre of DRA is simulated with different dielectric constant materials varying from 10 to 30. It is clear that as the dielectric constant increases, the resonant frequency and the bandwidth decreases. This behavior is expected since increasing the permittivity for a fixed dimension resonator results in a higher Q-factor.

Table 4.5: Table showing variation in dielectric constant of DRA on input impedance and resonant frequency

Dielectric constant of the DRA (ε_r)	Simulated Resonant Frequency from Return Loss Plot (GHz)	Simulated Resonant Frequency from Imedance Plot (GHz)	Re(Z11) At resonance (Ω)
10	2.59	2.60	44.33
20	2.36	2.35	55.50
30	2.15	2.15	63.58

Fig. 4.33 shows the simulated return loss curves for different values of dielectric constant of DRA, indicating the shift of the operating frequency band towards the lower band.

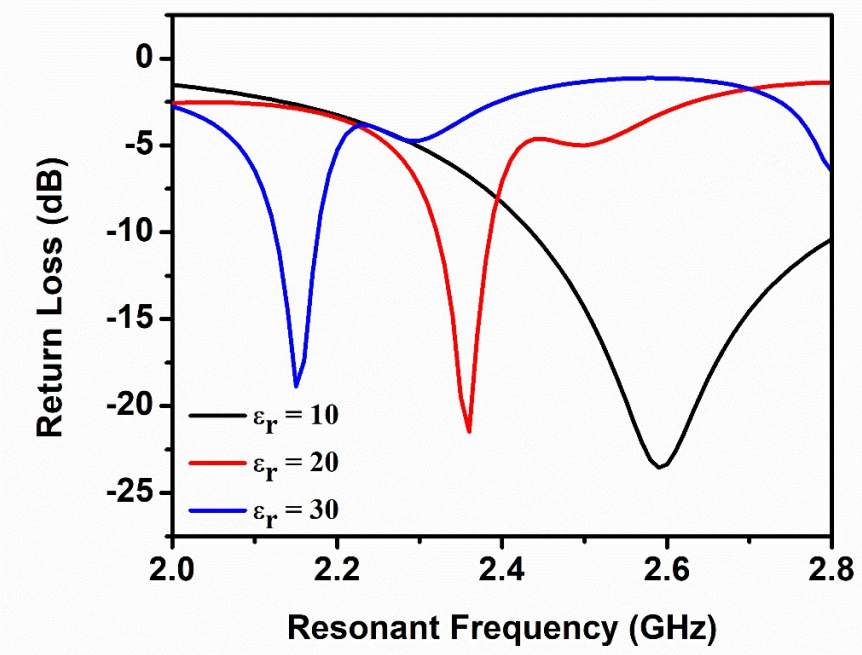

Fig. 4.33: Set of Return Loss curves with variation in Dielectric constant of DRA

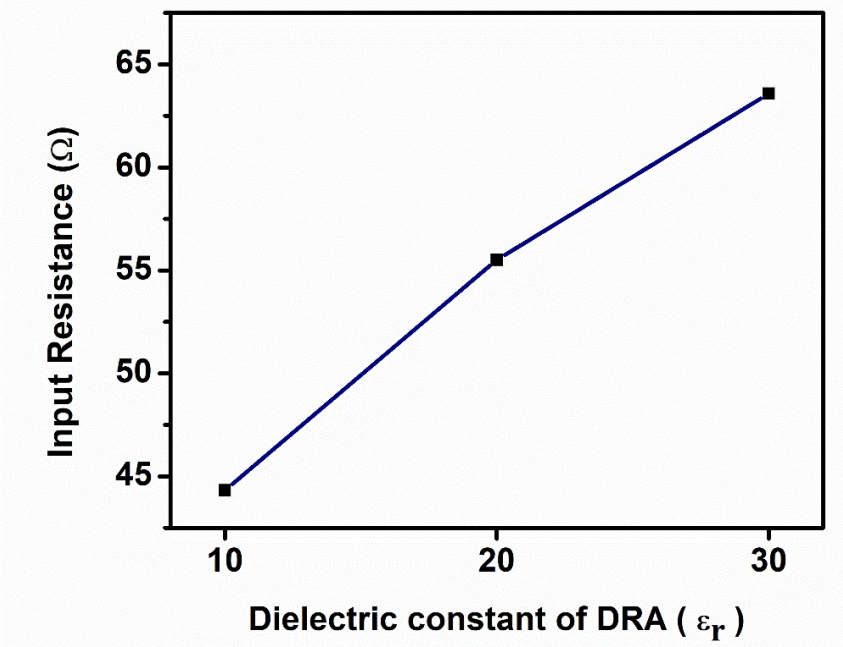

Fig. 4.34: Measured resistance versus variation in Dielectric constant of DRA

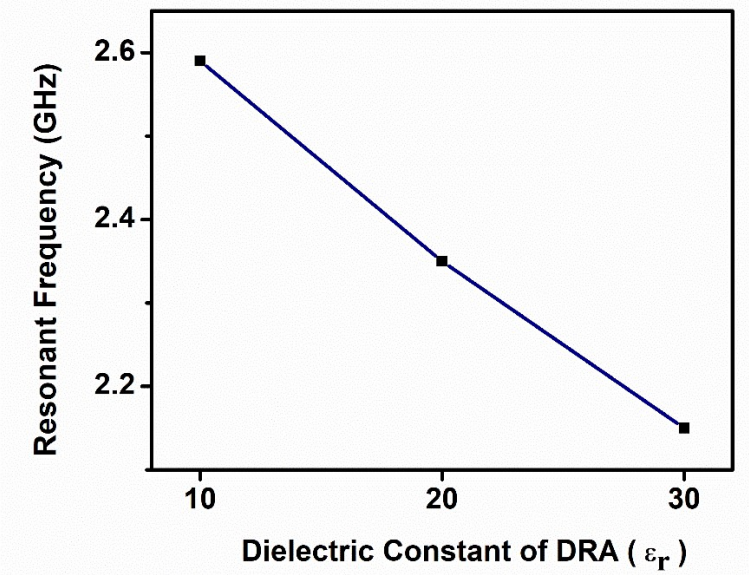

Fig. 4.35: Resonant Frequency versus change in Dielectric constant of DRA

The far-field radiation patterns of the antenna with change in dielectric constant of DRA is shown in the Fig 4.36. Figure a shows the plot of gain versus theta for H-field when phi is specified to 90˚ (i.e. Coplane) and phi is specified to 0˚ (i.e. Crossplane). Figure b shows the plot of gain versus theta for E-field when phi is specified to 0˚ (i.e. Coplane) and phi is specified to 90˚ (i.e. Crossplane). As it is evident from the graphs, there is larger variation in radiation patterns with the change in dielectric constant of DRA. From fig. 4.37, we can say that gain decreases with increase in relative permittivity of DRA.

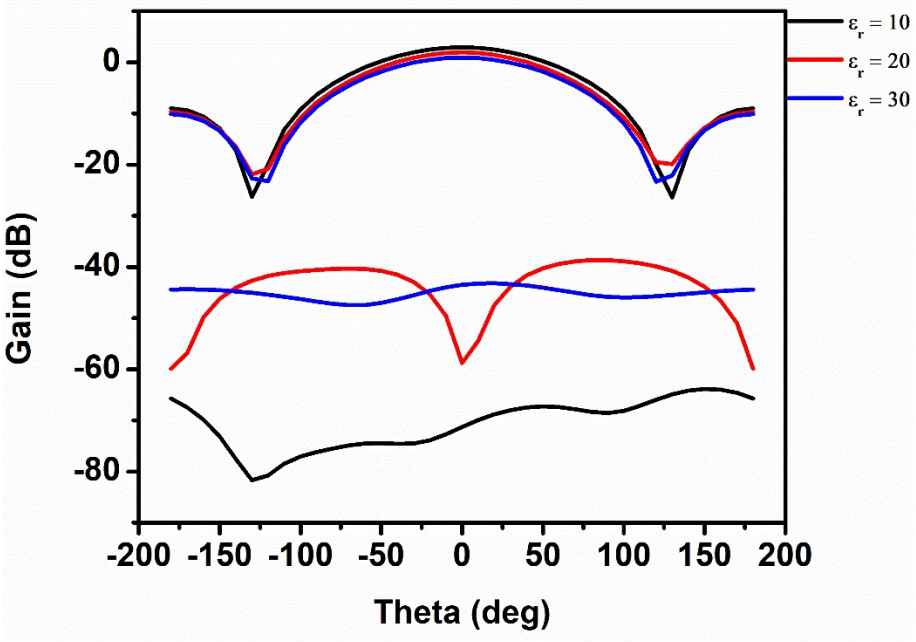

(a)

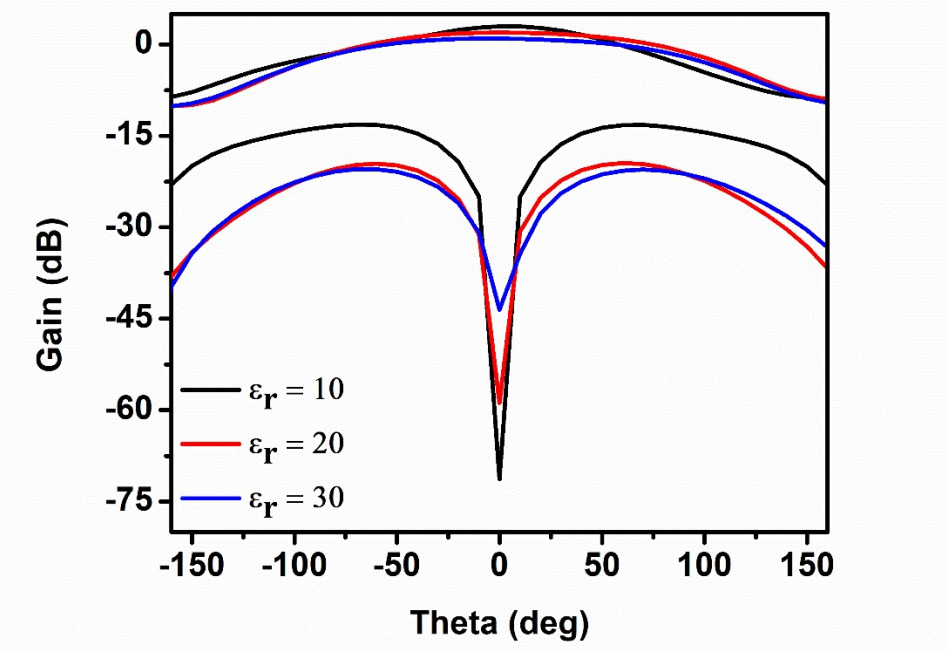

(b)

Fig. 4.36: (a) Gain vs theta for H-field at phi = 90˚ (Coplane) and phi = 0˚ (Crossplane) and (b) Gain vs theta for E-field at phi = 0˚ (Coplane) and phi = 90˚ (Crossplane) with change in dielectric constant of DRA

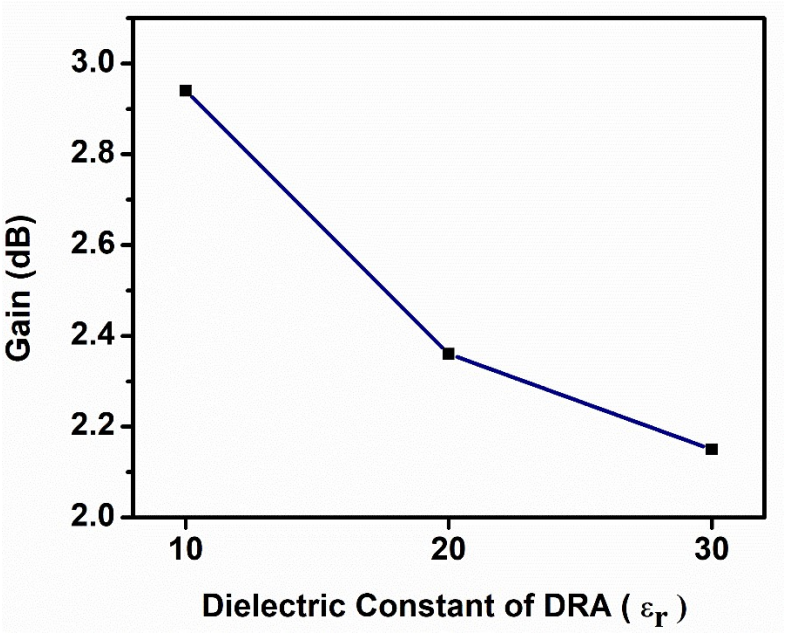

Fig. 4.37: Gain versus change in dielectric constant of DRA

4.5 Conclusion

Thus detailed analysis of various antenna parameters of probe-fed cylindrical DRA is simulated and its performance characteristics on return loss, resonant frequency, impedance, bandwidth, gain and radiation patterns are examined thoroughly and verified with the theoretical concepts.

References

[1] A. Petosa, Dielectric Resonator Antenna Handbook. Norwood, MA: Artech House, 2007.

[2] S. A Long, M. W. McAllister, and L.C .Shen, “The resonant cylindrical dielectric cavity antenna,” *IEEE Trans. Antennas Propag*., vol.AP-31, no.5, pp.406-412, May 1983.

[3] K. M. Luk and K. W. Leung, “Dielectric Resonator Antennas,” Eds. Baldock, U.K.: Research Studies Press, 2003.

[4] A. Petosa, A. Ittipiboon, Y. M. M. Antar, D. Roscoe, and M. Cuhaci, “Recent advances in dielectric-resonator antenna technology,” Antennas & Propagat. Mag., pp. 35–48, June 1998.

[5] G. P. Junker, A. A. Kishk, and A. W. Glisson, "Input impedance of dielectric resonator antennas excited by a coaxial probe," *IEEE Trans. Antennas Propagat.,* vol.42, pp. 960-966, July 1994.

[6] Vipul Ranjan Kaushik, “A Review on Dielectric Resonator Antenna and Its Analysis Setup”, International Journal of Scientific Research in Science, Engineering and Technology; Volume 4, Issue 7, Pages: 282-289, March-2018

CHAPTER 5

BANDWIDTH ENHANCEMENT USING DRA

5.1 Introduction

The use of the broadband devices in the modern communication systems is on the rise so a practical purposes antenna is supposed to have wider bandwidth. The bandwidth limitation of antennas is usually linked to their input impedance because it is the quantity which changes with frequency so improvement in impedance response can help us to enhance its bandwidth. The bandwidth of DRA depends on parameters such as the excitation method, shape, dimensional parameters like radius and height & dielectric constant of DRA material. Various bandwidth enhancement techniques are developed since the invention of DRAs like controlling permittivity and aspect ratio (a/h), use of matching networks, employment of multiple resonators, etc. But all these have few disadvantages like complexity in fabrication, costly and time-consuming. Hence, one of the easy methods for enhancing bandwidth is introducing air-gap between ground plane and DRA. It is easy to fabricate, does not require neither parasitic elements nor a complex matching network, and the technique takes up no additional real-estate. In this chapter, we will analyze the effect of air-gap between DRA and ground plane on input impedance and resonant frequency.

5.2 Antenna Design

To analyze the effect of air-gap between ground plane and DRA, a DRA of radius, a = 13mm, height, h = 26mm, probe length, l = 10mm, probe position = 9.8mm from centre of DRA, relative permittivity, ε_r = 10 is considered. The proposed structure is modelled with finite element solver Ansys HFSS v15.0. The DRA is first simulated without any air-gap then airgap is gradually increased from 1mm to 6mm and simulated results are analyzed thoroughly.

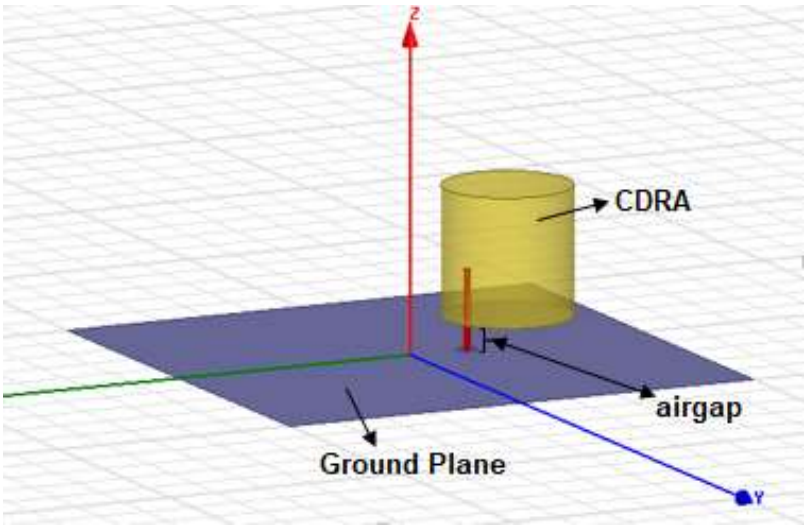

Fig. 5.1: Proposed DRA structure

5.3 Parametric Study

A parameter study is useful because it provides a comprehensive picture of the antenna's characteristics and allows understanding of the influence of the DR geometry parameters on the return loss of the antenna. Fig. 5.2, showing the simulated return loss for DRAs without airgap and then with increasing airgap. When there is no airgap, -10dB return loss resonant frequency is achieved around 2.53GHz, whereas with increasing airgap, it is around 3.29 GHz to 3.35GHz. Hence bandwidth of the antenna is enhanced.

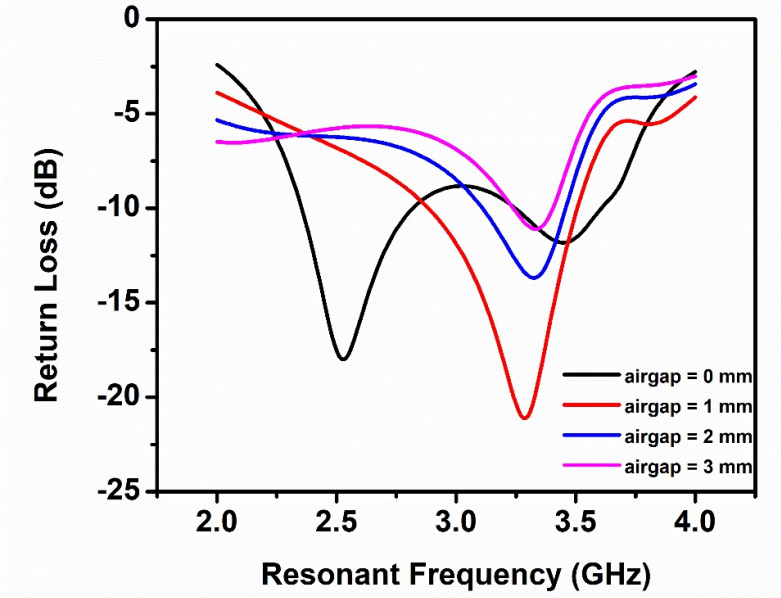

Fig. 5.2: Simulated return loss of proposed antenna with and without airgaps between ground plane and DRA

5.4 Result and Discussion

Fig. 5.3 shows the plot of input impedance as a function of resonant frequency without and with airgaps between ground plane and DRA. The airgaps are increased gradually from 1mm to 6mm. It is noticed that without airgap, input impedance was around 75Ω at 2.53GHz which increased to around 92 Ω - 177 Ω at frequency range 2.8GHz – 3.03GHz when airgaps are increased.

Table 5.1: Table showing variation of Resonant Frequency and Impedance with increasing airgaps between ground plane and DRA

Airgaps (in mm)	Simulated Resonant Frequency from Return Loss (S11) (GHz)	Simulated Resonant Frequency from Impedance Plot (GHz)	Re(Z11) At resonance (Ω)
0	2.53	2.53	75.18
1	3.29	2.88	92.64
2	3.33	2.96	107.25
3	3.34	3.00	122.82
4	3.32	3.01	139.10
5	3.31	3.02	157.97
6	3.30	3.03	176.81

Hence, it is evident from the plots that with increasing airgaps, input impedance as well as resonant frequency increases. Thus, bandwidth is also increased.

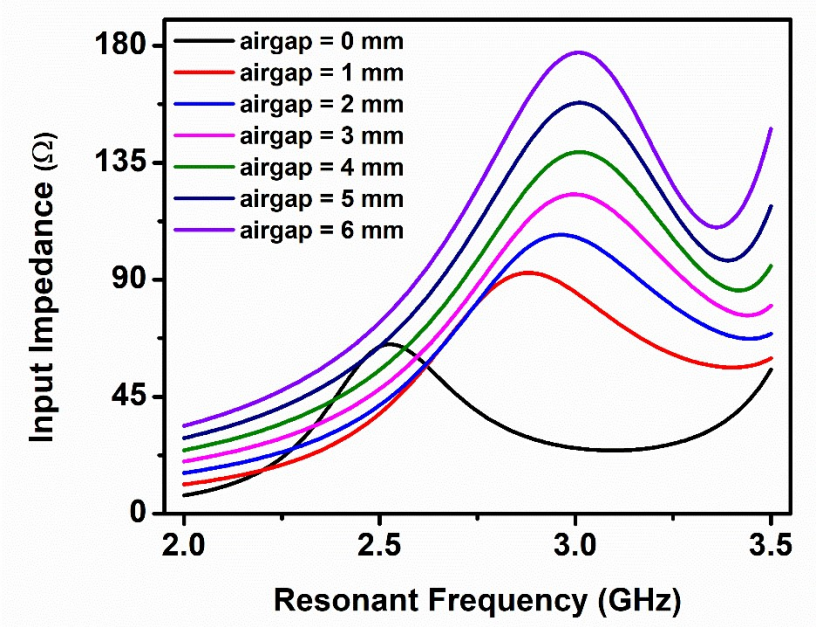

Fig. 5.3: Family of impedance curves with and without airgaps between ground plane and DRA

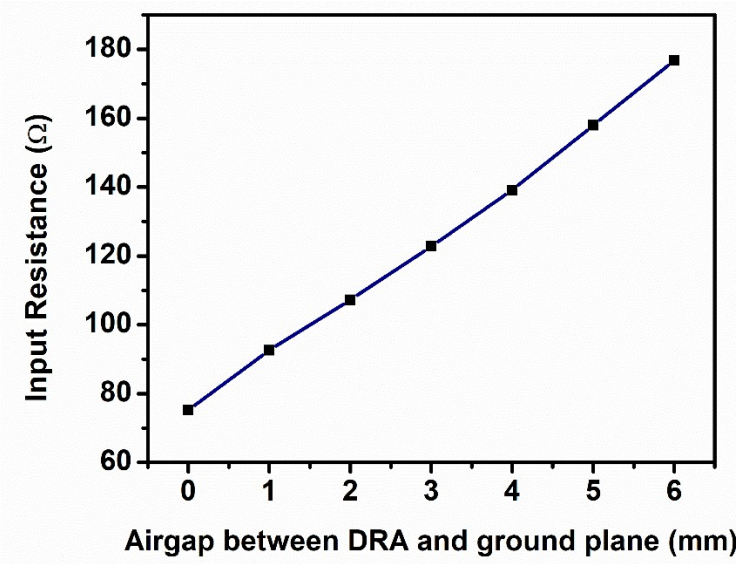

Fig. 5.4: Measured resistance versus with and without airgaps

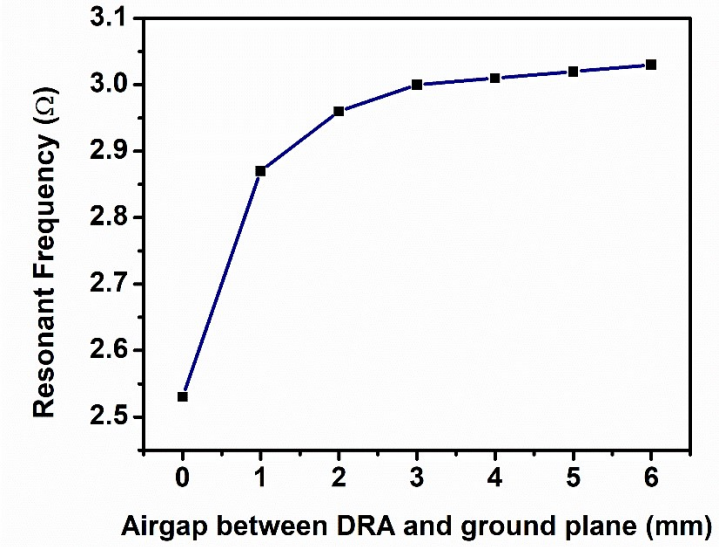

Fig. 5.5: Resonant Frequency versus with and without airgaps

The far-field radiation patterns of the DRA with and without airgaps between ground plane and DRA is shown in the Fig 5.6. Figure a shows the plot of gain versus theta for H-field when phi is specified to 90˚ (i.e. Coplane) and phi is specified to 0˚ (i.e. Crossplane). Figure b shows the plot of gain versus theta for E-field when phi is specified to 0˚ (i.e. Coplane) and phi is specified to 90˚ (i.e. Crossplane). As it is evident from the graphs, there is also variation in radiation patterns with increasing airgaps. From Fig. 5.7, it is noticed that with increase in airgaps, gain decreases gradually.

(a)

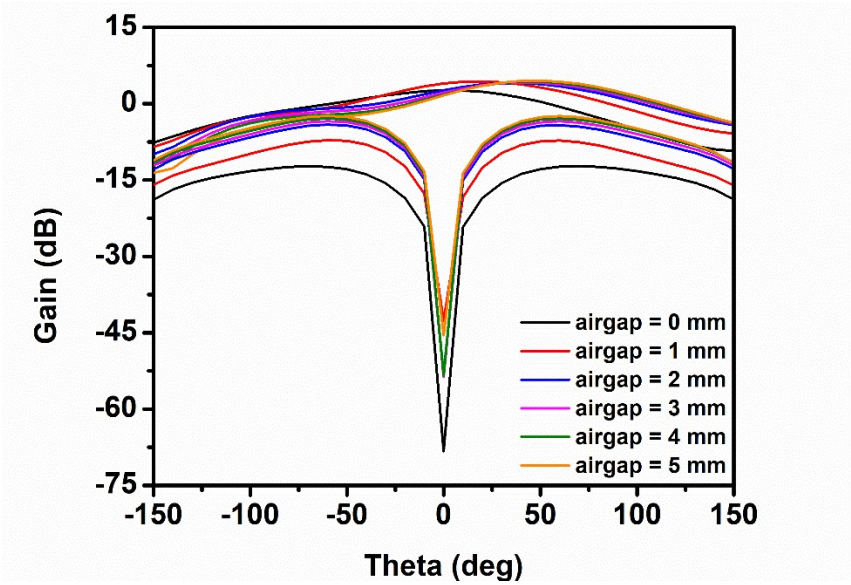

(b)

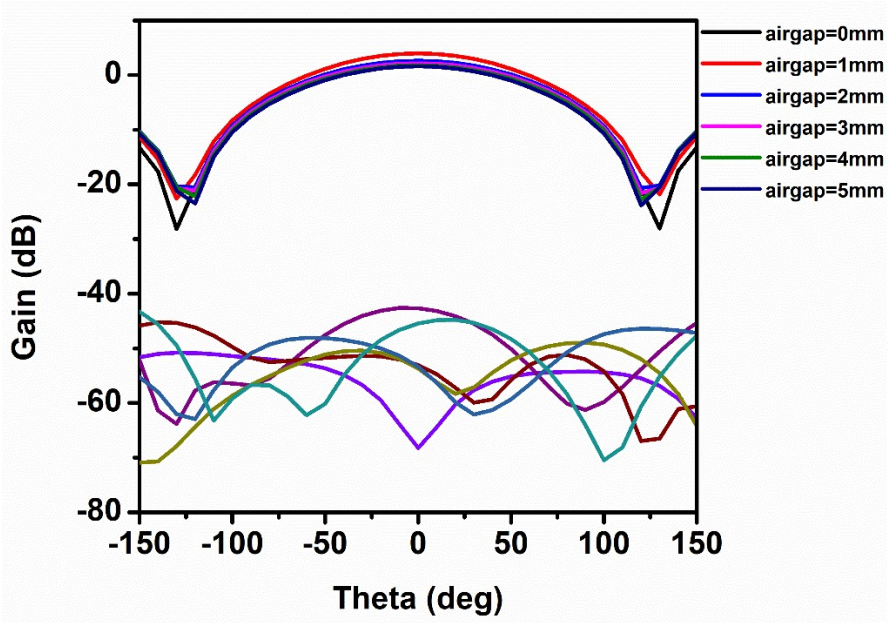

Fig. 5.6: (a) Gain vs theta for H-field at phi = 90˚ (Coplane) and phi = 0˚ (Crossplane) and (b) Gain vs theta for E-field at phi = 0˚ (Coplane) and phi = 90˚ (Crossplane) with and without airgaps

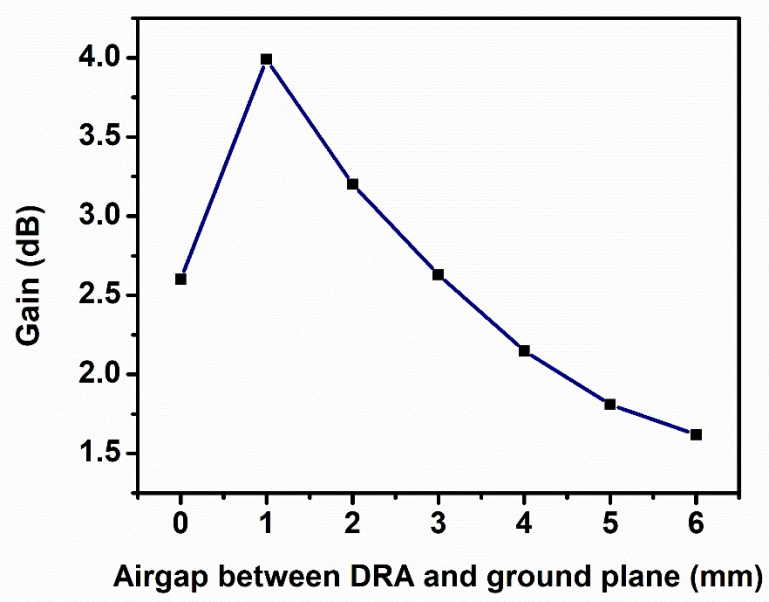

Fig. 5.7: Gain corresponding to variation in airgaps between ground plane and DRA

5.5 Conclusion

Thus we can conclude from the above study that by introducing airgaps between ground plane and DRA, we can enhance the impedance bandwidth of the antenna as it has a severe effect on antenna's input impedance and resonant frequency. This is one of the easiest and simplest methods among bandwidth enhancement techniques.

References

[1] A. Petosa, Dielectric Resonator Antenna Handbook. Norwood, MA: Artech House, 2007.

[2] S. A Long, M. W. McAllister, and L.C .Shen, "The resonant cylindrical dielectric cavity antenna," *IEEE Trans. Antennas Propag*., vol.AP-31, no.5, pp.406-412, May 1983.

[3] K. M. Luk and K. W. Leung, "Dielectric Resonator Antennas," Eds. Baldock, U.K.: Research Studies Press, 2003.

[4] G.P. Junker, A.A. Kishk, A.W. Glisson and D. Kajfez "Effect of air gap on cylindrical dielectric resonator antenna operating in TM or mode", *ELECTRONICS LETTERS* 20th January 1994 Vol. 30 No. 2

CHAPTER 6

EXPERIMENT SECTION

6.1 Introduction

A probe-fed cylindrical DRA is fabricated and measured its performance characteristics to analyze and compare with the simulated results. The simulation is performed using Ansoft HFSS and the experimental results are measured using vector network analyzer. The test results of the experimental antenna are in good agreement with the simulation results.

6.2 Antenna Design

The proposed cylindrical DRA structure is shown in Fig. 6.1. The DRA is placed above a conducting ground plane. Here, the ground plane size of 50mm×50mm×2mm is considered and fed by a coaxial connector. The dimensional parameters of the DRA are radius a=13mm, height h=26mm. The resonator material used has a dielectric constant of 10. The probe is located at the edge of the cylinder for the easy of fabrication. The feed probe is of length l = 10mm, and radius r =0.63 mm.

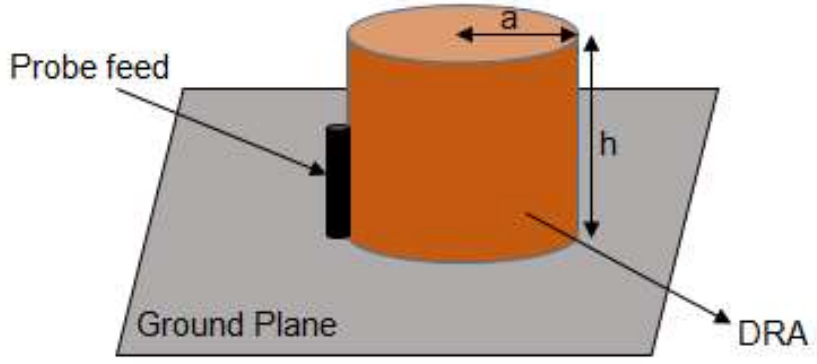

Fig. 6.1: Proposed antenna structure

(a)

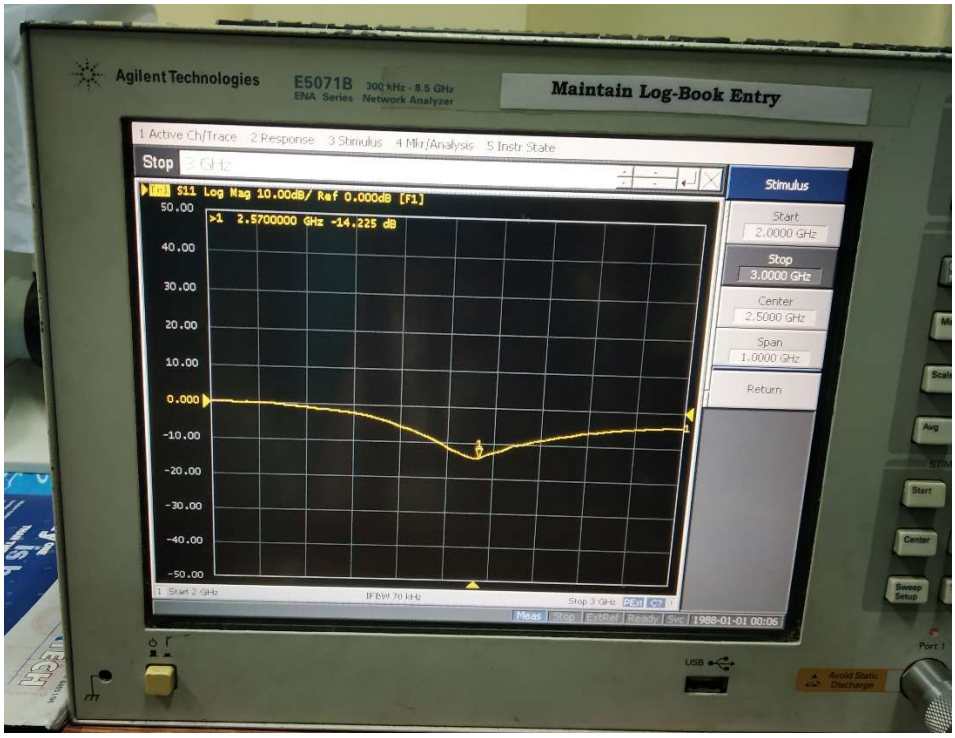

(b)

Fig. 6.2: Photograph of the fabricated antenna (a) proposed model and (b) Measurement using Vector Network Analyser (Model #5071 B) from Agilent Technologies

6.3 Result and Discussion

Fig.6.3 shows the typical simulated and measured antenna performance in terms of impedance bandwidth. It may be clearly seen that the two adjacent resonant frequencies are in the range of 2 GHz - 3GHz at |S11| ≤ -10 dB. It is worth noting that this prototype antenna has -10dB return loss resonant frequency at 2.57 GHz which is very close to the simulated value which is at 2.60 GHz.

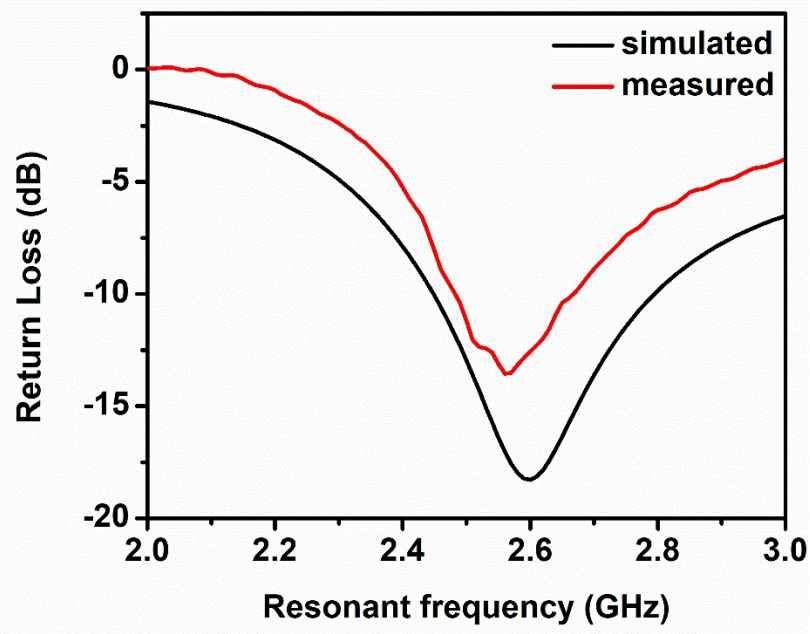

Fig. 6.3: Measured and simulated reflection coefficient $|S_{11}|$

Fig. 6.4 shows the simulated as well as measured input impedance of the proposed antenna. The test results of the experimental antenna are in good agreement with the simulation results.

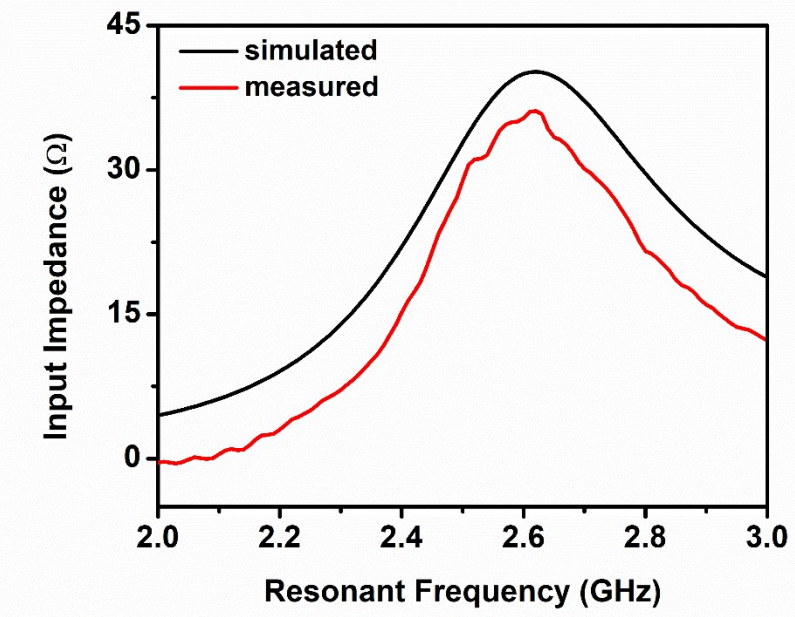

Fig. 6.4: Comparison of measured and simulated Impedance of the proposed antenna

Measurements of the far-field radiation patterns of the prototype antenna are performed in an anechoic chamber using an elevation-over-azimuth positioner, with the elevation axis coincident with the polar axis ($\theta = 0^{\circ}$) of the antenna's coordinate system. The azimuth drive thus generates cuts at constant ϕ. The fixed transmitting antenna was a broadband horn positioned 1m from the antenna being tested. The azimuth positioner was rotated from θ= -180 to 180 at increments of 10 for the selected measurement. Two patterns cuts, $\phi = 0^{\circ}$ and 90°, were taken at two selected operating frequencies for which the matching was optimal. Fig. 6.5 shows the simulated and measured normalized radiation patterns at resonance frequencies of 2.60 and 2.59 GHz. The electric and magnetic fields distributions are plotted on the xz and yz planes respectively.

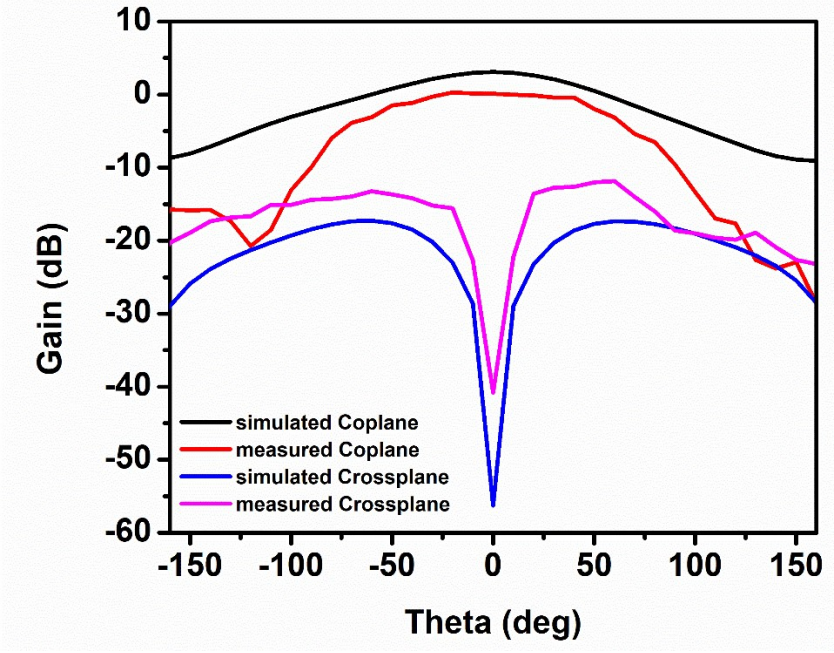

(a)

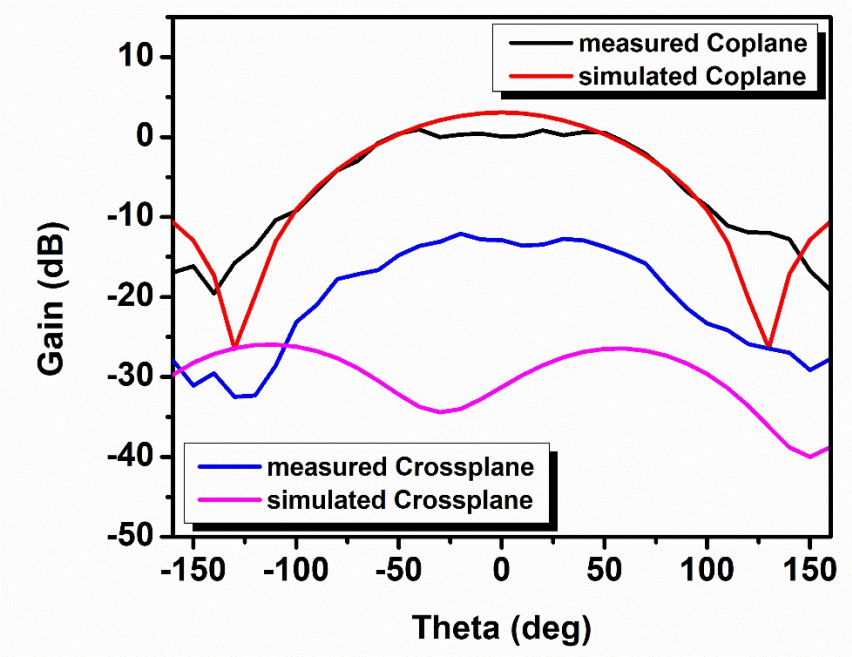

(b)

Fig. 6.5: Simulated and measured normalized radiation patterns (a) at xz plane (E field) and (b) at yz plane (H field)

6.4 Conclusion

Thus probe-fed cylindrical DRA is successfully designed, fabricated, measured and compared with the simulated results. The difference between simulated and measured results is because simulation measurements assume ideal conditions and for the designed antenna there may be effect of airgap or fabrication imperfections.

CHAPTER 7

CONCLUSION AND FUTURE SCOPE

7.1 Conclusion

The thesis emphasizes on the study and analysis of the performance characteristics of Cylindrical Dielectric Resonator Antenna. Prior to research in any field, fundamental knowledge of that field is first required followed by useful analytic and design techniques, and practical experience. These criteria are successfully achieved in this thesis. An effort was made to introduce HFSS as an effective tool for 3-D electromagnetic analysis and also impart understanding of the design process in HFSS. A comprehensive description of each step taken in creating the simulation of the DRA was presented.

Initially, a brief overview of Dielectric Resonator Antenna along with its historical development is studied. A literature survey is then carried out in the advancements of the cylindrical dielectric resonator antenna since its invention. After that, detailed theoretical analysis of cylindrical DRA is studied thoroughly which includes resonant modes, feeding mechanisms, different bandwidth enhancement techniques and MATLAB simulated results which verify theoretical formulations.

Using HFSS software, various simulations are then performed for comparative analysis of different parameters of DRA on input impedance, resonant frequency, bandwidth, gain and radiation patterns. Then, an antenna is designed and simulated to understand the effect of airgap on enhancing the antenna bandwidth. Finally, design and fabrication of a probe-fed cylindrical DRA is executed to make a comparative study of the antenna performance characteristics with the simulated results. Thus, we can conclude by stating that effective utilization of DRA characteristics can lead to a wider frequency range, low cost, high radiation efficiency antenna which is useful for various applications.

7.2 Future Scope

The future work plan could be constructed to extend the trends established in this thesis, resulting in detailed design strategies for the antennas and their response to the target operational environment. In recent years, interest in DRA antenna is due to its prospect of shrinking down the size of antennas for wireless applications and its potential in reducing the cost and ease of manufacturing. The difficulties faced in fabrication techniques are also a research statement. For innovative design in mobile and wireless system, research on hybrid modes creation is to be done for enhancing the bandwidth or develop multiband antenna. Considering the advantages of the DRA, the frequency range of antenna can be increased using DRA arrays. Improvisation in features of DRA can be done by changing excitation techniques and designing parameters.

Very recently, DRA can be used as a sensor to determine the relative permittivity of unknown materials, moisture content of fruits, the crack in a solid material, and biomedical applications like cancer cell determination in breast. So our further studies concentrated on design of DR accurately to predict above such parameters.